

**Analysis of NEIL3 Expression: A Possible  
Resistance Factor to Cancer  
Chemotherapy in Paediatric  
Cancer Cells.**

**Amira Duweb**

**School of Environment & Life Sciences.  
University of Salford, Salford, UK**

**A thesis submitted for the degree of MSc by Research, 2015**



1.3 <b><u>Types of DNA repair mechanisms</u></b> .....	31
1.3.1 Direct reversal.....	31
1.3.2 Nucleotide excision repair .....	32
1.3.3 Double-strand break repair .....	32
1.3.4 Mismatch repair .....	33
1.3.5 Base excision repair .....	33
1.4 <b><u>Oxidized base-specific DNA glycosylases in eukaryotic cells</u></b> .....	35
1.5 <b><u>NEIL family</u></b> .....	36
1.5.1 NEIL1.....	36
1.5.2 NEIL2.....	37
1.5.3 NEIL3.....	38
<i>1.5.3.1</i> Analysis of the structure of NEIL3 and its DNA glycosylase activity.....	39
<i>1.5.3.2</i> The role of NEIL3 in rapidly dividing cells.....	41
<i>1.5.3.3</i> The role of NEIL3 in replication-associated repair.....	42
<i>1.5.3.4</i> The immunological role of NEIL3.....	43
<i>1.5.3.5</i> NEIL3 and human immunodeficiency virus type1.....	43
1.6 <b><u>Telomeres</u></b> .....	44
1.6.1 Factors that influence telomere length.....	45
1.6.2 Factors regulating telomere homeostasis.....	47
1.6.3 Telomerase.....	48
1.6.4 The association between telomeric proteins and DNA repair mechanisms.....	51
1.7 <b><u>Genotoxic drugs</u></b> .....	52
1.7.1 Cisplatin.....	53
<i>1.7.1.1</i> Pharmacokinetic properties of cisplatin.....	54
<i>1.7.1.2</i> Pharmacodynamic properties of cisplatin.....	54
<i>1.7.1.3</i> Mechanisms of cisplatin resistance.....	55
1.7.2 <i>tert</i> -butyl hydroperoxide.....	56
<i>1.7.2.1</i> Pharmacokinetic properties of <i>tert</i> -butyl hydroperoxide.....	56

1.7.2.2 Pharmacodynamic properties of <i>tert</i> -butyl hydroperoxide.....	57
1.7.3 Doxorubicin.....	57
1.7.3.1 Pharmacokinetic properties of doxorubicin.....	59
1.7.3.2 Pharmacodynamic properties of doxorubicin .....	59
1.7.3.3 Mechanisms of doxorubicin resistance.....	61
<b>Aims of the project.....</b>	<b>62</b>
<b>Chapter 2: <u>Materials and Methods</u>.....</b>	<b>63</b>
<b>2.1 <u>Materials</u>.....</b>	<b>63</b>
2.1.1 Chemicals.....	63
2.1.2 Kits and other lab consumables.....	64
2.1.3 PCR Primers.....	65
<b>2.2 <u>Methods</u> .....</b>	<b>66</b>
2.2.1 Cell culture.....	66
2.2.1.1 Cell lines.....	66
2.2.1.2 Growing and maintaining the suspension cells.....	67
2.2.1.3 Splitting the suspension cells.....	67
2.2.1.4 Growing and maintaining the adherent cells.....	67
2.2.1.5 Splitting the adherent cells.....	68
2.2.1.6 Freezing the suspension cells and the adherent cells .....	68
2.2.1.7 Thawing the suspension cells and the adherent cells.....	68
2.2.1.8 Cell counting.....	69
2.2.1.9 Time course of cell growth.....	69
2.2.1.10 Preparation cell pellets for RNA extraction .....	69
2.2.2 RNA extraction.....	69
2.2.3 Reverse transcription.....	71
2.2.4 Reverse transcription PCR.....	72
2.2.5 Quantitative real time PCR.....	76
2.2.6 Cytotoxicity assays.....	78
2.2.6.1 MTS assay.....	78
2.2.6.2 MTT assay.....	81
2.2.7 qRT-PCR on treated HepG2 cells.....	82

2.2.7.1 Preparation of 2.5 $\mu$ M and 5 $\mu$ M <i>tert</i> -butyl hydroperoxide solution.....	82
<b>Chapter 3: <u>Results</u>.....</b>	<b>84</b>
3.1 Identification of the exponential growth phase of each cell line.....	84
3.2 RNA extraction from the cancer cell lines.....	86
3.3 Specificity of the PCR primers.....	89
3.4 Quantification of gene expression by qRT-PCR.....	91
3.5 Determination the cell growth inhibitory effect of genotoxic agents using the MTS assay.....	97
3.6 Determination the cell growth inhibitory effect of genotoxic agents using the MTT assay.....	100
3.7 Estimation of the effect of <i>tert</i> -butyl hydroperoxide on HepG2 cells on target gene expression by qRT-PCR.....	101
<b>Chapter 4: <u>Discussion</u>.....</b>	<b>103</b>
4.1 The significant role of NEIL3.....	103
4.2 The effect of oxidative stress on steroid sensitive and steroid resistant acute lymphoblastic leukaemia.....	105
4.3 The effect of oxidative stress on hepatoblastoma cells.....	106
4.4 The effect of cisplatin on steroid sensitive, steroid resistant acute lymphoblastic leukaemia and hepatoblastoma cells.....	107
4.5 The effect of doxorubicin on steroid sensitive, steroid resistant acute lymphoblastic leukaemia and hepatoblastoma cells.....	107
<b>Conclusion.....</b>	<b>108</b>
<b>Future perspectives.....</b>	<b>108</b>
<b>References.....</b>	<b>109</b>
<b>Chapter 5: <u>Appendix</u>.....</b>	<b>135</b>

## List of Abbreviations

5-OH-C	5-hydroxycytosine
5-OH-U	5-hydroxyuracil
8-oxoG	8-oxo-7,8-dihydroguanine
A	Adenine
ALL	Acute lymphoblastic leukaemia
ALT	Alternative lengthening of telomeres
APC	Adenomatous polyposis coli
AP site	Apurinic/Apyrimidinic site
APE	AP-endonuclease
Bcl-2	B-cell lymphoma 2
BER	Base excision repair
B-ME	2-mercaptoethanol
bp	Base pair
C	Cytosine
cALL	common ALL
cDNA	Complementary DNA
CEM-1-15	Human acute lymphoblastic leukaemia steroid resistant cell line
CEM-7-14	Human acute lymphoblastic leukaemia steroid sensitive cell line
Cg	cytosine glycol
CML	Chronic myeloid leukaemia
CNS	Central nervous system
CSR	Class switch recombination
Ct	Threshold cycle.
DEX	Dexamethasone
DHFR	Dihydrofolate reductase
DMEM	Dulbecco's Modified Eagle's Medium

DMSO	Dimethyl sulphoxide
DNA	Deoxyribonucleic acid
dNTP	Deoxyribonucleoside triphosphates
DOX	Doxorubicin
DSB	Double-strand break
dsDNA	double-stranded DNA
EDTA	Ethylene diamine tetra acetic acid
ETC	Electron transport chain
FapyA	4,6-diamino-5-formamidopyrimidine
FapyG	2,6-diamino-4-hydroxy-5-formamidopyrimidine
FBS	Foetal bovine serum
Fpg	Formamidopyrimidine DNA glycosylase
G	Guanine
G4	Guanine quadruplex
Gapdh	Glyceraldehyde-3-phosphate dehydrogenase
GCs	Glucocorticoids
Gh	Guanidinohydantoin
GPXs	Glutathione peroxidases
GR	Glucocorticoid receptor
GSH	Glutathione
GSSG	Glutathione disulphide
GST P1	Glutathione S-transferase P1
H <sub>2</sub> O <sub>2</sub>	Hydrogen peroxide
H2TH	Helix 2 turn Helix
HB	Hepatoblastoma
HepG2	Human hepatoblastoma cell line
HIV-1	Human immunodeficiency virus type 1
hNEIL3	Human NEIL3
HOS	Human osteogenic osteosarcoma cell line

hTERC	Human telomerase RNA component
hTERT	Human telomerase reverse transcriptase
lncRNAs	Long non-coding RNAs
MB	Medulloblastoma
MLL	Mixed-lineage leukaemia
MMR	Mismatch repair
Mmu NEIL3	<i>Mus musculus</i> NEIL3
nDNA	Nuclear DNA
NEIL	nei-like
NER	Nucleotide excision repair
NLS	Nuclear localization signal
Nth1	Endonuclease III homologue
O <sub>2</sub> <sup>-</sup>	Superoxide anion
OGG1	8-oxoguanine DNA glycosylase
OH·	Hydroxyl free radical
OS	Osteosarcoma
PBS	Phosphate buffered saline
PCNA	Proliferating cell nuclear antigen
PCR	Polymerase chain reaction
Ph chromosome	Philadelphia chromosome
PMS	Phenazine methosulfate
Pol β	DNA polymerase β
POT1	Protection of telomere protein 1
PRED	Prednisolone
Pro2	Proline amino acid at position 2
PRXs	Peroxiredoxins
qRT-PCR	Quantitative real-time PCR
RAR	Replication-associated repair
RE1	Repressor element 1



RNA	Ribonucleic acid
ROS	Reactive oxygen species
rRNA	ribosomal RNA
Saos-2	Human osteosarcoma methotrexate resistant cell line
SHH	Sonic Hedgehog pathway
SHM	Somatic hyper mutation
shRNA	Short hairpin RNAs
siRNA	small interference RNA
SOD	Superoxide dismutase
Sp	Spiroiminodihydantoin
ssDNA	Single-stranded DNA
T	Thymine
TBE	Tris/Borate/EDTA
<i>t</i> -BHP	<i>Tert</i> -butyl hydroperoxide
TC-32	Human medulloblastoma cell line
TE	Tris/EDTA
Tg	Thymine glycol
TRF	Terminal restriction fragments
TRF1	Telomere repeat factor 1
TRF2	Telomere repeat factor 2
tRNA	transfer RNA
U	Uracil
UDG	Uracil DNA glycosylase
Ug	Uracil glycol
UV	Ultraviolet
Val2	Valine amino acid at position 2
WNT	Wingless pathway
XP	Xeroderma pigmentosum

## Abstract

NEIL3 is the largest of three homologs of the bacterial Nei protein in mammalian cells. It has been shown to have DNA glycosylase activity *in vitro*, excising oxidised purine and pyrimidine bases from both single- and double-stranded DNA. Additionally, NEIL3 has recently been shown to release oxidised bases from telomeric regions of DNA. While NEIL3 shows a restricted expression pattern in normal human cells, previous studies have shown that NEIL3 is highly expressed in various cancer cell lines when compared with normal counterparts. Furthermore, high expression levels of NEIL3 were associated with development of metastases in patients with primary malignant melanoma. However, no one has looked at the expression of NEIL3 in paediatric cancer cells, or attempted to correlate the expression of NEIL3 with proteins involved in telomere length maintenance. Therefore, the aim of this project was to determine the gene expression levels of NEIL3 in paediatric cancer cell lines and to determine any association between the levels of NEIL3 expression and the presence or absence of telomerase in these cells. Gene expression of NEIL3, hTERT and POT1 was measured by qRT-PCR in two cell lines of acute lymphoblastic leukaemia (ALL; steroid sensitive and steroid resistant cells), osteosarcoma, hepatoblastoma and medulloblastoma tumours. An initial assessment of whether the levels of NEIL3 expression are indicative of the response of paediatric tumours to sensitivity to DNA damaging agents was also carried out using the hepatoblastoma and the ALL cells. The results confirmed that NEIL3 was highly expressed in all cell lines tested and that the relative levels of NEIL3 and telomerase mRNA was significantly higher in steroid resistant ALL cells than in the steroid sensitive ALL cells. However, there was no correlation between the expression of NEIL3 and the presence or absence of telomerase. ALL and hepatoblastoma cells were sensitive to cisplatin, doxorubicin and *tert*-butyl hydroperoxide (*t*-BHP), as a decrease in cell growth was observed at each concentration of the compounds tested. Results also indicate that following treatment with *t*-BHP, growth of the steroid sensitive ALL cells was significantly more inhibited than that of the resistant ALL cell line. Therefore, NEIL3 could be a resistance factor to cancer chemotherapy in paediatric cancer cells and may be a novel target for the treatment of paediatric cancers.

## **Declaration**

No part of this thesis has been submitted in support of an application for another degree or qualification of the University of Salford or any other university or other institute of learning.

## **Acknowledgments**

First of all I would like to express my great thanks to Allah for giving me the chance to improve my knowledge.

I gratefully acknowledge my supervisor Dr Rhoderick H. Elder for his kind support, encouragement and guidance. In particular, I would like to thank him for giving me the opportunity to work on this project.

For the valuable assistance, I am grateful to Professor Marija Krstic-Demonacos. Moreover, many thanks to Dr Patricia A. Ragazzon for her steady and great support.

Thanks to all my colleagues who I worked with at the University of Salford for support, motivation, inspiration and help. I would specially like to thank Michelle Hussain, Walid Almusrati, Ashraf Elgallali and Mustafa Albelazi.

A special thanks to my father Dr Ahmed Duweb, my mother Mrs Maghbula Mshawet, my wonderful sister Eshraq Duweb and my two brothers Mohamed Duweb and Moad Duweb who have supported me throughout these studies.

I would like to thank my lovely daughters Elyan Almusrati and Aren Almusrati for bearing with me during my study.

# Chapter 1: Introduction

## 1.1 Cancer

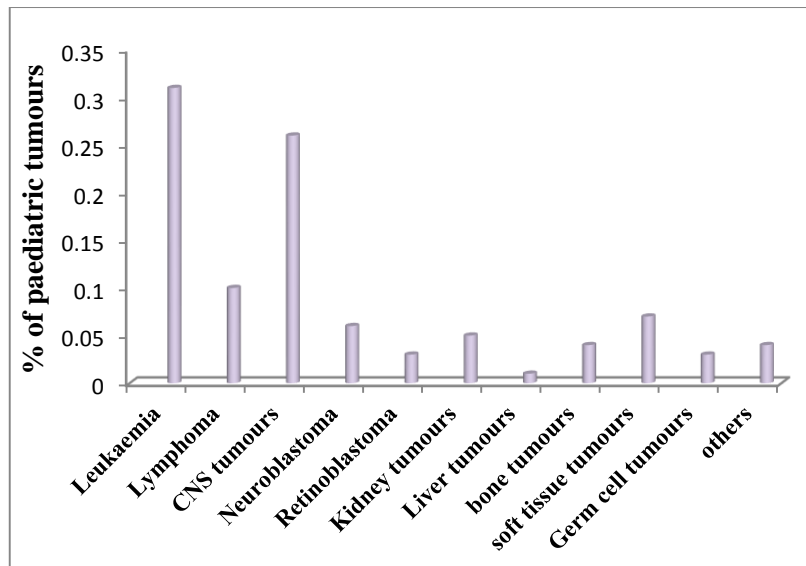
Cancer is a disease where cells begin to multiply rapidly and uncontrollably. All eukaryotic cells have a control centre, the nucleus where the chromosomes, which are composed of the genetic material, DNA, are located. Healthy cells control their growth through the complex interaction of the products of positive (proto-oncogenes) and negative (tumour suppressor genes) growth signals and any significant changes affecting the function of these signals allows the cells to continue growing and form a mass of malignant cells; these changes are called mutations. A multifactorial causation is behind the pathogenesis of these mutations. It is thought that a combination of genetic and environmental factors is responsible for the aetiology of cancer (Cancer Research UK, 2014).

Despite the breakthrough in the management of many cancers, the mortality rate is still high and some types of cancers exhibit resistance (either intrinsic or acquired) to chemotherapy. Thus, there remains an urgent quest for novel treatments and new therapeutic targets, especially for paediatric cancers where there is a high incidence of subsequent malignant neoplasms (Chen *et al*, 2014; Armenian *et al*, 2015).

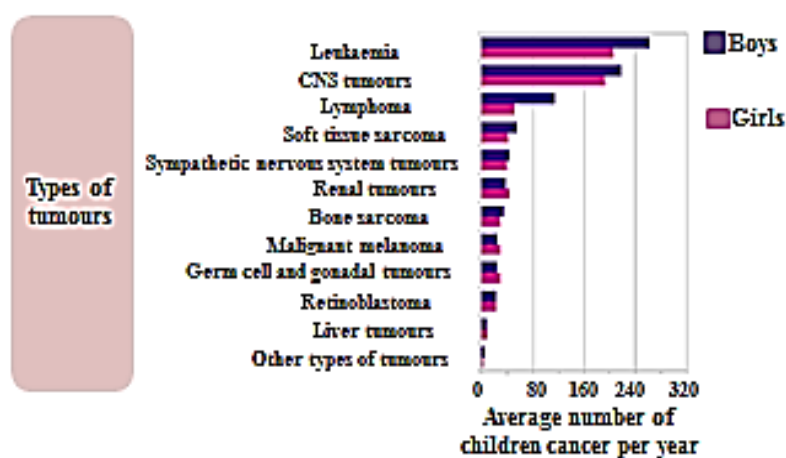
### 1.1.1 Childhood cancer

Leukaemia together with lymphoma, is the most frequent occurring cancer in children, while brain and spinal cord tumours are the commonest solid tumours in this age group (Figure 1.1). According to the latest estimated figures, which were collated by Cancer Research UK, between 2009-2011, an average of 1,574 children annually in the UK was diagnosed with cancer. While, about 252 children per year died from cancer in 2009-2011 in the UK. However, the 5- year survival rate in the UK was around 82% in 2006-2010 (Figure 1.2) (Cancer Research UK, 2014).

Integration of the molecular data together with the clinical features plays a significant role in identifying the exact classification of tumours and prediction of the prognostic factors in children who are suffering from neoplasms (López-Terrada, 2006).



**Figure 1.1:** Percentage of different types of childhood cancer below 14 years of age in the UK between 2001 and 2010. The vast majority of cases presented were leukaemias followed by CNS tumours (Adapted from Cancer Research UK, 2014).



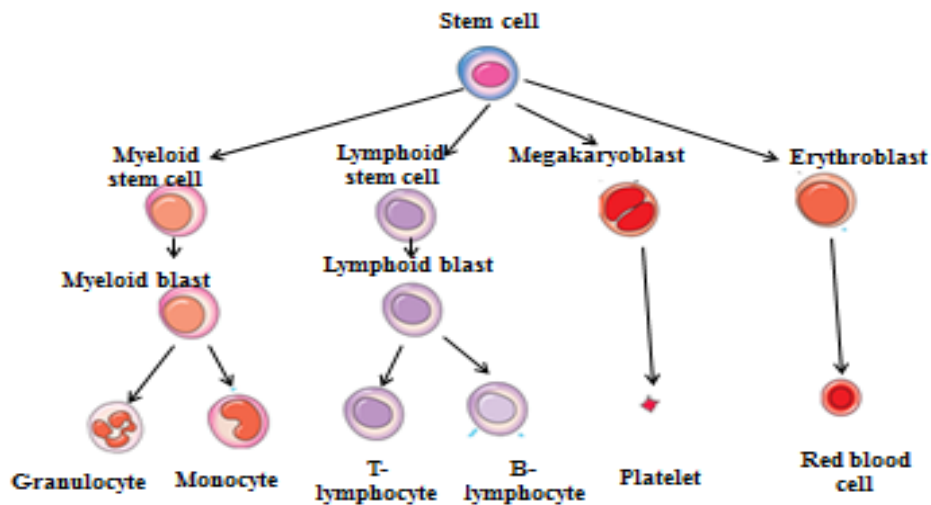
**Figure 1.2:** Average cases of paediatric tumour annually in UK among males and females, 2006-2008. Leukaemia presented the highest figures in both genders between 2006 and 2008 (Adapted from Cancer Research UK, 2014).

### 1.1.2 Leukaemia

The most predominant tumour among the paediatric age group is presented by leukaemia, accounting for approximately one third of all childhood malignancy. With the advances in the treatment protocol, about 80% of children cases can be cured

(Hagag and Nosair, 2015). However, it is predicted that the survival rate in patients with leukaemia should continue to increase, owing to a better understanding of the biology of the disease leading to more novel and cancer specific molecular targets being identified (Pui *et al*, 2012).

Leukaemia arises in the bone marrow from progenitor white blood cells (lymphoid blast cells or myeloid blast cells). The blast cells increase in number and then invade the blood stream. Thus, the function of the healthy cells is affected. Leukaemia is classified by oncologists into two main types: lymphoblastic leukaemia and myeloid leukaemia. This classification depends on which kind of hematopoietic cell is affected; whether from the lymphoid or myeloid lineage (Figure 1.3). Furthermore, each type is subdivided into acute or chronic leukaemia. In acute leukaemia, the cells divide rapidly in a short time, whereas in chronic leukaemia, the leukaemic cells divide more slowly over a longer period (Faderl *et al*, 2003; Shah and Kumar, 2013).



**Figure 1.3:** Differentiation of the hematopoietic cells from stem cells. A lymphoid stem cell differentiates into a lymphoid blast, which further differentiates to T-lymphocyte and B-lymphocyte (Adapted from Cancer Research UK, 2014).

### 1.1.2.1 Acute lymphoblastic leukaemia

Acute lymphoblastic leukaemia (ALL) is a tumour of lymphoid stem cells, usually affecting children between 2 to 5 years of age (Pui *et al*, 2008). Based on the type of clonal cell differentiation, it is divided into T-cell ALL and B-cell ALL. However, B

lymphocyte ALL accounts about 85% of childhood ALL (Garza-Veloz *et al*, 2015). ALL patients commonly present with symptoms such as fever, generalized weakness, joint pain and bleeding (Onciu, 2009). About 80% of leukaemic children are diagnosed with ALL (Bekker-Méndez *et al*, 2014) and it accounts for approximately 30% of the total paediatric cancers (Samuels *et al*, 2014).

High white blood cells number, metastasis through the central nervous system at the diagnosis, enlarged liver and spleen, alterations in the chromosomes, absence of the expression of CD10, failure to induce the remission after starting the therapy, the presence of lymphoid and myeloid antigens and infant age groups; all are bad prognostic factors in ALL (Pui and Evans, 1999).

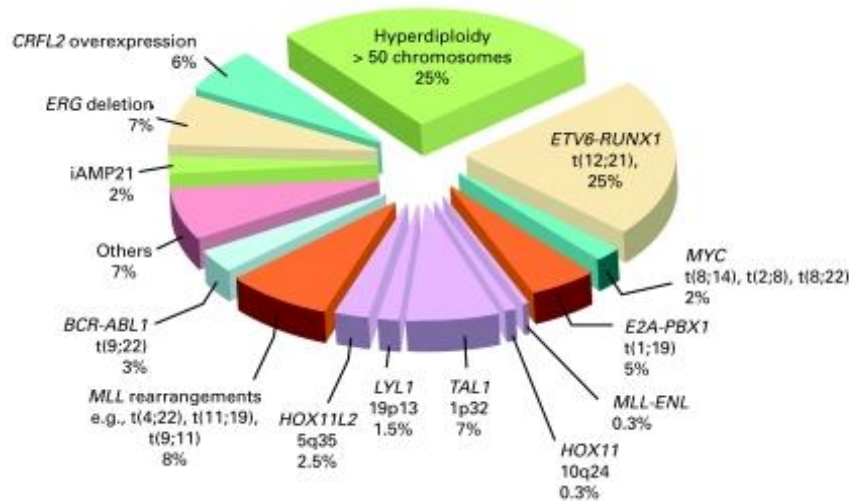
It has been estimated that the 5 year survival rates in leukaemic children is around 80%. To push the survival rate further, it is essential to understand the pathogenesis of leukaemia and therefore to analyse the molecular basis of ALL (including chromosomal abnormalities and the pattern of gene expression) (Pui *et al*, 2011).

The aetiology of ALL is related to environmental, socioeconomic, infectious and hereditary factors. However, Epstein Barr virus and human immunodeficiency virus are linked to the development of mature B-cell ALL. In comparison with the general population, children with Down syndrome (trisomy 21) have an increased risk of developing ALL by 20 times. Furthermore, ALL is associated with other genetic disorders *e.g.* Klinefelter syndrome, Fanconi anemia and ataxia telangiectasia. ALL in the second twin of both dizygotic and monozygotic twins occurs at a higher percentage than would be expected in the general population (Faderl *et al*, 2003).

#### **1.1.2.1 (i) The molecular genetic aspects of acute lymphoblastic leukaemia**

Over 75% of ALL cases have genotype mutations, which are identified via standard genome analysis (Pui *et al*, 2008). However, with the advantage of high-resolution genome-wide techniques, many new oncogenic abnormalities have been recognized (Pui *et al*, 2011). All leukaemic children can be categorised into subgroups with regard to the patterns of specific gene expression (Figure 1.4). In addition, cooperative oncogenic lesions are required in the pathogenesis of ALL and they were considered to have a role in drug responsiveness. Mullighan *et al* (2007) identified that deletion,

amplification, point mutation and structural rearrangement (which affects the genes regulating B lymphocyte differentiation) were implicated in the development of 40% of B-progenitor ALL cells.



**Figure 1.4:** The estimated percentage of genetic abnormalities in acute lymphoblastic leukaemia. Hyperdiploidy of more than 50 chromosomes and ETV6-RUNX1 t(12;21) account for the commonest cytogenetic aberrations in ALL patients (Pui *et al*, 2011).

According to the immunophenotypic features and cytogenetic-molecular markers, ALL has been classified into subtypes, which correlate with the prognosis (Faderl *et al*, 2003). In terms of immunophenotyping, ALL is divided into precursor-B cells (includes pre-pre-B ALL (pro-B ALL), common ALL (cALL), pre-B ALL), mature-B-cells and T-lineage ALL. However, the most presenting subtype among leukaemic children is cALL which is detected in 50% of Philadelphia positive ALL (Ph-positive ALL) and it carries with it a dismal prognosis (Faderl *et al*, 2003).

Based on the analysis of cytogenetic-molecular abnormalities, ALL can be caused by chromosomal translocations, chromosomal hyperploidy and alteration in the expression of transcription factors (Pui *et al*, 2004). Approximately 3% of ALL paediatrics possess Philadelphia (Ph) chromosome in which the ABL1 oncogene on chromosome 9 is reciprocally translocated to a breakpoint cluster region (BCR) on chromosome 22 t(9;22) (q34;q11) (Faderl *et al*, 1999). The Ph chromosome was the first cytogenetic aberration identified that linked to ALL and chronic myeloid leukaemia



(CML). The isoform p210<sup>BCR-ABL</sup> is related to CML, while the isoform p190<sup>BCR-ABL</sup> presents in Ph-positive ALL. BCR-ABL1 generates an activated tyrosine kinase, and ALL patients with BCR-ABL1 rearrangement have more blast cells than Ph-negative ALL at diagnosis (Prete *et al*, 1994).

Interestingly, the prognosis for BCR-ABL1-positive ALL patients is worse than for CML, suggesting that an additional factor is implicated in the progression of ALL (Mullighan *et al*, 2008). Mullighan *et al* (2008) identified a deletion on 7p12 of IKZF1 (it was deleted in 83.7% of ph<sup>+</sup> ALL but not in CML), which is responsible for coding the lymphoid transcription factor IKAROS, and appears to have a role in making the outcome of the Ph-positive ALL poor compared with CML (Iacobucci *et al*, 2009). Then Mullighan *et al* (2009) established that about 10% of BCR-ABL1-negative ALL have mutations in Janus kinases (JAK1, JAK2 and JAK3), and furthermore these mutations were combined with deletion of IKZF1. The authors suggested a great effort should be made to identify a therapeutic agent that targets JAK mutated ALL. Furthermore, Garza-Veloz *et al* (2015) recognized that overexpression of FLT3 and DEFA1 genes in B-ALL are poor prognostic factors, and they are associated with high mortality rate.

On the other hand, T-cell ALL is branched into numerous subsets according to genes alterations namely: HOX11L2, LYL1 plus LMO2, TAL1 plus LMO1 or LMO2, HOX11, and MLL-ENL. It was recognized that HOX11L2 is linked to an unfavorable prognosis, while HOX11 is associated with a better survival rate (Meijerink *et al*, 2009). Additionally, the presence of rearrangement of the mixed-lineage leukaemia (MLL) gene at chromosomal band 11q23 in T-ALL cell lines is correlated with poor prognosis. A histone methyltransferase is encoded by the MLL gene, which has a vital role in development of ALL via regulating the expression of HOX genes. The MLL locus can be affected by translocations, deletions, inversions, gene amplifications and internal duplications. Translocation abnormalities include t(4;11) (q21;q23), t(11;19) (q23;p13) and t(9;11) (p22;q23), however the former is the most common (Hilden *et al*, 2006; Beesley *et al*, 2010).

In spite of the high cure rate in children with ALL is high, some subgroups with chromosomal abnormalities need a combination of cytotoxic therapeutics and radiotherapy. However, allogeneic bone marrow transplant is required for the resistant

cases (Stanulla and Schrappe, 2009). The duration of the therapy in ALL after the induction phase can last up to 3 years (Samuels *et al*, 2014).

#### **1.1.2.1 (ii) The effect of glucocorticoids on acute lymphoblastic leukaemia**

In addition to the previously mentioned treatment for ALL, glucocorticoidal steroids (GCs) have been used by physicians as main antileukaemic regimen owing to their ability to induce apoptosis (programmed cell death) in lymphoid tumours. Nevertheless, in some occasions GCs cannot promote their apoptotic action on leukaemic cells when glucocorticoids face a cellular resistance. Dexamethasone (DEX) and prednisolone (PRED) are the most commonly used synthetic glucocorticoids in the treatment of ALL (Kaspers *et al*, 1994). Bindreither *et al* (2014) studied the mechanism of both steroids in ALL and the authors concluded that DEX and PRED regulate the same genes in childhood ALL and the disparity in the treatment efficacy of DEX and PRED was related to the difference in the pharmacokinetics and the pharmacodynamics of these agents.

GCs belong to steroid hormones, which exert their biological action via binding with the glucocorticoid receptor (GR). NR3C1 gene is responsible for encoding GR and the gene is located on chromosome 5 (5q31) (Bindreither *et al*, 2014). There are two GR-protein isoforms namely GR- $\alpha$  and GR- $\beta$ . GR- $\alpha$  is strongly linked to steroid sensitivity while GR- $\beta$  is linked to steroid insensitivity (Shah and Kumar, 2013).

Mutations in the transcription factor that regulates NR3C1 expression could explain the mechanism of the emergent resistance in ALL (Ploner *et al*, 2005). Glucocorticoid insensitivity occurs as one of two types: primary GCs resistance (present in about 10%-30% of leukaemic patients and this type of patients do not respond to the anti-lymphotic effect of GCs) or secondary GCs resistance (patients with this type of resistance, initially show response to the growth-inhibiting effect of GCs then after time GCs fail to induce blast cell arrest) (Kaspers *et al*, 1994).

Several studies have been carried out on lymphoid cells, aimed at identifying the genes that are responsible for regulation the intracellular function of steroids. However, experiments have been conducted on two subclones of lymphoblastic cell lines termed

CEM-7-14 (prototypical GR sensitive) and CEM-1-15 (prototypical GR resistant) which were obtained from a child with T-ALL cells, treated with DEX (Medh *et al*, 2003).

Schmidt *et al* (2006) reported that, FKBP5/FKBP51 and DDIT4/Dig-2 are upregulated in CEM-1-15 after induction the DEX. While, Beach *et al* (2011) identified E4BP4 is overexpressed in CEM-7-14 following initiating the treatment with DEX but not in CEM-1-15. Additionally the authors explained the mechanism of how E4BP4 displays DEX-evoked apoptosis in ALL and stated that the function is carried out through Bim upregulation. Moreover, Beesley *et al* (2010) reported that RNAi knockdown of MLL mRNA in T-ALL led the lymphoid cells to develop resistance to DEX and gamma radiation.

### **1.1.3 Central nervous system tumours**

Central nervous system (CNS) tumours are neoplasms of glial tissue involving the brain and the spinal cord, they are the second most common paediatric oncological diseases, presenting in more than a quarter of childhood cancers (Kheirollahi *et al*, 2015).

Globally around 200,000 people are affected each year by brain cancer. According to the clinical behaviour, brain tumours can be benign or malignant. Additionally, CNS tumours are classified into primary tumours (those originate in the brain) and secondary tumours (those begin in other organs then metastasize to the central nerve system) (Kheirollahi *et al*, 2015).

Primary brain cancer is less common than secondary cancer; usually the sources of the secondary brain tumours are breast tumour, cancer of colon, lung tumour, kidney tumour or melanoma. The presentation of brain tumours may include headaches, vomiting, convulsion, and difficulty in speech, abnormal gait, sensory deficit, hearing and vision problems (Barrow Neurological Institute, 2013).

Depending on which cells are being affected, brain tumours are subdivided into astrocytoma (tumours arise from astrocytes); these neoplasms present around 43% of brain tumours and the majority of them are benign. Embryonal tumours account the second most common CNS tumours, about 73% of this subgroup is accounted for medulloblastomas and the remaining CNS tumours are presented by ependymoma (Cancer Research UK, 2014).

### **1.1.3.1 Medulloblastoma**

Medulloblastoma (MB) was identified in 1925 by Harvey Cushing and his associate Percival Bailey (Li *et al*, 2013). Eighty percent of MB patients are diagnosed at the age of 15. MB follows the primitive neuroectodermal tumours (PNETs) and it is the most presenting nervous system malignancy in the paediatric age group. The primary originates in the cerebellar vermis and 10% of childhood neoplasm mortality is caused by these tumour cells. These poorly differentiated embryonal neuroepithelial tumours arise from the infratentorial site in the posterior fossa. (Santhana Kumar *et al*, 2015). These malignant cells are highly aggressive owing to their ability to spread through the leptomeningeal space and 30% of cases do not respond to treatment (Wang *et al*, 2014).

Although many patients with medulloblastoma have improved following treatments, which include surgery, chemotherapy and radiation, those who received radiotherapy suffer from the side effects of radiation such as secondary neoplasms and neurocognitive impairments (Jakacki *et al*, 2005; Mulhern *et al*, 2005). Thus, to lower the neurotoxicity caused by radiation, the planned management is to start with a prolonged course of chemotherapy, as the cytotoxic agents are effective in controlling the proliferation of the malignant cells in MB and to omit the radiotherapy except for relapsed patients (Duffner *et al*, 1993).

According to the histopathological features, MB is classified into five subgroups: classic medulloblastoma, nodular (desmoplastic), medulloblastoma with extensive nodularity, anaplastic and large cell medulloblastoma (Taylor *et al*, 2012).

#### **1.1.3.1 (i) The molecular genetic aspects of medulloblastoma**

Owing to advances in genome wide expression profiles, many genetic alterations are being discovered in medulloblastoma. However, mutations affecting the molecular pathways which control the proliferation of neural progenitor cells termed Wingless (WNT) and Sonic Hedgehog (SHH) pathways are the cornerstone in the oncogenesis of MB and numerous genes are linked to these pathways (Thompson *et al*, 2006).

The most common molecular abnormalities related to MB are the loss the short arm of chromosome 17 and the loss the long arm of chromosome 9 (Koch *et al*, 2001). About

10% of medulloblastomas are associated with mutations of the PTCH gene, which is located on chromosome 9q22.3. The encoded proteins of PTCH gene are believed to be receptors in the SHH pathway (Dong *et al*, 2000).

It was noticed that mutations in the adenomatous polyposis coli (APC) gene are associated with MB. However, many components in the WNT/SHH pathway are encoded via APC gene. Furthermore, APC protein has an important role in the regulation of  $\beta$ -catenine level in which it activates the degradation of cytoplasmic  $\beta$ -catenine, thereby leading to cellular growth inhibition. Additionally, mutations in CTNNB1 (which is a part of  $\beta$ -catenine) and deletion of AXIN1 were detected in around 20% of MB and they were linked to inappropriate activation of the WNT signal transduction pathway. Thus, AXIN1 acts as a tumour repressor gene in MB. It was found that AXIN1 mutations were linked to desmoplastic and classic types of MB (Dahmen *et al*, 2001).

Su *et al* (2006) identified that MB is often associated with overexpression of both the repressor of neuronal differentiation/neuron-restrictive silencer factor (REST/NRSF) and the MYC gene. The MYC family is composed of MYCn and c-MYC. These transcription factors have important functions, including regulation the cell proliferation, apoptosis and stem cell differentiation via encoding a nuclear phosphoprotein. Moreover, MYC proteins create heterodimers with Max, both of them contain Helix-loop-helix and leucine zipper protein. MYC/Max heterodimers bind to particular sequences on the DNA of target genes and regulate the transcription of these genes through inhibition or induction processes. However, high levels of MYC mRNA in MB are correlated with poor outcome (Grotzer *et al*, 2001; Swartling *et al*, 2012). Eberhart *et al* (2002) concluded that chromosomal losses are more frequent in anaplastic MB compared with other histological subtypes and that is a link between MYC gene amplification and loss of chromosome 17p. In addition, Kenney *et al* (2003) identified that MYCn is implicated in dysregulation of the SHH pathway and MB development. Nevertheless, c-MYC alone is not sufficient to generate MB.

REST/NRSF is a transcription repressor factor that controls the function of many neuronal genes through binding with a conserved 23 bp motif, namely repressor element (RE1). High levels of REST mRNA in neuronal cells suppress the transcription of

numerous neuronal differentiation genes and arrest these cells at a step before complete differentiation, which leads to MB neoplasm formation (Fuller *et al*, 2005).

Lawinger *et al* (2000) carried out transient transfection experiments and the authors designed a recombinant transcription factor (REST-VP16) by substituting the repressor domains of REST with the activation domain of the *adenovirus* (VP16) protein. The expression of REST-VP16 in MB cells was able to oppose the repression effects of endogenous REST on neuronal promoters, activate the cell death pathways. In addition, the authors confirmed that injection of REST-VP16 in medulloblastoma cells, which were grown in nude mice leads to inhibition of their growth. Thus, REST could be a novel target gene for MB therapy.

#### **1.1.4 Bone tumours**

The majority of childhood bone tumours are benign tumours. However, these benign cells are often asymptomatic and diagnosed accidentally during trauma or through evaluation the child for another presenting illness. Benign bone tumours are sub-classified into non-ossifying fibroma (mainly affects the metaphysis), desmoid fibroma (occurs commonly in the posterior medial condyle of the femur), osteochondroma (it has a unique sign on an X-ray which is obvious by the continuity of the cortex with the normal bone) fibrous dysplasia and chondroma (Vanel *et al*, 2009).

Malignant bone tumours are divided into osteosarcoma, Ewing sarcoma, chondrosarcoma and spindle cell sarcoma. The most common presenting symptoms in bone neoplasms are bone pain, which becomes severe during the night and swelling. (He *et al*, 2014).

##### **1.1.4.1 Osteosarcoma**

Osteosarcoma (OS) is the most frequent malignant tumour of bone that arises from primitive bone forming cells, termed mesenchymal cells, which produce osteoid and immature bone. Twenty percent of bone paediatric bone neoplasms are caused by these malignant osteoblast cells, affecting mainly teenagers. Therefore, OS is linked to the

growth spurt, the metaphysis growth plates of the long bones such as the distal femur, proximal tibia, and proximal humerus are the target sites (Richardson, 2014).

According to the histological features, OS is divided into chondroblastic OS and fibroblastic OS (He *et al*, 2014). Despite adjuvant chemotherapy, radiotherapy and surgery, osteogenic sarcoma still carries a poor prognosis due to their early metastasis (Bai *et al*, 2015). Most of OS tumours metastasize to the lung. More than 30% of OS patients suffer from pulmonary metastasis during the five years from the diagnosis. Therefore, more attention needs to be paid to understand the pathophysiology and the molecular pathways of lung metastasis in OS (Khanna *et al*, 2001).

#### **1.1.4.1 (i) The molecular genetic aspects of osteosarcoma**

It has been recognized that OS is associated with a high rate of drug resistance. Studies conducted to explain the mechanism of OS-induced drug resistance identified that high level of Bcl-2 mRNA (B-cell lymphoma 2) is correlated with developing tumour resistance to chemotherapeutics (Ye *et al*, 1998). Bcl-2 is an oncogenic protein as it has an anti-apoptotic role (Reed, 1997). Ferrari *et al* (2004) reported that OS cells, which exhibit high levels of Bcl-2 are high grade tumour cells and tend to induce early pulmonary metastasis. Similarly, Zhao *et al* (2009) confirmed that knockdown of Bcl-2 leads to an increased the effect of doxorubicin on OS. Therefore, the authors suggested that Bcl-2 could be used as a target in the treatment of OS.

Germ line mutations in retinoblastoma and p53 genes have been established to be related to increase the incidence of OS in the tumour suppressor genes (He *et al*, 2014). Moreover, Wong *et al* (2007) confirmed that OS cells, which express high levels of mutated p53 and p53-R273H are at a high risk of developing drug resistance.

Hattinger *et al* (2003) examined the Saos-2 cell line (human OS cell line; which is methotrexate resistant) to identify the chromosomal abnormalities related to the development of chemotherapy resistance in OS. The authors stated that gain of 8q22-qter and MYC (8q24.12-q24.13) along with low expression level of RFC (reduced folate carrier that allows the methotrexate to enter the cell through the cell membrane) gene is correlated with Saos-2 resistant cells. Therefore, RFC could be used to predict the chemosensitivity to methotrexate in OS (Ifergan *et al*, 2003). Notably, four altered

RFC proteins known as Leu291Pro, Ser46Asn, Ser4Pro and Gly259Trp are implicated in methotrexate OS resistance (Flintoff *et al*, 2004). Guo *et al* (1999) noticed that high levels of DHFR (dihydrofolate reductase) mRNA are linked to pulmonary metastasis in OS.

Upregulation of glutathione S-transferase P1 (GST P1) is associated with poor outcome in OS patients (Uozaki *et al*, 1997) GST P1 is a phase II detoxification enzyme that belongs to cytosolic GSTs, which have a major role in deactivation of many antitumour compounds (Uozaki *et al*, 1997). Moreover, Huang *et al* (2007) conducted RNAi knockdown of GST P1 on HOS cell lines (human osteogenic OS cell lines) and these cells were exposed to either cisplatin or doxorubicin. The authors concluded that suppression of GST P1 enhances the effect of these chemotherapeutic agents on OS cells, induces severe DNA damage and apoptotic cell death. In another study, Zhang *et al* (2012) found that OS patients with GST P1 Val/Val genotype have a shorter survival rate than those with GST P1 Ile/Ile genotype. Therefore, the authors suggested that polymorphisms of GST P1 gene could have a predictive value to identify the prognostic criteria in OS patients who received antineoplastic drugs.

To tackle GST P1-induced resistance in OS, an *in vitro* experiment evaluated the influences of NBDHEX [6-(7-nitro-2,1,3-benzoxadiazol-4-ylthio)hexanol], which acts as an GST P1 inhibitor, on the Saos-2 cell line. This study confirmed that NBDHEX could be applied to OS patients who show high level of GST P1 together with the chemotherapeutic drugs (Pasello *et al*, 2008).

A study carried out by Wang *et al* (2004) reported that overexpression of AP-endonuclease 1 (APE1) was associated with high mortality rate in OS individuals. In addition, the authors silenced APE1 in OS cell lines via siRNA and that led to increased sensitivity of OS cells to  $\gamma$ -radiation, oxidizing and alkylating DNA damaging agents. A further study revealed that a low level of ERCC4 mRNA (which is involved in nucleotide excision repair) in OS is linked to a high rate of chemotherapeutic resistance (Nathrath *et al*, 2001).



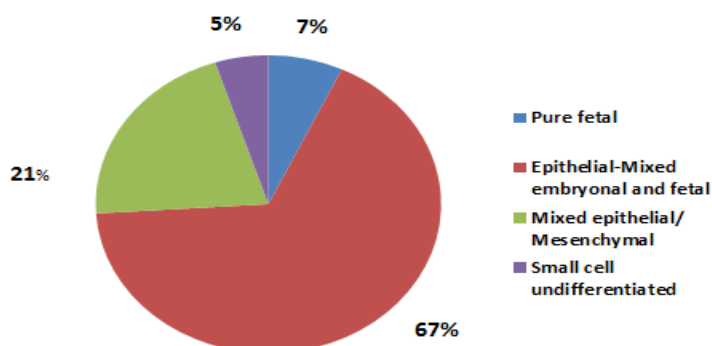
### **1.1.5 Hepatic tumours**

Slightly more than 1% of childhood tumours are hepatic tumours. Unfortunately, the vast majority of these neoplasms are malignant (about 60%), while the remaining 40% are benign. Patients usually complain of abdominal distension, malaise, abdominal discomfort and constipation. According to their histopathological character, malignant liver tumours are divided into hepatoblastoma, hepatocellular carcinoma, sarcoma, germ cell tumours and rhabdoid tumours. On the other hand, benign liver tumours include vascular tumours, hamartomas, adenomas, and focal nodular hyperplasia (Litten and Tomlinson, 2008).

#### **1.1.5.1 Hepatoblastoma**

Hepatoblastoma (HB) arises from hepatic primordium embryonic cells and was firstly recognized by Walter in 1896; at that time, it was termed paediatric hepatocellular carcinoma (Heywood *et al*, 2002). HB is the most common presenting tumour among children with liver neoplasms and is more frequent in boys than girls. Furthermore, HB follows an aggressive course with early metastasis through the lymphatic and blood vessels (Perilongo *et al*, 2012). The initial 3 years of life is the average age of presentation and in the last 30 years, the incidence of HB has increased significantly (Czauderna *et al*, 2014).

It has been suggested that the HB cells start to develop during the antenatal period as these stem liver malignant cells commonly occur in preterm neonates rather than in term neonates. The right hepatic lobe is the frequent affected part in the liver. In addition, HB has four main types, (each type has different cells) epithelial, mixed, small cell undifferentiated (has the worst prognosis), pure foetal (has the best prognosis) (Figure 1.5) (Litten *et al*, 2008).



**Figure1.5:** Percentage of the histological types of hepatoblastoma. Epithelial-Mixed embryonal and foetal type accounts the largest numbers (Adapted from Litten *et al*, 2008).

#### **1.1.5.1 (i) The molecular genetic aspects of hepatoblastoma**

Healthy cells possess a balance between the level of ROS and endogenous antioxidants enzymes, during liver damage; ROS activate hepatic stellate cells (which are responsible for synthesis of the extracellular matrix that is important for cellular growth and differentiation). However, chronic activation of hepatic stellate cells has been linked with enhancement of division of liver cells and the development of hepatic tumours. On the other hand, profound exposure to ROS resulted in cell death (Marra *et al*, 2011).

Different molecular alterations have been linked to the pathogenesis of HB. Through the analysis of different histological types of hepatoblastoma, López-Terrada *et al* (2006) found that mutations of the beta-catenin gene occur in more than 90% of HB tumours. Beta-catenin is an important gene in the Wnt pathway, which controls tumourgenesis (Sakanaka *et al*, 2000). Moreover, hepatoblastoma is correlated with some genetic diseases such as familiar adenomatosis polypi and Beckwith-Weidemann syndrome (Herzog *et al*, 2000).

Cuevas *et al* (2007) conducted a study on the HepG2 cell line (human HB cell line) to identify the factors that affect the growth of HB. The authors concluded that the proliferation of HepG2 is stimulated via insulin receptor substrate-4 (IRS-4). IRS-4

exerts its action through phosphatidylinositol 3-kinase and protein kinase B (Akt) pathways. In addition, HB is associated with overexpression of IRS-4 (Xia *et al*, 2014).

Dong *et al* (2014) reported that, lncRNAs (long non-coding RNAs) have a major role in the development of HB. Eukaryotic cells contain thousands of lncRNAs, they are longer than 200 nucleotides in length and regulate gene expression (Dinger *et al*, 2009; Ponting *et al*, 2009). Additionally, alterations in the level of expression of lncRNAs have been linked to the progression of several tumours (Ge *et al*, 2013; Sun *et al*, 2013).

## **1.2 DNA Damage**

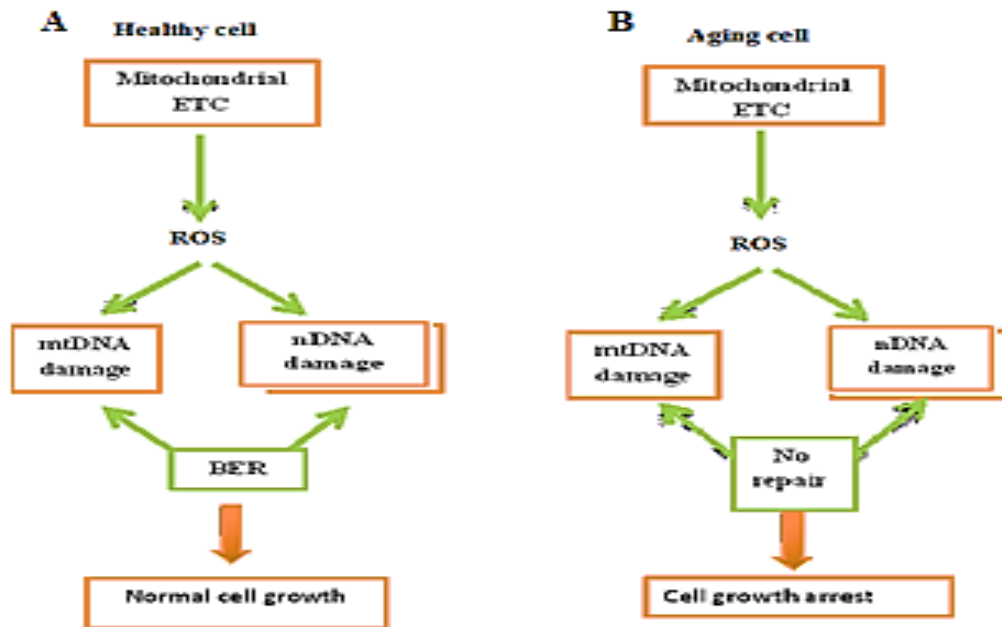
DNA contains the genetic information for achieving the appropriate growth, performance and breeding of living creatures (de Boer and Hoeijmakers, 2000). However, the biological stability of DNA *in vivo* is influenced by factors such as oxidation, hydrolysis and methylation (Lindahl, 1993).

A variety of innate responses to radiation and other oncogenic agents are exhibited by mammalian cells. Indeed the activation of oncogenes or deactivation of tumour suppressor genes was noticed to be responsible for the presentation of numerous neoplasms. In the majority of patients, mutation in a chromosome at a specific site is the commencement point in liberating cells from the dormant situation to the direction of uncontrolled cell proliferation. The connection between damaged DNA and carcinogenic activity indicates ineffectiveness in at least one of the pathways of DNA repair and is strongly implicated in carcinogenesis (Athas *et al*, 1991).

### **1.2.1 Aetiology of damaged DNA**

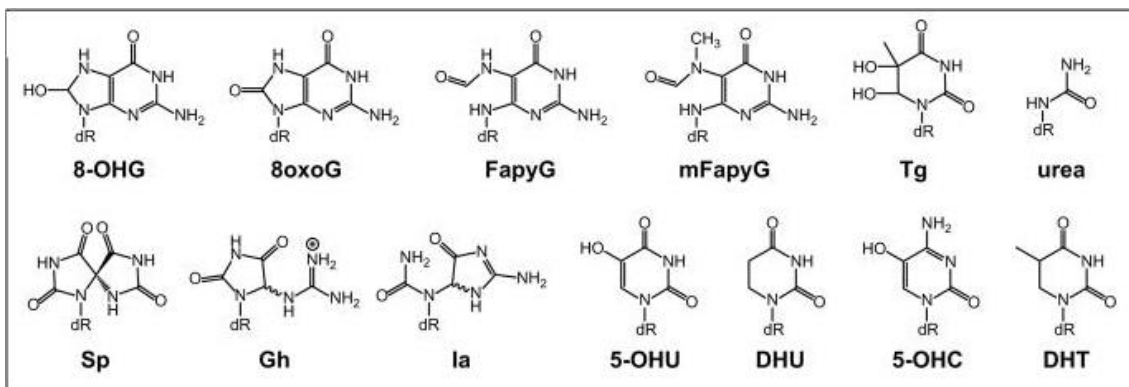
DNA in cells is frequently damaged by different genotoxins. The stability and the composition of DNA sequences might be disturbed endogenously by various replication errors and cellular metabolites or exogenously by radiation (such as UV-light and X-rays), oxygen radicals, alkylating agents, polycyclic aromatic hydrocarbons and chemotherapy drugs (Goode *et al*, 2002).

Different DNA damaging agents produce different DNA lesions; however, single-strand DNA breaks are caused by X-rays, oxygen radicals and indirectly by alkylating agents. In particular, the products of respiratory metabolism in mammalian cells release reactive oxygen species (ROS) (Figure 1.6), which lead to oxidative damage in the DNA molecule. Deamination and depurination are frequent hydrolysis reactions that occur due to intrinsic insults affecting the nucleotide; uracil is produced via deamination of cystine while depurination generates a non-coding abasic site. Bulky chemical adducts are induced by UV-light and polycyclic aromatic hydrocarbons. Double-strand DNA breaks occur because of X-rays and interstrand cross-links through the action of some genotoxic drugs, such as cisplatin (de Boer and Hoeijmakers, 2000).



**Figure 1.6:** The influence of reactive oxygen species (ROS) on mammalian cells. (A) A normal cell has the ability to repair the damaged mitochondrial DNA (mtDNA) and nuclear DNA (nDNA) caused by ROS. (B) Aging cells lack the ability repair the oxidative DNA damage to nuclear and mitochondrial DNA, which ends in cell growth arrest (Adapted from Yakes and Van Houten, 1997).

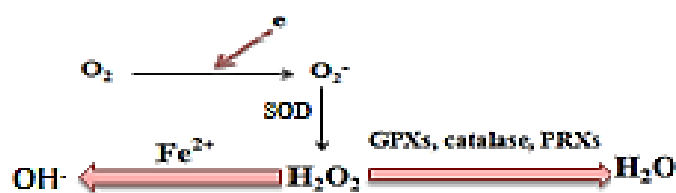
Oxidative DNA base damage (Figure 1.7) are mutagenic such as thymine glycol (Tg) produced by oxidation of thymine, 8-oxo-7,8-dihydroguanine (8-oxoG) produced by oxidation of guanine and 5-hydroxyuracil (5-OH-U) produced by oxidation of cytosine. These lesions lead to genomic instability either, as a result of blocking DNA polymerases or through base mispairing. Therefore, DNA base lesions should be repaired to maintain the stability of the genomic DNA (Brooks *et al*, 2013).



**Figure 1.7:** The most common oxidative DNA base damage. The figure illustrates different types of oxidative DNA base lesions (Brooks *et al*, 2012).

### 1.2.2 Reactive oxygen species

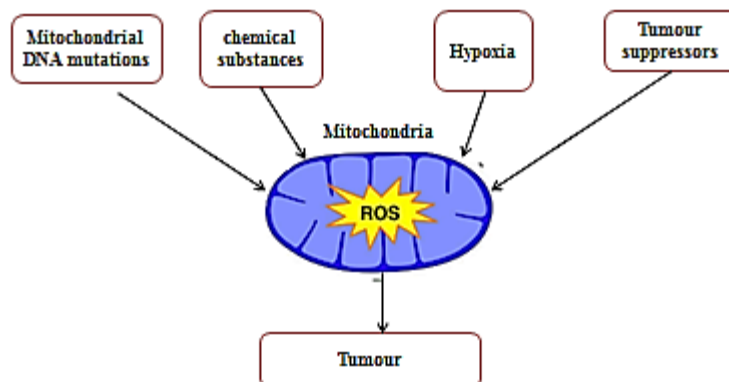
Reactive oxygen species (ROS) are free radical species that have a crucial role in all fields of biology as they are signalling molecules in living organisms involved in apoptosis (programmed cell death) and combat foreign organisms through oxidizing the cell components for instance: lipid, protein and DNA. It has been estimated that 1-3% of oxygen utilized by oxidative phosphorylation generate ROS through reduction of oxygen to water; this reaction involves adding electrons in four steps, which can lead to the production of superoxide anion ( $O_2^-$ ), hydrogen peroxide ( $H_2O_2$ ) and the hydroxyl free radical ( $OH\cdot$ ). ROS are generated from the electron transport chain (ETC) that occurs in the mitochondria of the mammalian cells (Figure 1.8) (Sullivan and Chandel, 2014).



**Figure 1.8:** ROS production pathway. Mammalian cells utilise oxygen in aerobic respiration to perform many vital functions. These processes lead to unstable reactive molecules. Superoxide ( $O_2^-$ ) is produced by adding an electron to an oxygen molecule, and then by the effect of superoxide dismutase (SOD), two molecules of superoxide are converted to hydrogen peroxide ( $H_2O_2$ ).  $H_2O_2$  is reduced to  $H_2O$  by glutathione peroxidases (GPXs), catalase and peroxiredoxins (PRXs). Hydroxyl radical ( $OH\cdot$ ) is generated through the Fenton reaction on  $H_2O_2$  (Adapted from Sullivan and Chandel, 2014).

ROS are also produced from macrophages and neutrophils during the inflammatory response against bacterial and viral infection. Moreover, exogenous reagents such as chemical substances, for example 4-nitroquinoline-1-oxide and ionizing radiation produce ROS (Figure 1.9) causing harmful effects in cells in the form of oxidative DNA lesions, abasic sites, and DNA strand break. ROS-induced base damage has been implicated in the pathogenesis of several diseases such as cancer, rheumatoid arthritis, arrhythmia, neurodegenerative disorder and aging. In comparison with other organs, the brain is more susceptible to the deleterious effect of ROS owing to it possessing low levels of antioxidant enzymes and high amount of unsaturated fatty acids, which are implicated in lipid peroxidation. To tackle all these hazards and conserve the cells from mutation, organisms have several DNA repair pathways (Nishioka *et al*, 1999; Quintanilla *et al*, 2012).

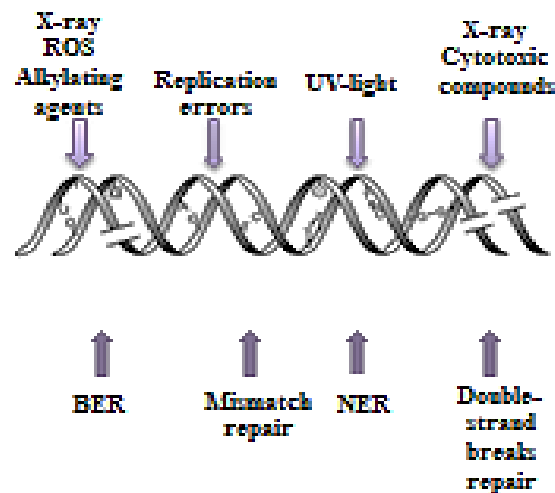
Exogenous antioxidants are another natural defence mechanism that acts against the effects of ROS. This mechanism is offered by fruit, vegetables and certain herbs, which have antioxidants in the form of vitamin C, vitamin E and carotenoids. Previous studies conducted on this mechanism concluded that consuming a diet rich in vegetables and fruit correlated with a lowered risk of developing cancer (Collins, 1999).



**Figure 1.9:** The pathogenesis of tumour formation. Several oncogenic pathways have been linked to cancer development, through generation of ROS, from the electron transport chain in mitochondria, to hypoxia, chemical substances, mutations affecting the mitochondrial DNA and loss of tumour inhibitors (Adapted from Sullivan *et al*, 2014).

### 1.3 Types of DNA repair mechanisms

DNA repair includes a number of sophisticated systems that play significant role in preventing the transcription, DNA replication of the damaged nucleotides. There are five methods, each one deals with particular sort of DNA damage: direct reversal repair, base excision repair (BER), nucleotide excision repair (NER), mismatch repair (MMR) and double-strand break (DSB) repair (Figure 1.10) (Goode *et al*, 2002; Hakem, 2008).



**Figure 1.10:** DNA repair mechanisms. The figure illustrates four DNA repair pathways: base excision repair, which repair the damaged DNA caused by X-ray, ROS and alkylating agents, while mismatch repair is responsible for repairing DNA replication errors. On the other hand, nucleotide excision repair DNA damage induced by UV-light and polycyclic aromatic hydrocarbons. Additionally, double-strand break repair repairs the DSB induced by ionizing radiation (Adapted from Goode *et al*, 2002).

#### 1.3.1 Direct reversal

Unlike other DNA repair pathways, direct reversal is a simple process that does not need the excision of the altered bases. Direct reversal repairs alkylated DNA lesions such as  $O^6$ -alkylguanine.  $O^6$ -alkylguanine is repaired in *Escherichia coli* by the Ogt and Ada proteins, while it is repaired in mammalian cells by  $O^6$ -methylguanine-DNA methyltransferase (MGMT). Moreover, 1-methyladenine (1meA) and 3-methylcytosine (3meC) are other damaged bases induced by alkylating agents, which are repaired in *E. coli* by AlkB and by the ALB homologs, ABH2 and ABH3 in vertebrate cells (Hakem, 2008).

### **1.3.2 Nucleotide excision repair**

Nucleotide excision repair (NER) has evolved to eliminate helix distorting DNA adducts and pyrimidine dimers caused by environmental agents such as UV light and certain chemical carcinogens. Several molecular studies conducted on NER illustrated that genetic abnormality in NER is associated with some rare genetic diseases such as xeroderma pigmentosum (XP). Patients with XP have a 2,000-fold risk of developing skin cancer compared to the rest of the population (Benhamou and Sarasin, 2000).

The NER mechanism is composed of four processes: First, via a complex of linked proteins, *e.g.* XPC and XPA, the damage is detected, and then the affected DNA segment is covered by the TFIIH complex. The next step involves making two incisions and removing a DNA portion (approximately 25-30 nucleotides), which is carried out by the ERCC1, XPF complex and XPE. The fourth step includes DNA polymerization by a DNA polymerase and ligation by DNA ligase (Goode *et al*, 2002).

### **1.3.3 Double-strand break repair**

There are two mechanisms that mediate DSB repair: homologous recombination (HR) and non-homologous end-joining (NHEJ). In yeast and prokaryotes, DSBs are repaired by HR, while in mammalian cells over 90% of DSBs are repaired by NHEJ (Hakem, 2008).

In NHEJ, the two broken DNA termini are ligated without need for a homologous DNA sequence. HR is complicated mechanism, as it requires several proteins to search for the homologous DNA template and to carry out DNA strand invasion. However, after resection, the DNA ends of the recently uncovered 3'-single-stranded tails invade into the double helical DNA to achieve an error free repair of the DSB (Goode *et al*, 2002). Mutations in the BRCA1, BRCA2 and XRCC3 genes (which have a role in the HR pathway) are associated with cancer of the ovary, breast and other tumours (Venkitaraman, 2002).



#### **1.3.4 Mismatch repair**

Mismatch repair (MMR) has a fundamental role in protecting the cells against DNA replication mistakes as a result of DNA polymerase errors. Impaired MMR genes (MLH1, MSH2, PMS2, and MSH6) lead to instability of short bases repeats (microsatellite instability) which have been linked to hereditary nonpolyposis colorectal cancer. MMR starts by detecting mismatch in the newly synthesized strand, and then the following steps are incision, excision, polymerization and ligation (Aquilina and Bignami, 2001).

#### **1.3.5 Base excision repair**

The mechanism of base excision repair (BER) was first described by Lindahl (1974). BER releases alkylated and oxidized bases and repairs apurinic/apyrimidinic (AP) sites and DNA single-strand breaks. Mammalian cells use highly conserved enzymes named DNA glycosylases, to identify and remove chemically modified bases from DNA (Krokan *et al*, 2000).

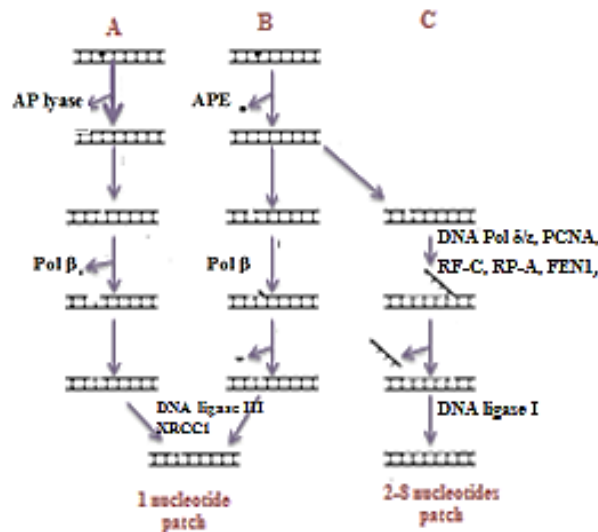
DNA glycosylases are divided into two major groups according to the type of DNA binding motif: Helix-hairpin-helix (HhH) or Helix 2 turn Helix (H2TH). OGG1, MutY and Nth have HhH structure, while MutM (Fpg), Nei and NEIL family follow H2TH group. However, all members in H2TH family have zinc finger motif except NEIL1, which has zincless finger motif (Liu *et al*, 2013).

OGG1 conserve the cells from the influences of 8-oxoG. 8-oxoG is the most oxidized purine, it implicates in tumour pathogenesis as this compound bind with A and C resulting in G: C → T: A transversions (Morland *et al*, 2002).

DNA glycosylases initiate BER by excision of the damaged base through splitting the N-glycosidic bond between the target base and the DNA sugar-phosphate backbone (deoxyribose) resulting in release of the nitrogenous base and creating an AP site. Moreover, certain DNA glycosylases are bifunctional and cause a break of the phosphodiester backbone 3' to the abasic site through their AP lyase activity that results in blocking the 3'-side of the AP site with 3'-phospho  $\alpha,\beta$ -unsaturated aldehyde (3'-PUA) or 3'-phosphate (3'-PO<sub>4</sub>), while the 5'-end has a phosphate (5'-PO<sub>4</sub>) residue. This

characteristic activity is a unique feature of oxidized base-specific DNA glycosylases. On the contrary, in monofunctional glycosylases the intact AP site is cleaved by an AP-endonuclease (APE) generating 3'-hydroxy (3'-OH) and 5'-deoxyribose phosphate (5'-dRP) termini. The basic disparity between both enzymes is related to the nucleophile compound, in that the activated water molecule is being used by APE dependent DNA glycosylases as the active site nucleophile, while an amine or N-terminal proline or valine is used by AP lyases as the nucleophile in attacking the sugar C1 (Lu *et al*, 2001).

Following incision of the phosphodiester backbone, BER can be either short patch or long patch. In short patch repair, replacement of one nucleotide is carried out, in which DNA polymerase  $\beta$  (Pol  $\beta$ ) uses the remaining DNA strand, as a template in DNA synthesis then DNA ligase III, XRCC1 are responsible for the ligation step. While, long patch repair involves gap filling of about 2-8 nucleotides, which requires DNA polymerase  $\delta/\epsilon$ , proliferating cell nuclear antigen (PCNA), replication factor C (RF-C), replication protein A (RP-A), flap structure-specific endonuclease 1 (FEN1) and DNA ligase I (Figure 1.11) (Nakanishi *et al*, 2007).



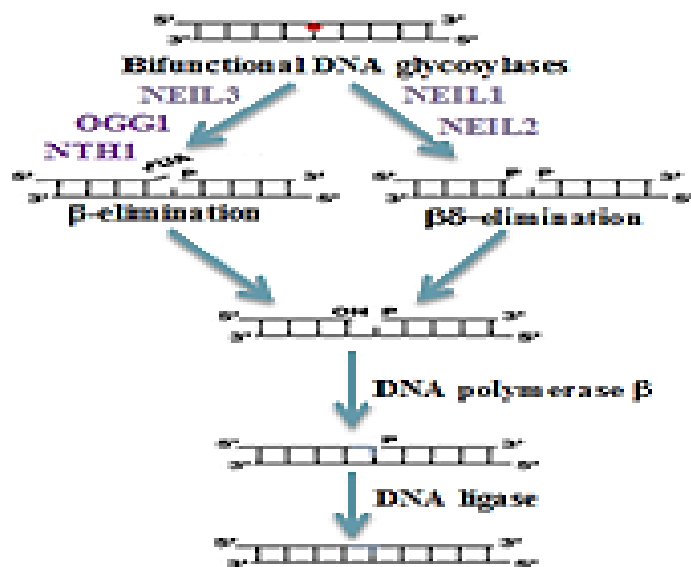
**Figure 1.11:** Base excision repair mechanism. (A) Bifunctional DNA glycosylases, in which their action is mainly carried out via internal AP lyase residue. (B) Monofunctional DNA glycosylases, in which the action is achieved by AP endonuclease. Both A and B illustrate short patch repair, in which filling the gap with single nucleotide is achieved via DNA Pol  $\beta$ , DNA ligase III and XRCC1. (C) Long patch repair, in which the BER conducted with replacement of several nucleotides via DNA Pol  $\delta/\epsilon$ , PCNA, RF-C, RP-A, FEN1, DNA ligase I (Adapted from Krokan *et al*, 2000).

#### **1.4 Oxidized base-specific DNA glycosylases in euokaryotic cells**

Oxidative stress generated from hydrogen peroxide, superoxide and hydroxyl radicals have been implicated as a cause of mutagenic base lesions affecting purines and pyrimidines. It has been estimated that the genomic DNA in each cell is liable to  $10^4$ - $10^5$  lesions each day (Lindahl, 1993).

The pathway of BER was initially determined in *E. coli*, and further experiments revealed that the mechanism occurs in mammalian cells as well. Therefore, DNA glycosylases are expressed in both prokaryotic and eukaryotic cells. Although, for each type of DNA glycosylase there is a preferred kind of base damage and sometimes the substrate specificity overlaps. These enzymes are small proteins, approximately 30-50 kDa (Krokan *et al*, 2000; Hegde *et al*, 2008).

DNA glycosylases specific for oxidized bases in *Homo sapiens* are bifunctional by virtue of an AP lyase activity and are classified into two major families named Nth family and Fpg (MutM)/Nei (Endonuclease VIII) family. NTH1 and OGG1 are included in the Nth family, while NEIL1, NEIL2 and NEIL3 are members of the Fpg/Nei family. Depending on the elimination reactions at AP site, Nth family uses  $\beta$ -elimination activities and leaves 3'-PUA at the DNA strand break. In comparison, the NEIL family with the exception of NEIL3 utilizes a  $\beta\delta$ -elimination reaction and liberates 3'-PO<sub>4</sub> termini at the strand break (Figure 1.12) (Hegde *et al*, 2008; Edmonds and Parsons, 2014).



**Figure 1.12:** Bifunctional DNA glycosylases with  $\beta$ -elimination reaction and  $\beta\delta$ -elimination reaction. NEIL1 and NEIL2 use  $\beta\delta$ -elimination reaction at AP site, while NEIL3, OGG1 and NTH1 use  $\beta$ -elimination reaction. DNA synthesis is carried out by DNA polymerase  $\beta$  and DNA ligation via DNA ligase (Adapted from Liu *et al*, 2013).

## 1.5 NEIL family

NEIL family is Nei-like protein in vertebrate genome (Hazra *et al*, 2002). The genes for NEIL1, NEIL2 and NEIL3 are located on chromosomes 15, 8 and 4 in human cells respectively (Takao *et al*, 2002).

### 1.5.1 NEIL1

NEIL1 (endonuclease VIII-like I) is a 44 kDa protein. According to the catalytic activity there is a considerable similarity between NEIL1 and both Nei and Fpg. However, NEIL1 is closer to Nei than Fpg in that, 8-oxoG-C pair-containing DNA or oligos are poor substrates for NEIL1. Nevertheless, NEIL1 and Fpg have similar excisional activity as both prefer ring-opened purines such as the formamidopyrimidines FapyA (4,6-diamino-5-formamidopyrimidine) and FapyG (2,6-diamino-4-hydroxy-5-formamidopyrimidine). Additionally, NEIL1 has the ability to excise 8-oxoG, Tg and 5-OH-U. It was concluded that NEIL1 takes part in replication-associated repair of the oxidized bases as its expression level rises sharply by about

seven-fold in S-phase compared with that in G<sub>0</sub>/G<sub>1</sub>. NEIL1 utilises the N-terminal proline amino acid at position 2 (Pro2) as the nucleophile, while the C-terminal end has the nuclear localization signal (NLS), which is essential for nuclear translocation (Takao *et al*, 2002; Yamomoto *et al*, 2014).

Unlike NEIL2 and NEIL3, which have zinc finger motifs, NEIL1 has a characteristic feature by lacking the loop that carries the zinc residue, thus NEIL1 exerts its DNA glycosylase activity through a zincless finger. However, the zinc finger motif is also absent in other members of the Fpg family namely *Arabidopsis thaliana* Fpg and *Candida albicans* Fpg (Doublié *et al*, 2004).

In addition, the role of NEIL1 in repairing the damaged genome was demonstrated by knocking down the level of NEIL1 in embryonic stem cell lines through RNAi. The results showed that the cells become highly sensitive to the effect of low dose of gamma radiation (Rosenquist *et al*, 2003).

It was confirmed that NEIL1 is involved in humoral immunity as a study was conducted on NEIL1 showed that NEIL1 is highly expressed in germinal centre (GC) B cells. However, when mouse NEIL1 (Mmu NEIL1) was deleted, the frequency of immunoglobulin gene hypermutation was lowered and the clonal expansion and the responses of GC B cells against T cell-dependent antigen decreased (Mori *et al*, 2009).

### **1.5.2 NEIL2**

NEIL2 (endonuclease VIII-like II), a 37 kDa protein, is expressed in testes and voluntary muscles whereas the level of NEIL1 mRNA is highly expressed in liver, pancreas and thymus. In contrast to that, the expression of NEIL1 decreases dramatically in muscles and testes. The previous variations conclude that, the function of NEIL1 is complementary to NEIL2 (Hazra *et al*, 2002).

Furthermore, there are some similarities between NEIL1 and NEIL2, in that both have N-terminal Pro2 to fulfil their roles as DNA glycosylases. Additionally, NEIL2 and NEIL1 are mainly located in the nucleus. Nonetheless, the protein level of NEIL2 is not regulated during the cell cycle. Notably, NEIL2 has a strong repair tendency toward the lesions that are produced via oxidation of cytosine (C), and its preferred substrate is 5-

OH-U. However, NEIL2 has a marginal activity to 5-hydroxycytosine (5-OH-C) and 5,6-dihydrouracil and it has unmeasured activity to 8-oxoG, 2-hydroxyadenine, hypoxanthine and xanthine (Hazra *et al*, 2002).

Several studies conducted on the influence of ROS-induced DNA damage reveal that the products of oxidized cytosine are the most common mutagens leading to GC → AT transitions; the C → T transition is the most frequent base replacement affecting the genomic DNA. This was explained by the following: initially cytosine oxidation leads to cytosine glycol (Cg). Due to the instability of Cg, it is either dehydrated to 5-OH-C or deaminated to uracil glycol (Ug). The third compound is 5-OH-U is formed by either removing the amine group from 5-OH-C or removing the water from Ug (Figure 1.13). These uracil derivatives are mispaired with adenine during DNA replication (Kreutzer and Essigmann, 1998).



**Figure 1.13:** Cytosine oxidation. Exposure of cytosine to ROS generates an unstable cytosine glycol (Cg) product. Further reactions that include dehydration and deamination will lead to three pre-mutagenic lesions namely: 5-hydroxycytosine (5-OH-C), uracil glycol (Ug) and 5-hydroxyuracil (5-OH-U) (Adapted from Kreutzer and Essigmann, 1998).

### 1.5.3 NEIL3

NEIL3 (endonuclease VIII-like III) is a 68 kDa protein. Recently, NEIL3 has been discovered as a third mammalian oxidative base pair DNA glycolysase that homologous

to the *E. coli* DNA glycolysases Fpg and Nei. The hNEIL3 (human NEIL3) gene is situated on chromosome 4q34.3 and is encoded via the plus strand. In addition, the hNEIL3 locus is flanked by two genes namely AGA gene (aspartylglucosaminidase) which is situated on the telomeric end and another gene located on the centromeric side termed VEGFC gene (vascular endothelial growth factor c). Nevertheless, both genes are encoded via the minus strand. The NEIL3 gene has 10 exons and consists of 1818 bp in the coding sequences, which gives the full length of hNEIL3 protein of 605 amino acids (Liu *et al*, 2013).

NEIL3 is mainly present in the cell nuclei (Torisu *et al*, 2005). It has been observed that there is a significant increase in the protein level of hNEIL3 in G2 phase and the Ras dependent ERK-MAP kinase pathway has been implicated in the enhancement of the transcription of hNEIL3 in early S phase. There are several transcription factors affecting the level of gene expression, in a manner that they increase or decrease the level of NEIL3 mRNA for instance, the E2F family, which consists of eight factors that adhere with the target promoters, thus control their expression. Members of E2Fs family also bind with DP1 or DP2 and create active DNA binding heterodimers. Additionally, they bind with pocket protein group such as retinoblastoma (RB) tumour suppressor, p107 and p130. DREAM complex consists of E2F4, DP1, RB p130 and MuvB core complex. However, the DREAM complex possesses an important role in suppression the expression of NEIL3 mainly in G0 dormant cells (Neurauter *et al*, 2012).

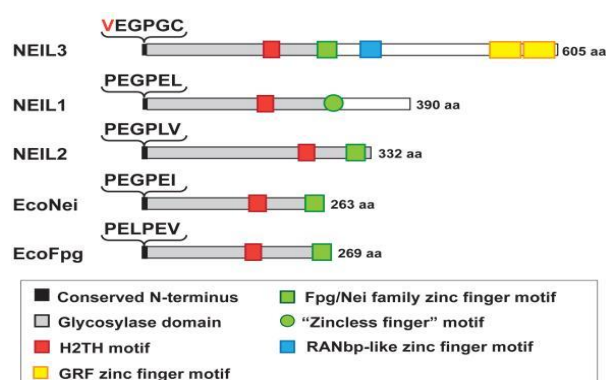
### **1.5.3.1 Analysis of the structure of NEIL3 and its DNA glycosylase activity**

Regarding the protein structure, hNEIL3 has a unique long C terminal domain that contains a Ranbp-like zinc finger motif and tandem GRF zinc finger motifs in addition to the H2TH motif (Figure 1.14). Moreover, NEIL3 has an N-terminal valine amino acid at position 2 (Val2) instead of the usual Pro2 residue. Thus, NEIL3 uses this amino acid to form a transient catalytic Schiff base. The valine nucleophilicity is also a characteristic feature of another DNA glycosylase named MvNei2 (*Acanthamoeba polyphaga mimivirus*) (Liu *et al*, 2010).

The preferred substrates for NEIL3 are hydantoin lesions such as spiroiminodihydantoin (Sp) and guanidinohydantoin (Gh) in both single-strand DNA (ssDNA) and double-

strand DNA (dsDNA). However, NEIL3 has no excisional activity toward 8-oxoG. Nonetheless, NEIL3 has a unique feature, in that it is the only repair enzyme that excises Sp and Gh in ssDNA. Also it was found that Neil3 exerts some excisional activity toward 5-OH-C and 5-OH-U in ssDNA. On the other hand, there is no activity shown by NEIL3 on 5-OH-C and 5-OH-U in dsDNA. Compared with NEIL1 and NEIL2, which both have a robust  $\beta\delta$ -lyase activity, NEIL3 has very weak  $\beta$ -lyase activity forming 3'-PUA at the DNA strand break (Liu *et al*, 2013).

Additionally, several experiments were carried out on Mmu NEIL3 (mouse NEIL3, *Mus musculus*) concluded that NEIL3 is responsible for releasing the mutagenic FapyG base lesion. Indeed there is overlapping in the activity toward the specific substrates between hNEIL3, Nth1, NEIL2 and NEIL1 (Liu *et al*, 2013).



**Figure 1.14:** Structural comparison between NEIL3, NEIL2, NEIL1, *E. coli* nei and *E. coli* Fpg. *E. coli* nei, *E. coli* Fpg and NEIL2 have an Fpg/Nei family zinc finger motif, H2TH motif and conserved N-terminal Pro2 residue, while NEIL1 possesses additional features such as a zincless finger motif. On the other hand, NEIL3 has a GRF zinc finger motif and a RANbp-like zinc finger motif at C-terminus, H2TH motif and conserved N-terminal Val2 amino acid instead of Pro2 terminus (Liu *et al*, 2013).

Mmu NEIL3 has been characterized through crystal structure analysis of two domains, which form the catalytic core and resembles Fpg glycosylases (Liu *et al*, 2013). The N-terminal domain consists of two layers of helices, while the C-terminal domain forms a stalk of  $\alpha$ -helices, the H2TH motif form two of them and the zinc finger motif are placed after H2TH motif. Between the N-terminal domain and C-terminal domain, there is a fissure with positive charges that create an electrostatic attraction toward DNA. The catalytic task of Mmu NEIL3 is carried out via the Val2, which is located in the fissure.

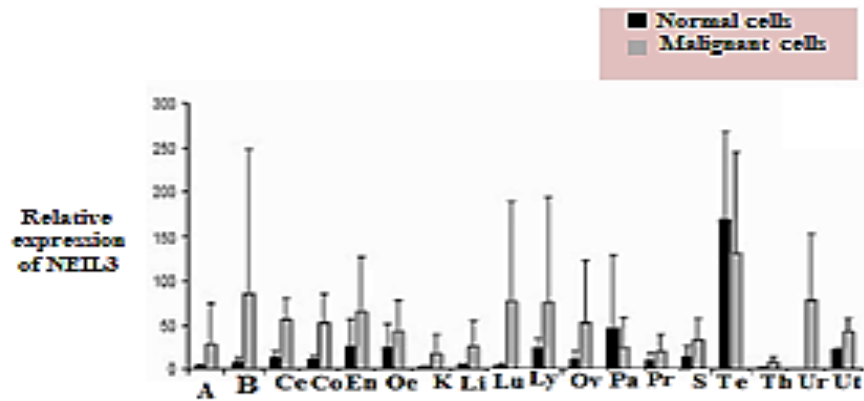


In addition, the 8-oxoG capping ring, which harbours the 8-oxoG in prokaryotic Fpg proteins is very small in NEIL3, thus this enzyme is unable to trap the 8-oxoG in the binding place. Furthermore, the absence of two void-filling residues in Mmu NEIL3, which are responsible for stabilisation of the complementary DNA strand after removing the base damage, along with the presence of the negative charge residues, which prevent the NEIL3 from binding with the opposite DNA strand. However, all these features explain the high excision activity of NEIL3 toward ssDNA (Takao *et al*, 2009; Liu *et al*, 2013).

### **1.5.3.2 The role of NEIL3 in rapidly dividing cells**

It has been suggested that NEIL3 has a major role in repairing the damaged bases in rapidly dividing cells, as the level of NEIL3 is highly expressed during the embryogenesis phase in brain regions containing many stem cells. In addition, the level of hNEIL3 mRNA was examined in 18 different tumour tissues and healthy tissues. The result showed that there was a significant increase in the level of NEIL3 in tumour cells except testes and pancreas compared with the normal cells (Figure 1.15) (Hildrestrand *et al*, 2009).

Despite all the previous research and the achieved results on NEIL3, its biological role remains an enigma because of issues related to purification of the protein. However, a great effort is needed to illustrate the task of NEIL3 in mammalian cells and the purpose of being a unique component of eukaryotes (Hildrestrand *et al*, 2009).



**Figure 1.15:** The relative level of NEIL3 mRNA in different tumours and healthy organs. q-RT-PCR was carried out on cDNA obtained from different human cell lines. The relative expression of NEIL3 mRNA was calculated via normalization with  $\beta$ -actin. The selected cell lines were A: Adrenal gland, B: Breast, Ce: Cervix, Co: Colon, En: Endometrium, Oe: Oesophagus, K: Kidney, Li: Liver, Lu: Lung, Ly: Lymph nodes, Ov: Ovary, Pa: Pancreases, Pr: Prostate, S: Stomach, Te: Testis, Th: Thyroid gland, Ur: Urinary Bladder, Ut: Uterus (Adapted from Hildrestrand *et al*, 2009).

Interestingly, high expression levels of NEIL3 and other DNA repair proteins has been correlated with the development of metastasis and high mortality rates in patients with primary malignant melanoma (Kauffmann *et al*, 2008). Thus, it has been suggested that high levels of DNA repair genes might explain the resistance of melanoma to chemotherapy and radiotherapy (Kauffmann *et al*, 2008).

### **1.5.3.3 The role of NEIL3 in replication-associated repair**

There is a strong suggestion that NEIL3 has a specific role in repair the replicating 1 genome due to alignment of the NEIL3 sequence with proliferating cell nuclear antigen (PCNA) binding proteins and replication protein A binding proteins.

Replication protein A is a single-strand DNA binding protein, which is required during DNA metabolism (Morland, 2002), while PCNA is a ring-shaped protein that surrounds the DNA and enhances the processivity of DNA synthesis by binding the catalytic subunit of the replicative DNA polymerase with the DNA template. PCNA has additional tasks in the nucleus as it deals with remodeling the chromatin structure and it is a cofactor for DNA polymerase  $\epsilon$ , which explains the function of the PCNA in DNA repair. Moreover, PCNA exerts its role in genome replication through stimulation DNA polymerase  $\delta$  (Kelman, 1997).

#### **1.5.3.4 The immunological role of NEIL3**

Since Mmu NEIL3 is highly expressed in spleen, lymph nodes, thymus, B cells and bone marrow along with a marginal decline in the numbers of mouse white blood cells after NEIL3 knockout, it has been suggested that NEIL3 has a function in the immune system (Torisu *et al*, 2005; Hildrestrand *et al*, 2009).

Furthermore, several DNA glycosylases are involved in promoting the mutated immunoglobulin genes. A good example of this is uracil DNA glycosylase (UDG) which recognizes the mismatched base pairs (dU: dG) in the immunoglobulin genes during B cell differentiation by class switch recombination (CSR) and somatic hyper mutation (SHM). dU: dG damages are produced via deamination of deoxycytidine (dC) residues in the single-strand DNA which leads to antibody gene diversification. However, UDG initiates the switch recombination through cleaving the strand at abasic sites by using the AP-endonuclease (Rada *et al*, 2004; Dominguez and Shaknovich, 2014).

#### **1.5.3.5 NEIL3 and human immunodeficiency virus type 1 (HIV-1)**

HIV-1 is an RNA virus that belongs to the retrovirus family. Due to the fact that the length of the HIV-1 genome is about 9.8 kb and it is responsible for encoding only 15 proteins, HIV uses host proteins to complete all the steps of its reproductive cycle. These steps include entrance of the nucleoprotein core of the virus into the host cell, followed by reverse transcription phase then the viral double-stranded DNA is imported into the cell nucleus and integrated into the target chromosomes. After that, the provirus is transcribed into viral mRNA and translated into viral proteins then the assembled new viral particles are released to the cytoplasm (Goff, 2007; Lama and Planelles, 2007).

Although there have been major advances in antiretroviral therapy, many patients are still suffering from drug resistance. It was estimated that about 35.3 million people are infected globally by HIV-1. As the current antiretroviral agents block the viral enzymes, which include viral protease, reverse transcriptase and integrase, mutation emerges in these enzymes that can make the HIV-1 therapeutics ineffective. For that reason, there is a need for novel antiretroviral drugs that target the host proteins (Asamitsu *et al*, 2015).

To illustrate the cellular factors that are linked to HIV-1 replication, Zhou *et al* (2008) carried out genome-wide small interference RNA (siRNA) experiment on HeLa P4/R5 cells. These cells were transfected with siRNA and after 24 h they were infected with HIV-1 and the DNA was isolated. siRNA is a technique used to identify the biological role of specific genes by applying small double-strand RNA (sdRNA) to the cytoplasm of the cell which results in silencing the expression of the target gene (Elbashir *et al*, 2001). About 311 cellular genes were detected in this screen, which influence the existence of HIV-1. Of these, 267 genes are not previously recognized. Interestingly, NEIL3 was discovered as one of the host cellular cofactors, which are needed for integration the HIV-1 cDNA into the host genome. However, this virus host interaction is very important for the life cycle of HIV-1 and for its replication as knocking down of NEIL3 mRNA led to decrease the HIV infection and hinder its integration to the cell. Furthermore, cDNA rescue experiments were conducted in a non-targeted form, which confirm the function of the identified host genes (Zhou *et al*, 2008).

## **1.6 Telomeres**

The termini of mammalian linear chromosomes are capped with telomeres, which serve as one of the biological indicators for aging. Telomeres were first recognized in the 1930s and consist of nucleoprotein complexes in a form of approximately 9-15 kb telomeric repeated 5' TTAGGG 3' sequences and telomeric binding proteins (Wang *et al*, 2015).

In addition, telomeres end with a conserved structure of about 150 bp 3'G overhanging single-strand (Raynaud *et al*, 2008; Zhou *et al*, 2015). Telomeres have vital functions in which they hinder uncontrolled cell proliferation and they conserve the subtelomeric regions from end to end fusion and the deleterious effects of nucleolytic activities such as DNA degradation. Furthermore, the peripheral parts of chromosomes are distinguished from double-strand DNA breaks by the structure of the telomeres and thereby the genomic integrity is protected (McEachern *et al*, 2000; Hug and Lingner, 2006; Degerman *et al*, 2014).

### **1.6.1 Factors that influence telomere length**

Studies conducted on telomere length have demonstrated the factors, which are implicated in loss of telomere repeats. These factors are divided into environmental, genetic and cellular factors; telomeres become significantly shortened as a result of the cellular factors and this decline in telomere length is enhanced via environmental factors (Njajou *et al*, 2007).

Owing to the process of DNA replication, which is incapable of entirely replicating the telomeric DNA (the activity of DNA polymerases is unidirectional 5'→3'), gradual shortening of the telomeres occur. In addition, degenerative activities and nonhomologous end-joining of telomeric DNA shorten the telomeres as well. However, short telomeres promote replicative senescence or chromosome instability, which ends with generation of cancer cells (Andrew *et al*, 2006). Alter *et al* (2012) measured the length of the telomere by automated multicolour flow fluorescence *in situ* hybridization in peripheral white blood cells subtypes. The authors concluded that short telomere length is linked to inherited genetic diseases such as dyskeratosis congenita (inherited bone marrow failure syndrome), aplastic anemia and mutation in some genes *e.g.* TERT. Additionally, the authors noticed that the length of telomere reflects the severity of the associated diseases and decrease with aging. Moreover, short telomere length is related to dementia, atherosclerosis and cardiovascular diseases (Saretzki and Von Zglinicki, 2002; Andrew *et al*, 2006).

In terms of the environmental factors and their effects on telomere length, Valdes *et al* (2005) tested the association between telomeres, body weight and cigarette smoking. The authors reported that the length of telomeres in obese females reduced by 240 bp when they were compared with telomeres of the normal females and every pack-year smoked was equal to 5 bp of telomeres lost. Therefore, oxidative stress is implicated in telomere attrition. In addition, Gardner *et al.* (2005) examined the relation between insulin hormone and the length of telomeres in leukocyte cells. The authors stated that white blood cells telomere length is inversely correlated with insulin resistance. Additionally, poorly controlled type 2 diabetes mellitus and hypertension are linked with short leukocyte telomeres (Aviv, 2002; Biron-Shental *et al*, 2015; D'Mello *et al*, 2015).

There is a wide disparity in the length of telomeres in human organs and among people. Takubo *et al* (2002) tested the telomere lengths in the human cerebral cortex, myocardium, liver, renal cortex and the spleen in relation to the age. The authors reported that the telomeres decrease by 29-60 base pair (bp) per year in liver, spleen and renal cortex. However, the authors confirmed that the reduction rates of telomere do not involve the myocardium and cerebral cortex and the myocardium has the longest telomeres, whereas the renal cortex and liver have the shortest telomeres.

Moreover, Okuda *et al* (2002) examined telomere length by calculating the mean length of the terminal restriction fragments (TRF) in different ages and in both sexes. The authors sum up that all intrauterine fetuses have different lengths of telomeres but that telomere length in their organs is similar. Then as a result of postnatal circumstances, this length was subjected to change. Additionally, comparing both genders, telomere lengths are shorter in men than in women, which were explained by the influences of estrogen on a female's telomeres, as it stimulates the degradation of ROS (Aviv *et al*, 2002).

ROS are generated via  $Fe^{2+}$ -mediated Fenton reaction and these species enhance numerous abnormalities in all cellular components. As oxidative agents prefer G-rich sequences, thus telomeres are favored to be altered as they have runs of triplet guanines. Furthermore, telomeric DNA has high binding activity to  $Fe^{2+}$  (Rai *et al*, 2005).

However, the most common oxidized base lesion in telomeres is 8-oxoG, which is repaired by OGG1. 8-oxoG interrupts telomerase, reduces the activity of the binding proteins (TRF1 and TRF2) and even the DNA repair mechanism at telomeres is less effective compared with non-telomeric DNA as a result of the failure of OGG1 to remove 8-oxodG from the 3'-overhang (Rhee *et al*, 2011).

Kawanishi and Oikawa (2004) concluded that oxidative stress accelerates telomere shortening through the generation of oxidized guanine in the telomeric DNA. In addition, it was confirmed that oxidative stress induces single-strand breaks in telomeric DNA (Von Zglinicki *et al*, 2000; Honda *et al*, 2001).

To assess the effect of genetics on telomere length, many studies were carried out. Nawrot *et al* (2004) said that telomere repeat factor (TRF) length is linked to X chromosome. Furthermore, another report revealed the pattern of inheritance in

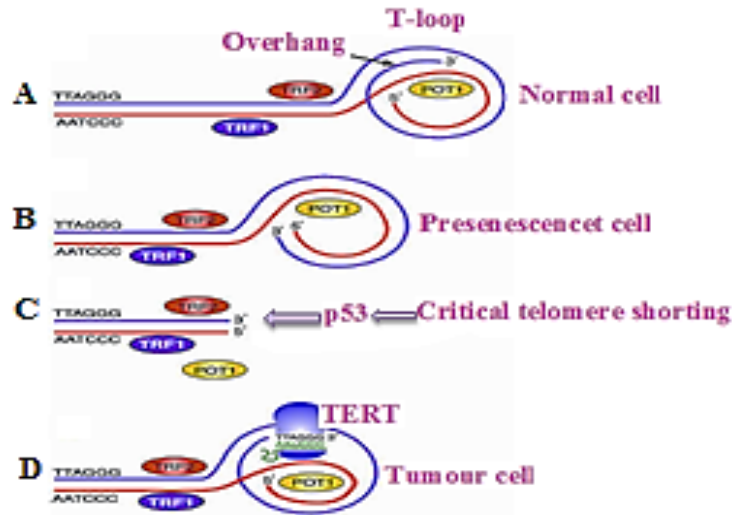
telomeres is father-to-offspring (Nordfjäll *et al*, 2005). In addition, Vasa-Nicotera *et al* (2005) identified the mean TRF length is linked to a locus on chromosome 12. Then Andrew *et al* (2006) measured the mean TRF length via Southern blotting analysis in both homozygotic and dizygotic twins; the authors stated that a robust association between the telomere length and loci on chromosomes 14q23.2, 10q26.13 and 3p26.1. However, recently it has been demonstrated that maternal factors are also implicated in telomere length maintenance (Asghar *et al*, 2015).

### **1.6.2 Factors regulating telomere homeostasis**

To tackle the issues caused by decreasing the telomere length, vertebrate cells maintain the stability of the genomic telomeres with each cell cycle proliferation by many genes, including TERT, UP1, Tankyrase, EST1, EST2, EST3, YKU70, SIR4 and RIF2 (Njajou *et al*, 2007).

Telomeric DNA sequences are bound by six specific chromosomal proteins, collectively known as shelterin: telomere repeat factor 1 and 2 (TRF1, TRF2), TRF-1 interacting nuclear factor 2 (TIN2), repressor activator protein 1 (Rap1), tripeptidyl peptidase 1 (TPP1) and protection of telomere protein 1 (POT1) (Raynaud *et al*, 2008). POT1 binds to single-stranded G-rich telomeric sequences and it plays a major role in maintaining telomere length. This function was illustrated by loss of the telomeric DNA following the deletion of the POT1 gene (Baumann and Cech, 2001).

Shelterin has numerous roles to prevent the loss of the genomic sequences such as controlling the protection of telomeres via telomerase, inhibition of the ATM and ATR kinase signaling pathways and avoidance of nonhomologous end fusion (de Lange, 2005; Palm and de Lange, 2008). Shelterin proteins assist telomeres to exist in a T-loop form with 3'-single-stranded overhang invading double-strand telomeric DNA. The stability of telomeres is affected by interruption of the T-loop, therefore the 3'-overhang will be exposed (Figure 1.16) (Rhee *et al*, 2011).

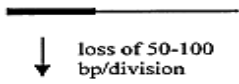
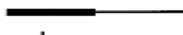
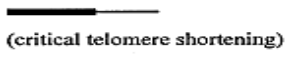

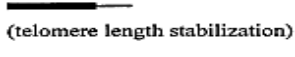
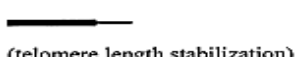


**Figure 1.16:** Structure of telomere. (A) Shelterin proteins such as TRF1, TRF2 and POT1 help in stabilisation telomere into a structure known as T-loop. T-loop is formed by folding back of the 3' G-rich, single-stranded overhang then it invades the double-strand part of telomeric DNA. (B) During DNA replication, shortens of telomere occur. (C) Loss of telomere is recognized by DNA damage response genes such as p53 which ends in apoptotic cell death. (D) TERT is the catalytic subunit of telomerase that is responsible to maintain the length of telomere in cancer cells (Adapted from Ben-Porath and Weinberg, 2004).

### 1.6.3 Telomerase

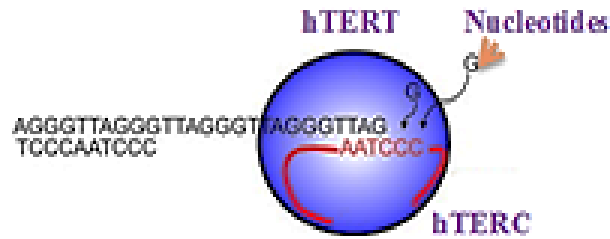
Telomerase (telomere terminal transferase) is ribonucleoprotein complex; the activity of which was first identified by Greider and Blackburn (1985) in the protozoan *Tetrahymena* (Vaziri *et al*, 1993). Then the telomere terminal transferase was detected in human tumour cells by Morin (1989). The structure of telomerase allows the addition *de novo* of telomeric TTAGGG repeats to overcome the loss of telomere length that accompanies each cell division. Subsequently, it was confirmed that telomerase plays a very important role in immortal cells such as neoplastic cells and germ line cells (Figure 1.17) (Aviv *et al*, 2002).



Cell phenotype/stages	Relative telomere length	Size	Telomerase expression
A. Normal somatic dividing cells		10-15 kb	Absent
B. Presenescent cells		8-10 kb	Absent
C. Senescent phase M1		5-8 kb	Absent
D. Crisis phase M2 (transforming event)		shorter than the sizes at M1 phase	↑
E. Immortalized cells		varies	↑↑
F. Tumor cells (benign / malignant)		varies (but generally shorter than normal telomerase-positive cells)	↑↑↑

**Figure 1.17:** The activity of telomerase in different cell types. (A) Normal cells lose about 50-100 bp of telomere length with each proliferation cycle. (B) The size of telomere in pre-senescent cells is about 8-10 kb. (C) Telomere length decreases significantly in senescent cells and its final size is around 5-8 kb. (D) Owing to marked shortening in telomere, cells in phase M2 start to express telomerase. (E) Telomere length is synthesized by telomerase. (F) Cancer cells immortalized express high levels of telomerase (Saldanha *et al*, 2003).

Telomerase is an RNA-dependent DNA polymerase that is composed of two components; an RNA template known as human telomerase RNA component (hTERC) which adheres to the 3' overhang of telomeres. This subunit contains 11 nucleotides (5'-CUAACCCUAAC) complementary to telomeric hexanucleotides sequences. The second component of telomerase is human telomerase reverse transcriptase (hTERT) and this catalytic subunit synthesizes TTAGGG repeats from hTERC (Newbold, 2002) (Figure 1.18). hTERC gene is mapped to chromosome 3q26.3, while hTERT gene is localized on chromosome 5p15.33 (Bryce *et al*, 2000).



**Figure 1.18:** The activity of telomerase on the telomeric termini. The two components of telomerase (hTERT and hTERC) act to replace the loss in the telomeric sequences (Adapted from Raynaud *et al*, 2008).

It was found that more than 85% of neoplastic cells express telomerase (telomerase-positive cells) and the level of telomerase in these cells is higher than in germ cells and stem cells. Significantly, most somatic cells do not express telomerase. In addition, the activity of telomerase is controlled via hTERT; c-myc, interleukin-6 and insulin-like growth factor lead to hTERT upregulation. On the other hand, retinoblastoma protein, protein phosphatase 2A (PP2A), cyclin-dependent kinase inhibitor p21 and p53 cause hTERT downregulation (Tahtouh *et al*, 2015).

Furthermore, the level of hTERT mRNA is strongly correlated with the activity of telomerase and induction of this activity induces tumourgenesis (Newbold *et al*, 2002). Recently, telomeric repeat-containing RNA (a long noncoding RNA) which arises from subtelomeric sites has been shown to have a vital role in telomerase homeostasis (Giardini *et al*, 2014).

Approximately 15% of cancer cells are telomerase-independent cells, including soft tissue sarcoma, osteosarcoma, some types of brain cancer such as medulloblastoma, glioblastoma, astrocytoma and oligosarcoma, ovarian carcinoma, breast carcinoma, gastric carcinoma, hepatoblastoma and adrenocortical carcinoma. Many studies have been conducted to identify the mechanism that allows these cells to maintain the length of telomeres, as the average telomere length in cancer cells lacking telomerase is between 3 kb-59 kb (Morrish *et al*, 2013). This mechanism was named alternative lengthening of telomeres (ALT) and was first recognized by Bryan *et al* (1995). ALT is a homologous recombination-based DNA replication pathway and it is regulated through numerous genes, including Rad50, Rad51, MRN complex, SMC5/6, Mus81-EME1 Top3a, FANCD2 and FANCA (Morrish *et al*, 2013).

Importantly, telomerase-negative cancer cells have a unique feature by possessing C-overhang structure (cytosine-rich single-stranded 5' telomeric overhang) and this structure was identified as having a significant role in the ALT mechanism. Thus, 5'-C-overhangs could be targeted in the treatment of telomerase-negative neoplastic cells (Oganesian and Karlseder, 2011; Školáková *et al*, 2015).

#### **1.6.4 The association between telomeric proteins and DNA repair mechanisms**

Many DNA repair proteins exert a vital role in maintenance of telomere length (Slijepcevic, 2006). The telomeric DNA of mammalian cells possesses repetitive noncoding sequences of G-rich oligonucleotides. *In vitro* experiments, which were done under physiological salt conditions, illustrated that; telomeric sequences were folded to generate guanine quadruplex (G4) structures (Smith and Feigon, 1992).

The basic structure of G4 is two or more layers of four guanines. Each layer composed of four guanines, which bind together through Hoogsteen base pairs. Monovalent cations *eg* Na<sup>+</sup> and K<sup>+</sup> fix each layer onto the other (Zhou *et al*, 2013).

Additionally, G4 telomeric structures were implicated in the loss of the stability of telomeres via blocking the action of telomerase. Moreover, they have an essential role in the control of DNA replication, transcription and mRNA translation (Lipps and Rhodes, 2009).

Taking all the previous information together, medical intervention should be targeted toward telomeric guanine quadruplexes in the treatment of tumours (Neidle and Read, 2000; Chen *et al*, 2008). However, many suggestions were raised about the formation of G4 in mammalian cells (Biffi *et al*, 2013). Yang *et al* (2009) first confirmed the existence of G4 structure in human telomeres by designing a novel cyanine dye supramolecular assembly. By this means, more than  $3.0 \times 10^4$  quadruplex sequences in the genomic DNA of vertebrates was estimated (Wu and Brosh, 2010).

Of all the four bases in DNA, guanine is more liable to oxidative damage. Therefore, G4 is the preferred target for oxidative stress, which is produced via DNA charge transport (Coluzzi *et al*, 2014). Oikawa *et al* (2001) examined the influence of UVA irradiation on telomeric sequences in mammalian cells and reported that 8-oxoG was induced over

5 fold more frequently in telomeric DNA than in nontelomeric DNA sequences. This led the authors to conclude that UVA radiation leads to loss of the telomere length via DNA damage at guanine sequences. Moreover, Szalai *et al* (2002) stated that the activity of telomerase is affected by the deleterious effects of the oxidized guanine. Furthermore, shelterin proteins such as TRF1 and TRF2 are disrupted by 8-oxoG (Opresko *et al*, 2005). Further oxidation of 8-oxoG leads to the generation of Gh and Sp and it has been shown that Gh and Sp led to blocking of the DNA polymerase at the telomeric sequences. Thus, the replication of the telomeric DNA will be discontinued (Aller *et al*, 2010).

Therefore, repair of telomeric oxidative DNA lesions should be carried out to preserve genomic integrity. Zhou *et al* (2013) investigated the activity of the mammalian oxidative DNA glycosylases (NTH1, OGG1, NEIL1, NEIL2 and Mmu NEIL3) on telomeric quadruplex guanine; the results showed that Mmu NEIL3 has the ability to excise Tg, Gh and Sp from the damaged telomere, while NEIL1 can remove Sp and Gh from G4. On one hand, the authors found Tg is a preferred substrate for Mmu NEIL3, while on the other, NEIL1 exerts high excisional activity towards Gh in the telomeric DNA. Nonetheless, the authors were unable to identify any physical relation between NEIL3 and shelterin proteins such as TRF1 and TRF2 in mammalian cancer cell lines by co-immunoprecipitation. Moreover, the authors emphasised neither NEIL1, Mmu NEIL3 nor OGG1 have the ability to excise 8-oxoG from the telomeric G4. Therefore, in comparison with the other parts of chromosomes; telomeric DNA has abundant of 8-oxoG lesions. Recently, Zhou *et al* (2015) have confirmed the significant role of both NEIL1 and the DNA glycosylase domain of human NEIL3 on removing the oxidized base damage from telomeres via BER. Thus, the stability of telomeres will be maintained.

### **1.7 Genotoxic drugs**

Since cytotoxic drugs have been incorporated in the management protocol to treat different sorts of tumours, significant improvement in the mortality rate has been observed. Nevertheless, there are some issues, which hinder the effectiveness of these agents. One of the main issues is drug toxicity as the chemotherapeutic drugs destroy both malignant cells and healthy cells. Thus, novel medical interventions should be

discovered to target specific markers of tumour cells. In addition, optimization the chemotherapeutic doses has an essential role in decreasing the side effects of these medications (Pfister *et al*, 2006; Weidmann *et al*, 2014).

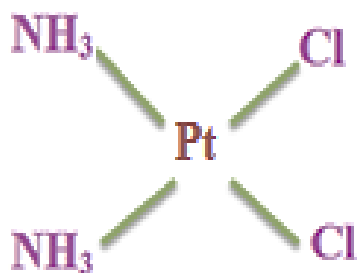
Another issue is drug resistance, which could be inherent or acquired, and it occurs through many mechanisms; changes in the drug target, loss of the drug activity, decline in drug accumulation via elevated drug efflux or reduced drug uptake and avoidance of apoptosis. Therefore, further experiments should focus on the molecular pathways of drug resistance to design new antitumour compounds, which have high sensitivity and specificity (Brabec and Kasparkova, 2005).

### **1.7.1 Cisplatin**

Platinum-derivative compounds such as cisplatin, carboplatin and oxaliplatin are a specific class of chemotherapeutic agents that are widely used by many oncologists to treat patients with tumours (Hato *et al*, 2014).

Cisplatin was first synthesized in 1845 by Michel Peyrone (de Biasi *et al*, 2014). Then Rosenberg *et al* (1965) confirmed the inhibitory effect of cisplatin on *E. coli* cell division. Four years later, Rosenberg discovered the antineoplastic activity of cisplatin in a mouse model. Subsequently, this result led scientists to test cisplatin on human cancer cells. Since that time, cisplatin has become one of the most commonly used antitumour drugs (de Biasi *et al*, 2014).

Cisplatin [cis-diamminedichloroplatinum (II)] is an inorganic metal-based cytotoxic drug, (Figure 1.19) which has been used frequently to treat both children and adult neoplasms such as germ cell, lung, testes, ovary, cervix, bladder, head and neck tumours. Furthermore, cisplatin can be used as monotherapy or in combination with other chemotherapy drugs. Despite the effectiveness of cisplatin in limiting the proliferation of cancer cells, numerous adverse effects have been caused by this drug *e.g.* nephrotoxicity, ototoxicity, peripheral neuropathy and bone marrow suppression (Shiraishi *et al*, 2000).



**Figure 1.19:** Chemical structure of cisplatin (Adapted from Pinato *et al*, 2013).

### **1.7.1.1 Pharmacokinetic properties of cisplatin**

Cisplatin has the ability to enter the cells via the following steps: simple passive diffusion, active transport mechanisms through a protein gate that binds with Na<sup>+</sup> K<sup>+</sup>-ATPase pump, H<sub>2</sub>O phase endocytosis, organic cation transporter (OCT) and copper transporters (CTR1/SLC31A1, ATP7A and ATP7B). While cisplatin efflux, is regulated by melanosomes, ATP7B dependent vesicles, ATP7A protein and MRP1-5 proteins (Hall *et al*, 2008; Burger *et al*, 2010; Amable and Fain, 2014). In the cytoplasm of cells; through hydrolysis, cisplatin losses the chloride ions and generates reactive mono-aqua and di-aqua derivatives. However, these water molecules are positively charged electrophiles, which react with nucleophilic sites on DNA (Mandic *et al*, 2003).

Detoxification of cisplatin occurs via its conjugation with glutathione by glutathione-S-transferase (GSTs), thus, patients with low activity of GSTs have a better response to cisplatin. On the other hand, these patients may suffer from cisplatin toxicity (Roco *et al*, 2014).

### **1.7.1.2 Pharmacodynamic properties of cisplatin**

Cisplatin is an alkylating DNA-damaging agent that inhibits DNA synthesis via a mechanism of DNA cross-links. This mechanism leads to the formation of different types of cisplatin-DNA adducts including intra- and interstrand cross-links (Roco and Cayún, 2014). These adducts occur at the nitrogen in position 7 of guanine (N7) (Pinato *et al*, 2013).

Cisplatin-DNA adducts bend and unwind the DNA leading to impairment in the DNA repair pathways including nucleotide excision repair, mismatch repair and homologous recombinational repair. Finally, the cisplatin modified DNA blocks transcription and DNA replication, subsequently ends in cell apoptosis. Moreover, several studies conducted on cisplatin-induced cell death revealed that two pathways are implicated in cell-cycle arrest, which include the tumour-suppressor protein p53 and the p53-related protein p73 (Jordan and Carmo-Fonseca, 2000; Zhang *et al*, 2010). Although, cisplatin is cell cycle-independent, in a few situations it leads to prolongation of G2 phase cell-cycle arrest (Roco *et al*, 2014).

In addition, cisplatin binds with biomolecular targets other than DNA to exert its antitumour activity such as proteins and RNA (Mandic *et al*, 2003). Interestingly, cisplatin forms DNA-protein cross-links with sulphur-containing proteins such as glutathione and albumin (Wang and Guo, 2007; Pinato *et al*, 2013). Moreover, it was identified that cisplatin has immunogenic effect as it modulates the immune system by the following pathways: cisplatin increases the expression of MHC class I, enhances the growth of macrophages and T lymphocytes, induces the lytic activity of the cytotoxic cells and reduces the immunosuppressive parts of the tumour microenvironment (de Biasi and Adusumilli, 2014).

Zhang *et al* (2010) examined the cytotoxic effect of cisplatin on the HepG2 cell line after abrogation of the XRCC1 gene via transfection of the short hairpin RNAs (shRNA). The results showed that inhibition of XRCC1 enhanced the sensitivity of the malignant cells to cisplatin. Wu *et al* (2003) confirmed that knockdown of XPA by antisense RNA transfection in human lung cell lines decreases the expression of NER and sensitises the malignant cells to cisplatin.

### **1.7.1.3 Mechanisms of cisplatin resistance**

It has been considered that the cellular resistance to cisplatin is multifactorial, which involves limitation in the formation of cisplatin-DNA adducts and prevents apoptosis following cisplatin-induced damage by enhancement of DNA repair mechanisms. In addition, alterations in the influx cellular transporters of cisplatin such as cMOAT, OCT-hSLC22A2, copper transporters and a cis-configuration specific platinum influx

transporter have been attributed to decrease the amount of drug accumulation. Subsequently, this has led malignant cells to acquire resistance to cisplatin treatment (Hall *et al*, 2008; Burger *et al*, 2010). Moreover, a high level of cMOAT mRNA (A multidrug resistance associated protein that is located on 10q24 chromosome) was detected in cisplatin resistant tumour cells (Taniguchi *et al*, 1996).

Much research has been carried out to explore the mechanisms of cisplatin resistance in tumour cells. Jordan *et al* (2000) stated that alterations in the mismatch repair pathway are associated with cisplatin unresponsiveness. In addition, Ferry *et al* (2000) reported that upregulation of the ERCC1 and XPF genes (NER genes) is related to cisplatin resistant cancer cells, while Amable *et al* (2014) concluded that Gli1 (upstream regulator of NER) has an important role in protecting the malignant cells from the DNA damaging effects of cisplatin via its effect on c-jun and ERCC1.

### **1.7.2 tert-butyl hydroperoxide**

Tertiary-butyl-hydroperoxide (*t*-BHP), is a short chain organic hydroperoxide (simple lipophilic alkyl hydroperoxide) that has frequently been used as a model substance to illustrate the biological pathways of oxidative stress in many organs such as renal, liver, brain and skeletal muscle (Haidara *et al*, 2008; Tan *et al*, 2011; Jho *et al*, 2013). *t*-BHP has been found to have a similar mode of action to lipid hydroperoxides, as it generates ROS and produces mitochondrial dysfunction (Cheng *et al*, 2007).

#### **1.7.2.1 Pharmacokinetic properties of tert-butyl hydroperoxide**

*t*-BHP is metabolised by two pathways and both of them lead to oxidative damage. The first pathway is mediated via cytochrome P450, which generates peroxy and alkoxy radicals. The second pathway involves the action of glutathione peroxidase, which ultimately induces *t*-butanol and glutathione ( $\gamma$ -L-glutamyl-L-cysteinylglycine, GSH). However, GSH is oxidized to glutathione disulphide (GSSG) (Cacciatore *et al*, 2010; Tan *et al*, 2011; Kučera *et al*, 2014).



### **1.7.2.2 Pharmacodynamic properties of *tert*-butyl hydroperoxide**

Several articles have investigated the different mechanisms of how *t*-BHP causes cytotoxic biochemical changes. Schnellmann (1988) examined the mechanism of oxidative injury caused by *t*-BHP in the proximal renal tubules of rabbit stating that *t*-BHP exhibits its cytotoxic action via enhancement of lipid peroxidation of polyunsaturated fatty acids, which alters the permeability of the cell membrane. In addition, Buc-Calderon *et al* (1991) reported that *t*-BHP increases the level of intracellular calcium ions and reduces the level of cellular GSH (GSH is a powerful antioxidant protein); both of them lead to apoptotic cell death (Kang *et al*, 2011; Choi *et al*, 2015).

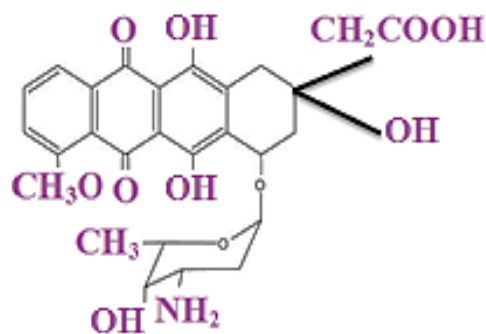
Adams *et al* (1994) recognized that *t*-BHP is a neurotoxic agent that exerts its action through its major metabolite (*tert*-butanol) on different sorts of brain cells (astrocyte cells, oligodendrocyte cells and endothelial cells) and *t*-BHP has a major role in damaging dopaminergic, GABAergic and cholinergic neurons. Furthermore, Guidarelli *et al* (1997) concluded that *t*-BHP induces single-strand DNA breaks and it is implicated in hydrogen peroxide formation.

Haidara *et al* (2002) conducted a study on rat liver cells by applying *t*-BHP to identify the pathogenesis of oxidative stress-induced apoptosis based on cytochrome c as an apoptotic signal. Finally, the author stated two main conclusions. Firstly, the involvement of the cytosolic cytochrome c as it was released from the mitochondrial membrane in response to oxidative damage. Secondly, *t*-BHP induces two types of cell death depending on its concentration; a dose less than 0.4 mM is associated with apoptosis, while a dose higher than 0.4 mM is associated with necrosis. Furthermore, Lin *et al* (2014) stated that *t*-BHP is an oxidative stress-inducing drug that causes oxidative DNA damage in many cells mainly by alkoxy and alkyl radicals.

### **1.7.3 Doxorubicin**

Doxorubicin (DOX), also known as Adriamycin, belongs to the anthracycline group of compounds (Figure 1.20). DOX was the first anthracycline compound to be identified and was first isolated from the soil bacterium *Streptomyces peucetius* var. *caesius* in the 1970's (Thorn *et al*, 2011; Yang *et al*, 2014).

DOX is a highly effective antineoplastic antibiotic, which is commonly used by many oncologists to treat different types of tumours including sarcoma, lymphoma, leukaemia, bladder, liver, lung, thyroid and breast cancer (O'Brien *et al*, 2004; Smith *et al*, 2010; Girotti and Minotti, 2013).



**Figure 1.20:** Chemical structure of doxorubicin (Adapted from Kostrzewa-Nowak *et al*, 2005).

DOX has significant side effects that limit its pharmacological use, such as cardiac contractility dysfunction, which leads to dose-cumulative cardotoxicity and skeletal muscle myopathy. However, it has been identified that DOX-mediated muscle toxicity is mainly caused by the emission of mitochondrial ROS and stimulation of the cysteine protease calpain. Therefore, a highly selective mitochondrial-targeted anti-oxidant agent along with calpain inhibitor should be offered to ameliorate the undesirable effects of DOX on both skeletal and cardiac muscles (Min *et al*, 2015).

Interestingly, molecular studies conducted to understand the mechanism of DOX-induced myopathies, revealed that DOX increases the expression of FoxO (forkhead-box O) gene and that exercise can protect the muscles from DOX toxicity (Kavazis *et al*, 1985). Furthermore, the active metabolite of DOX, doxorubicinol, inhibits the calcium pumps of the endoplasmic reticulum, interferes with the regulation of iron and subsequently leads to the initiation of ROS-induced cell death. Taken together, iron chelator compounds such as dexrazoxane protects the cardiomyocytes from the toxic influences of DOX (Thorn *et al*, 2011).

In addition to the previously mentioned DOX-associated side effects, a single dose of DOX might lead to hair loss, nausea, vomiting, bone marrow suppression and mucositis (O'Brien *et al*, 2004).

### **1.7.3.1 Pharmacokinetic properties of doxorubicin**

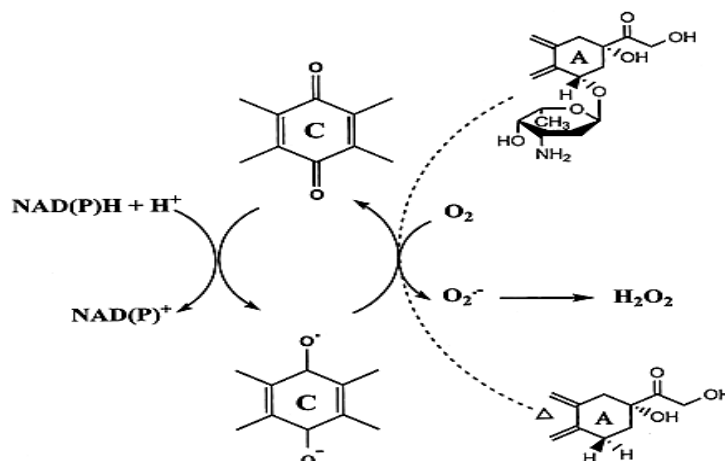
Recently it has been shown that individual genetic differences can influence the pharmacokinetics of DOX. The half-life of DOX presents three phases; between 5 to 10 min, 0.5 to 3 h and 24 to 36 h. About 74%-76% of DOX is bound to albumin. Importantly, DOX is metabolized via liver enzymes then it is excreted through the biliary tract and it is reduced via carbonyl reductases and aldoketoreductases to its active metabolite doxorubicinol. On the other hand, aglycones, glucuronides and sulphates are inactive DOX metabolites (Ryu *et al*, 2014).

### **1.7.3.2 Pharmacodynamic properties of doxorubicin**

Doxorubicin exhibits its anti-cancer activity by blocking the activity of topoisomerase II. Topoisomerase II is an ATP-dependent enzyme, which has two isoforms in eukaryotic cells named topoisomerase II $\alpha$  and topoisomerase II $\beta$ . Interestingly, it has been shown that DOX exerts its anti-neoplastic action via topoisomerase II $\alpha$ , while topoisomerase II $\beta$  is responsible for DOX-mediated cardiotoxicity (Zhang *et al*, 2012; Yang *et al*, 2014). Moreover, topoisomerase II $\beta$  inhibitors conserve the cardiac muscles from the toxicity of DOX. The previous literature confirmed the inhibition of topoisomerase II by DOX prevents DNA synthesis, RNA transcription and replication (Vavrova *et al*, 2013).

DOX is a bioreductive agent that induces free radicals through cellular oxidoreductases such as NADH dehydrogenase, NADPH cytochrome P450 reductase, xanthine oxidase and nitric oxide synthase. However, these oxidoreductases convert DOX to an unstable semiquinone radical through a pathway of one-electron reduction then followed by reoxidation process with oxygen molecule to quinone that ends with the generation of ROS (Kostrzewa-Nowak *et al*, 2005; Finn *et al*, 2011) (Figure 1.21). ROS leads to protein oxidation, lipid peroxidation and DNA cross-linking (Gewirtz, 1999;

Macpherson and Evans, 2009). Recently, it has been shown that DOX generates double-strand DNA breaks around promoters of active genes (Yang *et al*, 2015).



**Figure 1.21:** One-electron redox cycling of doxorubicin. The addition of one-electron to quinone moiety in DOX generates semiquinone, which reproduces quinone through oxygen reduction to ROS. This cycle is enhanced via NADPH oxidoreductases. (Minotti *et al*, 2004).

The cytotoxic impact of DOX on cancer cells can be promoted through the formation of DOX-DNA adducts. DOX has a high tendency to bind to adjacent GC base pairs. However, the linkage of DOX to one strand of DNA is stabilized via a covalent bond between DOX and guanine, which is based on formaldehyde, while DOX is linked to the guanine on the other DNA strand through a hydrogen bond. Importantly, it has been identified that DOX-sensitive neoplastic cells have higher levels of formaldehyde than DOX-unresponsiveness neoplastic cells. Thus, more DOX-DNA adducts have an essential function in increase the responsiveness of tumour cells to DOX (Forrest *et al*, 2012; Yang *et al*, 2014).

DOX-induced apoptosis is also mediated by increase the release of ceramide. Ceramide consists of sphingosine and a fatty acid and is implicated in cellular growth arrest (Senchenkov *et al*, 2001; Kawase *et al*, 2002).

Pang *et al* (2013) identified a novel mechanism that allows anthracycline agents independent of topoisomerase II to cause apoptotic cell death; this mechanism has been termed histone eviction. DOX, which does not trap topoisomerase II, evicts histone

variant H2AX. H2AX has an essential role in the DNA damage signalling pathway. Therefore, H2AX eviction is linked to impairment in the genome repair mechanism.

### **1.7.3.3 Mechanisms of doxorubicin resistance**

Tumour cells are characterized by developing numerous pathways to counteract the toxic effect of DOX. However, high level of MDR1 mRNA, which encodes the membrane-bound glycoprotein, known as P-glycoprotein has been recognized to be related to DOX resistant tumour cells. P-glycoprotein has a high molecular weight of 170 kDa and it functions as a drug discharge pump; therefore, it decreases the accumulating intracellular drug level (Ueda *et al*, 1987; Senchenkov *et al*, 2001). Thus, to reverse the resistance that arises from alteration in P-glycoprotein, a novel delivery method of DOX was designed to treat osteosarcoma resistant tumour cells, namely lipid-modified dextran-based polymeric nanoparticles. This new drug delivery mode enables co-delivery of DOX and MDR1 siRNA and promises to oppose the effect of P-glycoprotein induced DOX resistance in cancer cells (Susa *et al*, 2010). Additionally, Akman *et al* (1990) stated that high levels of glutathione peroxidase mRNA is associated with DOX resistance in tumour cells.

It has been reported that tumour cells which express low levels of topoisomerase II are resistant to DOX, whereas neoplastic cells with high levels of topoisomerase II are sensitive to DOX. Thus, the activity of topoisomerase II could be used to predict the clinical response of malignant cells to topoisomerase II targeted chemotherapeutics (Holden, 1997). In addition, the amplification of human epidermal growth factor receptor-2 (HER-2/ERBB2) which is close to topoisomerase II $\alpha$  on chromosome 17 has been identified to have an association with DOX-resistant cells (Oakman *et al*, 2009; Thorn *et al*, 2011). Additionally, Itoh *et al* (2003) confirmed that low levels of ceramide are associated with DOX-insensitive cells. Furthermore, overexpression of GCS (glucosylceramide synthase enzyme that is responsible for converting ceramide to glucosylceramide) is correlated with loss of response to DOX on tumour cells (Uchida *et al*, 2004).

## **Aims of the project**

Although previous studies have shed light on the biochemical and cellular role of NEIL3, particularly in the developing brain (Hildrestrand *et al*, 2009), the question of why its expression is conserved in vertebrate cells has not been answered. In cancer cells, high levels of NEIL3 have been determined when compared with normal cells. Moreover, recent work has shown that NEIL3 is involved in the excision of hydantoin lesions from telomeric and other G-quadruplex regions in DNA. Therefore, it was hypothesized that NEIL3 might decrease the sensitivity of paediatric tumour cells to certain genotoxic chemotherapeutic compounds. The main purpose of this study was to verify the gene expression of NEIL3, hTERT and POT1 in several paediatric cancer cell lines of different origin and then to determine any association between the levels of NEIL3 expression and the presence or absence of telomerase in these cells. In addition, the sensitivity of ALL and hepatoblastoma cells to cisplatin, doxorubicin and *tert*-butyl hydroperoxide (*t*-BHP) was determined in order to compare the response of these cells to the levels of NEIL3 determined.

## Chapter 2: Materials and Methods

### 2.1 Materials

The materials used in this study include chemicals, kits and primers. All of them are illustrated in the following Tables with their catalogue numbers and the suppliers.

#### 2.1.1 Chemicals

All the chemicals (include reagents, cell culture media, and cytotoxic drugs) required to carry out the experiments are listed in Table 2.1

**Table 2.1: List of Chemical substances**

No	Name of the chemical substances	Supplier company	Catalogue number
1	MEM Non-essential Amino Acid Solution (100×)	Sigma-Aldrich, UK	M7145-100ML
2	Dulbecco's Modified Eagle's Medium (DMEM)	Sigma-Aldrich, UK	D6429-6X500ML
3	RPMI-1640	(SLS) Scientific Laboratory Supplies, UK	LZ12-167F24
4	Lonza McCoy's 5A with glutamine and 25mM Hepes (500 ml)	(SLS) Scientific Laboratory Supplies, UK	LZBE12-168F
5	Foetal bovine serum heat inactivated (FBS)	(SLS) Scientific Laboratory Supplies, UK	F9665-50ML
6	95% Ethanol	Fisher, UK	E/0600/05
7	Penicillin/Streptomycin	Labtech	LM-A4118/100
8	Phosphate buffer saline 10X (PBS)	Fisher, UK	10214733
9	Dimethyl sulfoxide hybri-max sterile filtered (DMSO)	(SLS) Scientific Laboratory Supplies, UK	D2650-5X5ML

10	Trypsin 1X (500 ml)	Labtech	LM-T1705/500
11	L- glutamine 1X (100 ml)	Labtech	XC-T1715/100
12	Boric acid	Fisher, UK	BP168-1
13	Agarose	Bioline, UK	BIO-41025
14	Virkon	Fisher, UK	005414182
15	EDTA-sodium-salt	Sigma-Aldrich, UK	E6760
16	GelRed Nucleic acid stain	Biotinum	41002
17	Hyperladder I marker, 1 kb	Bioline, UK	BIO-33026
18	NaOH	Sigma-Aldrich, UK	S8045-500G
19	Phenazine methosulfate $\geq 90\%$ , (PMS)	Sigma-Aldrich, UK	P9625-1G
20	CellTiter 96AQueous MTS Reagent Powder, 250mg (MTS)	Promega, UK	G1112
21	MTT [3-(4,5-dimethylthiazol-2-yl)- 2,5-diphenyltetrazolium bromide]	Sigma-Aldrich, UK	M2122-5G
22	Cisplatin	Sigma-Aldrich, UK	C2210000
23	Doxorubicin hydrochloride 98.0-102.0% (HPLC)	Sigma-Aldrich, UK	D1515-10MG"
24	<i>tert</i> -butyl hydroperoxide solution 70% (w/v)	Sigma-Aldrich, UK	458139-25ML
25	NaCl B.P. 0.9% (w/v)	Fisher, UK	BP358-1
26	RNase free water.	Fisher, UK	BP561-1
27	Tris base	Fisher, UK	BP152-1
28	2-mercaptoethanol (B-ME)	Sigma-Aldrich, UK	M3148
29	MyTaq Red Mix, 2X	Bioline, UK	BIO-25044
30	Bromophenol blue	Sigma-Aldrich, UK	114391-5G

### **2.1.2 Kits and other lab consumables**

All kits and other lab consumables used in the study are shown in Table 2.2



**Table 2.2: List of kits**

No	Name of kit	Supplier company	Catalogue number
1	ISOLATE II RNA Mini Kit	Bioline, UK	BIO-52072
2	GoScript Reverse Transcription System	Promega, UK	A5000
3	Sensi Fast SYBR Lo-ROX Kit 500 x 20 µl Reactions	Bioline, UK	BIO-94005
4	8-Strip PCR Caps, Flat (X-Clear)	Starlab, UK	I1400-0900
5	96-Well PCR Plate, Skirted, Low-Profile	Starlab, UK	E1403-5209
6	6 well plate standard with lid	Greiner bio-one	657102
7	96 Well Cell Culture Plate Sterile, U-bottom with lid	Greiner bio-one	650180
8	96 Well Cell Culture Plate Sterile, F-bottom with lid	Greiner bio-one	655180

**2.1.3 PCR Primers**

The sequences of primers used to assess the expression of the target genes are shown in Table 2.3, all of them were purchased from Eurofins Genomics.

**Table 2.3: Real time PCR primers**

No	Real time PCR Primers	Sequence 5' to 3'	Tm
1	Gapdh 1014 (Forward)	GGTGGTCTCCTCTGACTTCAACA	61.82°C
2	Gapdh 1140 (Reverse)	GTTGCTGTAGCCAAAATCGTTGT	60.55°C
3	NEIL3 1651 (Forward)	CGCCTCTGCATTGTCCGAGT	62.29°C
4	NEIL3 1798 (Reverse)	TGGAACGCTTGCCATGGTTG	61.80°C
5	TERT 2605 (Forward)	GGAGAACAAGCTGTTTGCGG	60°C
6	TERT 2744 (Reverse)	AGCCATACTCAGGGACACCT	59.96°C
7	POT1 1416 (Forward)	GTCGGGGAATCAGGGTCTTG	60.11°C
8	POT1 1555 (Reverse)	AGAGCTTGGAAGCTGTCGT	59.61°C

**Table 2.4: Composition of buffers**

Buffer	Preparation
0.5 M EDTA (Ethylene diamine tetra acetic acid)	18.61 g EDTA-sodium-salt was dissolved in 70 ml d-H <sub>2</sub> O, NaOH was added to adjust the pH at 8, and then the final volume was made at 100 ml by adding d-H <sub>2</sub> O.
5X TBE (Tris/Borate/EDTA) buffer	54 g Tris was added to 27.5 g Boric acid + 900 ml d-H <sub>2</sub> O, 20 ml 0.5 M (4.65 g) EDTA then the total volume of 1 L was achieved by adding d-H <sub>2</sub> O (pH 8.3)
TE (Tris/EDTA) buffer	0.1 ml of 1 M Tris-HCl was mixed with 0.02 ml of 500 mM EDTA, then through adding NaOH the pH was adjusted to 8
Agarose gel loading buffer	25 mg Bromophenol blue was added to 4 g sucrose and 2.4 ml of 0.5 M EDTA. Finally, d-H <sub>2</sub> O was added to make a total volume of 10 ml.

## 2.2 Methods

### 2.2.1 Cell culture

#### 2.2.1.1 Cell lines

Two main types of cell lines were chosen to conduct different experiments of this research; suspension cells and adherent cells. The suspension cells were two clones of human ALL cell lines: CEM-7-14 and CEM-1-15. On the other hand, the adherent cells were human medulloblastoma TC-32, human hepatoblastoma HepG2 and two types of human osteosarcoma; HOS and Saos-2. The Saos-2 cell line was purchased from Sigma-Aldrich, UK (code number: 89050205-1VL), while HepG2 cell line was a kind gift from Dr Patricia A Ragazzon, University of Salford.

### **2.2.1.2 Growing and maintaining the suspension cells**

CEM-7-14 and CEM-1-15 cell lines were cultured in complete cell culture medium (Table 2.5; RPMI-1640 medium supplemented with 10% foetal bovine serum (FBS), 1% Penicillin/Streptomycin and 2 mM L- glutamine) and they were maintained in a T75 flask. These flasks were incubated at 37°C, 5% CO<sub>2</sub> and a humidified atmosphere.

**Table 2.5: Composition of the complete cell culture media; RPMI-1640, DMEM and McCoy's 5A**

Reagent	Suspension cells	HOS/TC-32	HepG2	Saos-2
RPMI-1640	89 ml	89 ml		
DMEM			89 ml	
McCoy's 5A				89 ml
MEM Non-essential Amino Acid			10 ml	
FBS	10 ml	10 ml	10 ml	10 ml
Penicillin/Streptomycin	1 ml	1 ml	1 ml	1 ml
200 mM L- glutamine	1 ml	1 ml	1 ml	1 ml

### **2.2.1.3 Splitting the suspension cells**

The suspension cells were subcultured every 48-72 h when these cells were 70%-80% confluent. The cells were passaged by transferring them to a sterile 30 ml centrifuge tube (universal tube), and centrifuged for 3 min at 2000 rpm. After the centrifugation was complete, the supernatant was discarded and the cell pellet was resuspended in 2 ml of fresh complete medium. Subsequently, each 1 ml of cell suspension was split in a new flask containing 9 ml of complete medium to obtain a total amount of 10 ml and a dilution of 1:10. Finally, these flasks were returned to the CO<sub>2</sub> incubator.

### **2.2.1.4 Growing and maintaining the adherent cells**

The TC-32 cell line and HOS cell line were grown in RPMI-1640 medium, while Dulbecco's Modified Eagle's Medium (DMEM) was used to grow the HepG2 cells and McCoy's 5A medium was used for the Saos-2 cell line. All the previously mentioned media were supplemented with 10% FBS, 1% Penicillin/Streptomycin and 2 mM L- glutamine as shown in Table 2.4. In addition to that, DMEM medium was supplied with

MEM Non-essential amino acid solution. These cells were cultured in their media in a T75 flask then kept in a humidified atmosphere in a 5% CO<sub>2</sub> incubator at 37°C.

#### **2.2.1.5 Splitting the adherent cells**

The growth of the cells was observed every 2-3 days and the cells split when they were more than 70% confluent. The medium was removed and the cells washed with 8 ml PBS followed by swirling the flask for about 2 min. After that, PBS was replaced with 1 ml trypsin and the flask was incubated at 37°C for 3 min. After this period, the flask was tapped to increase the detachment of the cells, which was confirmed under microscopic examination. Deactivation of the trypsin was achieved by the addition of 10 ml complete medium and the cell suspension was centrifuged for 3 min at 2000 rpm. Cells were suspended in 2 ml of medium and 1 ml transferred to a previously prepared flask with 9 ml of complete cell culture medium.

#### **2.2.1.6 Freezing the suspension cells and the adherent cells**

The freezing medium was prepared by adding 1.8 ml FBS to 200 µl DMSO. The cell pellets of suspension cells and adherent cells were suspended in 2 ml freezing medium. Two aliquots of 1 ml of each cell suspension then added to 2 ml cryovials. After that, the cryovial was transferred to -80°C for 24 h, before the final storage in liquid nitrogen at -196°C.

#### **2.2.1.7 Thawing the suspension cells and the adherent cells**

Frozen cells in cryovial were taken from the liquid nitrogen and placed in a water bath at 37°C for a few minutes. After that, 1 ml of complete medium was added to the cell suspension followed by centrifugation at 2000 rpm for 3 min to avoid the cytotoxic effect of DMSO on the cells. The supernatant was removed and the cell pellet then resuspended in 1 ml of the appropriate complete medium. The cells were then added to a T75 flask containing 9 ml of complete medium and incubated at 37°C, 5% CO<sub>2</sub>

### **2.2.1.8 Cell counting**

Counting of the cells was carried out by taking 500 µl of cell suspension from each flask and transferring them into a universal tube. After that, 10 µl of the cell suspension was transferred onto a haemocytometer and the cells in the four large squares were counted by placing the haemocytometer under the light microscope using the objective 10X. The average cell number was then calculated.

### **2.2.1.9 Time course of cell growth**

The growth pattern of the cells was observed for 96 h to determine the best time for the preparation of the cell pellet and RNA extraction. Each cell line was set up with duplicate flasks containing  $2 \times 10^6$  cells/12 ml medium and the cells were counted every 24 h over a period of 96 h.

### **2.2.1.10 Preparation of cell pellets for RNA extraction**

The time course of cell growth indicated that, all cell lines were in the exponential phase of growth at 72 h and therefore this was a suitable time for analysing and comparing gene expression. Therefore, each cell line was grown for 72 h in a duplicate flask, which was loaded with  $2 \times 10^6$  cells in 10 ml of complete medium. On the third day, the number of cells in four flasks was calculated to insure the increasing in growth rate of these cells. Subsequently the volume of the cell suspension containing  $5 \times 10^6$  cells for four flasks was calculated and centrifuged to form a cell pellet, 1 ml PBS was added and these suspensions transferred to 1.5 ml microcentrifuge tubes. Subsequently, they were centrifuged at 1200  $\times g$  for 5 minutes to form a pellet. The supernatants were discarded and the 1.5 ml microcentrifuge tubes were placed in dry-ice before storage at  $-80^\circ\text{C}$  until used for RNA extraction.

### **2.2.2 RNA extraction**

RNA extraction was carried out from the stored pellets of the different cell lines using the ISOLATE II RNA Mini Kit following the manufacturer's guidelines; 350 µl of

Lysis Buffer was added to the cell pellet followed by 3.5 µl B-ME (2-mercaptoethanol) and mixing on a vortex. The Isolate II Filter was placed in a 2 ml collection tube and the lysate was loaded in it, then it was centrifuged at 11,000 *xg* for 1 min. The flow-through was transferred into a 1.5 ml microcentrifuge tube, then 350 µl of 70 % ethanol was added and mixed by vortexing (2 x 5 s).

Pipetting up and down of the lysate was carried out 3 times before it was transferred to a 2 ml collection tube which was placed in an Isolate II RNA Mini Column and centrifuged at 11,000 *xg* for 30 s. After that, the column was put in a new 2 ml collection tube and the silica membrane was desalted by adding 350 µl of Membrane Desalting Buffer and the membrane was dried through centrifuging at 11,000 *xg* for 1 min.

DNase I reaction mixture was prepared by adding 10 µl of reconstituted DNase I to 90 µl Reaction Buffer for DNase I (RDN) and mixing conducted by gently flicking the tube. Genomic DNA was digested by adding 95 µl DNase I reaction mixture directly onto the centre of the silica membrane and incubated at room temperature for 15 min.

The silica membrane was then washed several times, first by adding 200 µl of Wash Buffer RW1, followed by centrifugation at 11,000 *xg* for 30 s. The second wash was carried out by adding 600 µl Wash Buffer RW2, then it was centrifuged at 11,000 *xg* for 30 s, the flow-through was discarded and the column was placed into a new collection tube. The last wash was achieved by adding 250 µl wash Buffer RW2 followed by centrifugation at 11,000 *xg* for 2 min and the column was placed into a nuclease free 1.5 ml collection tube.

Finally, the RNA was eluted by adding 60 µl RNase-free water directly onto the centre of the silica membrane followed by centrifugation at 11,000 *xg* for 1 min.

Estimation the concentration of RNA in the extracted samples is an important step before proceeding in any molecular experiment, particularly when comparing the gene expression levels between different cell lines. Nucleic acids only absorb a light with 260 nm wavelength. Thus, RNA concentration was measured at 260 nm via a photo-detector in the spectrophotometer (Bustin *et al*, 2009).

The concentration and the purity of the extracted RNA were measured at an absorbance of 260 nm using a Nanodrop 2000 Spectrophotometer (Thermo scientific) by loading 1 µl from the final product of RNA on the Nanodrop machine.

The integrity of the extracted RNA was assessed by using 1% agarose gel electrophoresis, which was prepared by mixing 0.5 g agarose with 50 ml 0.5X TBE in a 100 ml flask then heating the mixture in a microwave oven. After the agarose had cooled, 2 µl GelRed was added and all the contents were placed in a gel tray. Five microliters from each RNA sample was mixed with 3 µl loading buffer and 3 µl d-H<sub>2</sub>O then 2 µl, 4 µl and 5 µl from this mixture was loaded into the gel along with 6 µl Hyperladder I marker (prepared by dissolving 2 µl Hyperladder I and 2 µl loading buffer in 2 µl d-H<sub>2</sub>O). The gel was subjected to electrophoresis at 100 V for 70 min. The bands were imaged and recorded by using UV transillumination Gene snap software.

### **2.2.3 Reverse transcription**

mRNA in the extracted RNA samples was reverse transcribed into cDNA using the GoScript Reverse Transcription System kit (Promega) following the manufacturer's instructions. One microgram of RNA was mixed with 1 µl (0.5 µg) oligo (dT)<sub>15</sub> and nuclease-free water to make a final volume of 5 µl (Table 2.6) and incubated at 70°C for 5 min. Immediately, it was placed in ice for 5 min then centrifuged for 10 s and kept in ice until the reverse transcription mix was added. The reaction mixture for reverse transcription was prepared by mixing 4 µl GoScript 5X reaction buffer with 1.5 µl (1.9 mM) MgCl<sub>2</sub>, 1 µl nucleotide mix (0.5 mM each dNTP), 0.5 µl of recombinant RNasin ribonuclease inhibitor (20 units), 1 µl GoScript reverse transcriptase and 7 µl nuclease free water. The RNA – oligo (dT)<sub>15</sub> was added to the reaction mixture to make a final volume of 20 µl. This was incubated at 25°C for 5 min to ensure annealing of the oligo (dT)<sub>15</sub> to the mRNA, followed by 42°C for 60 min. The reverse transcriptase was inactivated by heating the reaction at 70°C for 15 min.

**Table 2.6: Amount of RNA, oligo (dT)<sub>15</sub> and nuclease-free water which were used to carry out the reverse transcription experiment**

Cell line	Amount of RNA to obtain 1 µg	0.5 µg Oligo (dT) <sub>15</sub>	nuclease-free water
CEM-1-15	2.5 µl	1.0 µl	1.5 µl
CEM-7-14	3 µl	1.0 µl	1 µl
HOS	3.25 µl	1.0 µl	0.8 µl
TC-32	1.6 µl	1.0 µl	2.4 µl
HepG2	1.25 µl	1.0 µl	2.75 µl
Saoa-2	3.7 µl	1.0 µl	0.3 µl

The obtained cDNA was amplified at targeted gene sequences by using specific primers through PCR.

#### **2.2.4 Reverse transcription PCR**

Amplification of cDNA sequences of the target genes (NEIL3, hTERT, POT1 and Gapdh) was carried out through reverse transcription PCR. Three different concentrations of cDNA template were prepared by diluting 1 µl of cDNA with 4 µl TE buffer (1:5), 1 µl cDNA with 9 µl TE (1:10) and one sample was used without dilution. The primers were prepared by diluting 1 µl (100 pmol) with 9 µl TE (1:10). Each cDNA sample was mixed with 2X MyTaq RedMix, forward primer, reverse primer (Table 2.3 illustrates the sequences of the primers) and the total reaction was made up to 25 µl by adding d-H<sub>2</sub>O (Table 2.7). Table 2.8 shows the conditions of the PCR reaction.

**Table 2.7: Composition of the PCR reaction**

PCR reaction	Amount
Template cDNA	1 µl
2X MyTaq RedMix	12.5 µl
10 µM Forward primer	0.5 µl
10 µM Reverse primer	0.5 µl
d-H <sub>2</sub> O	10.5 µl
Total	25 µl



**Table 2.8: PCR conditions, denaturation, Annealing and Extension were set up for 30 cycles.**

PCR Conditions	Temperature	Time	
Pre-denaturation	95°C	1 min	
Denaturation	95°C	10 s	30 Cycles
Annealing	60°C	10 s	
Extension	72°C	10 s	
Final extension	72°C	5 min	
Soak while end	4°C	Hold	

Two microliters from each PCR reaction was mixed with 2 µl loading buffer and 6 µl d-H<sub>2</sub>O then 10 µl was loaded on a 1.5% agarose gel (prepared by mixing 0.75 g agarose with 50 ml 0.5X TBE) along with 10 µl Hyperladder I marker (made by dissolving 1 µl Hyperladder I and 2µl loading buffer in 7 µl d-H<sub>2</sub>O). The gel was subjected to electrophoresis at 100 V for 70 min. The bands were imaged and recorded using UV transillumination and Gene Snap software. Design of hTERT and POT1 primers was achieved through NCBI website (Figures 2.1 and 2.2).

**POT1 cDNA:**

```

1  gtcagtattt cgccaaacct ccaggcgcca tcagtgtgtg aaccgttaacg cagctgggtcc
61  accgcggggcg gagaacaagc gactatgccc agggatcctg cacgcatgcg tggagctgaa
121 ccgtcagcgt gcggtgtgacg tcacctgcgc gcccgcctaa actcttcccta gggttcttcc
181 tagagtacggcagcaagttg tcagattccc tagttgaatt tgctttggac atcagtggtga
241 agcagaactg atatgccact tgaattaata aaggaagtca atggggtgcc tgaagttcag
301 ccgctgagta aattacataa agtagatttc ggatccctac agccaggta caattatagc
361 aagaaatata ttcagggaaa actttcactt atctcttctt taacttatcg tggaaataaa
421 acagctgttt tgcagattgg actacaagga caccattgca gtggctagat ttattgtttt
481 tttagcttct tcacttacia gcagagatgg taaaccttgc atatttttga aagcatttga
541 agacctcaa tcaactgttt atgtttatgt caaatcttta agagattttt ctacagaatc
601 aatgtcttttggttcagcaa caaattatat atatacacc ctgaatcaac ttaagggtgg
661 tacaattgtc aatgtctatg gtgtttgtgaa gttctttaag ccccatatc taagcaaagg
721 aactgattat tgctcagttg taactattgt ggaccagaca aatgtaaac taacttgctt
781 gctcttttagt ggaaactatg aagcccttcc aataatttat aaaaatggag atattgttcc
841 ctttcacagg ctgaagattc aagtatataa aaaggagact cagggtatca ccagctctgg
901 ctttgcactc ttgacgtttg agggaacttt gggagcccct atcatacctc gcacttcaag
961 caagtatttt aacttcaacta ctgaggacca caaatggta gaagccttac gtgtttgggc
1021 atctactcat atgtcaccgt cttggacatt actaaaattg tgtgatgttc agccaatgca
1081 gtattttgac ctgacttgtc agctcttggg caaagcagaa gtggacggag catcatttct
1141 tctaaaggta tgggatggca ccaggacacc atttccatct tggagagtct taatacaaga
1201 cttgttctt gaaggtgatt taagtcacat ccatcggcta caaatctga caatagacat

```

```

1261 tttagtctac gataaccatg ttcattgtggc aagatctctg aagggttgaa gctttcttag
1321 aatctatagc cttcatacca aacttcaatc aatgaattca gagaatcaga caatgttaag
1381 tttagagttt catcttcatt gaggtaccag ttacggtcgg ggaatcaggg tcttgccaga
1441 aagtaactct gatgtggatc aactgaaaaa ggatttagaa tctgcaatt tgacagccaa
1501 tcagcattca gatgttatct gtcaatcaga acctgacgac agctttccaa gctctggatc
1561 agtatcatta tacgaggtag aaagatgtca acagctatct gctacaatc ttacagatca
1621 tcagtatttg gagaggacac cactatgtgc cttttgaaa caaaaagctc ctcaacaata
1681 ccgcatccga gcaaaattga ggtcatataa gcccagaaga ctatttcagt ctgttaaact
1741 tcattgcctt aaatgtcatt tgctgcaaga agttccacat gagggcgatt tggatataat
1801 ttttcaggat ggtgcaacta aaacccaga tgtcaagctc caaaatacat cattatatga
1861 ttcaaaaatc tggaccacta aaaatcaaaa aggacgaaaa gtagcagttc attttgtgaa
1921 aaataatggt attctcccgc tttcaaatga atgtctactt ttgatagaag gaggtacact
1981 cagtgaatt tgcaaactct cgaacaagtt taatagtgtg attcctgtga gatctggcca
2041 cgaagacctg gaacttttgg acctttcagc accatttctt atacaaggaa caatacatca
2101 ctatggatgt aaacagtggt ctagtttgag atccatacaa aatctaaatt ccctgggtga
2161 taaaacatcg tggattcctt cttctgtggc agaagcactg ggtattgtac cctccaata
2221 tgtgtttggt atgaccttta cacttgatga tggaaacagga gtactagaag cctatctcat
2281 ggattctgac aaattcttcc agattccagc atcagaagtt ctgatggatg atgaccttca
2341 gaaaagtgtg gatatgatca tggatatggt ttgtcctcca ggaataaaaa ttgatgcata
2401 tccgtggttg gaatgcttca tcaagtcata caatgtcaca aatggaacag ataatacaat
2461 ttgctatcag atttttgaca ccacagttgc agaagatgta atctaaatatt gccatccaat
2521 ttagcataca taaaatggtg ccaactcact tccctgtttg agcttctttt cctgacctga
2581 gttttgtatc agcaatggtg atgatgttag catgggtatg ggattagaaa atgtccttac
2641 cttaaactc tttgctttta ctgggtgcaa ggtaataaat ggctatggat tttgttttgc
2701 tttctgtttt gcttttgtac aaagagacct gcttaacaa gtactgctga gataagtgtc
2761 tgatcaagct acagtgtact ttaagtagaa atggcaaagt tgctttgttg ggggtgctgat
2821 actgatgatt ttaggataaa ttcatttctt taaacttgta atacatgggt ttattgcttg
2881 tttctctcca ggatagtaga gatttctcta tttcacctca acctataaaa agtggtcaga
2941 tttataatgt taatgactta atattatcct tttctaatag tctcatgtaa aatatgccgc
3001 tattacaact tacaactaat tgaatgagat gtttaacttag taaaatagtt tgatttttac
3061 ctgacagtgt ttgtcaaatt taaaatcatg aatattcaat tttatacaaa catttatata
3121 tatatatata gatttgtgta tgttatttgc caaagacaga tataaattac ctggtttaat
3181 attagtgaag aataaataag tgcacacatt tcaactgttt cttttatttg cctaagttg
3241 agctgaaaaa tgatatgagg caaagaatcg aataggtgt ggcaatgcag cagatgttta
3301 gggctgtcta catcccaggt actgtgctaa gcactaaaca tgtatttgat cctcacagca
3361 acctattttt ccgataagaa atctgaggct tgattgataa gctgacttga ctaagttcac
3421 acagtttgta aaagctagag tctgtgcctt aattcacata atctctattc agagcctgta
3481 ctgttaacca ctcaaggatt ctggaacaga agctaacagt tttctgcaac gagtctttga
3541 cttaaacatc tgaataaaca ttggaatag attataagag gagtcagtgt gtttttctat
3601 agtttcaaaa tacttttaac atcttattgt caaaaagatt ggataactga ctttctttgc
3661 tcataataac tctaaattct agttcctgag tacattaaca catcttcttt acctaacac
3721 caatgtcccc catcatcgac ttatcagctt gtttgagaca atgagaaaga ctgattttat
3781 tttcaagaat atagactcct ggttcaaac attttcagga aaaatatttt aaaacctac
3841 agttgaacag gtgtgtttcc gtgttgatga tgtgctcagg atacaaaggt gaaataaaca
3901 tttttctgac cttcaggaag cctcaatct agaagagtag aggtccaaag gtgccatag
3961 ttcacactgt gagcctgcaa gatctccagc ttaacaaagg aaaactcttc ctatgaatct
4021 tcatgatgat aggccatgtc tcttcttatt tttgttttaa ataaacatcc accttatcat
4081 ga aaaaaaaaa aaaaa

```

**Figure 2.1:** Human POT1 cDNA. The position of the PCR primers used in this study are indicated in red.

## hTERT cDNA

```
1 caggcagcgc tgcgtcctgc tgcgcacgtg ggaagccctg gccccggcca cccccgcgat
61 gcccgcgcgt ccccgctgcc gagccgtgcg ctccctgctg cgcagccact accgcgaggt
121 gctgccgctg gccacgttcg tgcggcgcct ggggccccag ggtggcgggc tggcgcagcg
181 cggggacccg gcggccttcc gcgcgctggt ggcccagtgc ctgggtgtgcg tgccctggga
241 cgcacggccg cccccgcgcg cccctcctt ccgccaggtg tctgctga aggagctggt
301 ggcccagagt ctgcagaggc tgtgcgagcg cggcgcgaag aacgtgctgg ccttcggctt
361 cgcgctgctg gacggggccc gcgggggccc ccccaggcc ttaccacca gcgtgcgcag
421 ctacctgcc aacacggtga ccgacgcact gcgggggagc gggcgctggg ggctgctgct
481 gcgccgcgtg ggcgacgacg tgctggttca cctgctggca cgctgcgcgc tctttgtgct
541 ggtggctccc agctgcgcct accaggtgtg cgggcccgcg ctgtaccagc tcggcgtgc
601 cactcaggcc cggccccgc cacaagctag tggacccga aggcgtctgg gatgcaaacg
661 ggcttgaac catagcgtca gggaggccgg ggtccccctg ggctgccag cccgggtgc
721 gaggaggcgc gggggcagtg ccagccgaag tctgccgtt cccaagaggc ccaggcgtgg
781 cgctgcccct gagccggagc ggacgcccgt tgggcagggg tctgggccc acccggcag
841 gacgcgtgga ccgagtgacc gtggtttctg tgtggtgtca cctgccagac ccgccgaaga
901 agccacctct ttggagggtg cgctctctg cagcgcacc tcccacccat ccgtgggccc
961 ccagcaccac gcgggcccc catccacatc gcggccacca cgtccctggg acagccttg
1021 tccccgggtg tacgccgaga ccaagcactt cctctactcc tcaggcgaca aggagcagct
1081 gcggccctcc ttctactca gctctctgag gccagcctg actggcgctc ggaggctcgt
1141 ggagaccatc tttctgggtt ccaggccctg gatgccaggg actccccga ggttgccccg
1201 cctgcccag cgctactggc aatgcccggc cctgtttctg gagctgcttg ggaaccacgc
1261 gcagtgccc tacggggtgc tctcaagac gcactgccc ctgcgagctg cggtcacccc
1321 agcagccggt gtctgtgccc gggagaagcc ccagggctct gtggcggccc ccgaggagga
1381 ggacacagac ccccgctgcc tggcgcagct gctccgccag cacagcagcc cctggcaggt
1441 gtacggcttc gtgcgggctt gctgcgcgc gctggtgccc ccaggcctct ggggctccag
1501 gcacaacgaa cgccgcttc tcaggaacac caagaagttc atctccctgg ggaagcatgc
1561 caagctctcg ctgcaggagc tgacgtgaa gatgagcgtg cgggactgcg cttggctgcg
1621 caggagccca ggggttggct gtgttccggc cgcagagcac cgtctgcgtg aggagatcct
1681 ggccaagttc ctgcaactgc tgatgagtg gtacgtcgtc gagctgctca ggtctttctt
1741 ttatgtcag gagaccacgt ttcaaaagaa caggctcttt ttctaccgga agagtgtctg
1801 gagcaagttg caaagcattg gaatcagaca gcacttgaag agggcgcagc tgcgggagct
1861 gtcggaagca gaggcagcc agcatcggga agccaggccc gcctgctga cgtccagact
1921 ccgcttcac cccaagcctg acgggctgcg gccgattgtg aacatggact acgtcgtggg
1981 agccagaacg ttccgcagag aaaagagggc cgagcgtctc acctcgaggg tgaaggcact
2041 gttcagcgtg ctcaactacg agcgggcccg gcgccccggc ctccctgggg cctctgtgct
2101 gggcctggac gatatccaca gggcctggcg caccttcgtg ctgcgtgtgc gggcccagga
2161 cccgcccct gagctgtact ttgtcaaggt ggatgtgacg ggcgcgtacg acaccatccc
2221 ccaggacagg ctcacggagg tcatgccag catcatcaa cccagaaca cgtactcgt
2281 gcgtcggat gccgtggtcc agaaggccc ccatgggccc gtcgcgaagg ccttcaagag
2341 ccacgtctct accttgacag acctccagcc gtacatgcga cagttcgtgg ctcacctgca
2401 ggagaccagc ccgctgaggg atgccgtcgt catcgcagcag agtcctccc tgaatgaggc
2461 cagcagtggc ctcttcgacg tcttctacg cttcatgtgc caccagccg tgcgcacag
2521 gggcaagtcc tacgtccagt gccaggggat cccgcagggc tccatcctct ccacgctgct
2581 ctgcagcctg tgctacggcg acatggagaa caagctgttt ggggggatte ggcgggacgg
2641 gctgctcctg cgtttggtgg atgatttctt gttggtgaca cctcacctca cccacgcgaa
2701 aaccttctc aggaccctgg tccgaggtgt ccctgagtat ggctgcgtgg tgaacttgcg
2761 gaagacagtg gtgaacttcc ctgtagaaga cgaggccctg ggtggcacgg cttttgttca
2821 gatgccggcc cacggcctat tcccctggtg cggcctgctg ctggataccc ggaccctgga
2881 ggtgcagagc gactactcca gctatgccg gacctccatc agagccagtc tcaacttcaa
2941 ccgccccttc aaggctggga ggaacatgcg tcgcaaactc tttggggtct tgcggctgaa
3001 gtgtcacagc ctgtttctgg atttgcaggt gaacagcctc cagacgggtg gcaccaacat
```

```

3061 ctacaagatc ctctgctgc aggcgtacaggtttcacgca tgtgtgctgc agctcccatt
3121 tcacagcaa gtttgaaga accccacatt tttcctgcgc gtcacatctg acacggcctc
3181 cctctgctac tccatcctga aagccaagaa cgcagggatg tcgctggggg ccaagggcgc
3241 cgccggccct ctgccctccg aggcctgca gtggctgtgc caccaagcat tctgctcaa
3301 gctgactcga caccgtgtca cctacgtgcc actcctgggg tcactcagga cagcccagac
3361 gcagctgagt cggaagctcc cggggacgac gctgactgcc ctggaggccg cagccaaccc
3421 ggcaactgcc tcagacttca agaccatcct ggactgatgg ccaccgccc acagccaggc
3481 cgagagcaga caccagcagc cctgtcacgc cgggctctac gtcccaggga gggagggcg
3541 gccacaccc aggcccgcac cgctgggagt ctgaggcctg agtgagtgtt tggccaggc
3601 ctgcatgtcc ggctgaaggc tgagtgtccg gctgaggcct gagcagagtgt ccagccaagg
3661 gctgagtgtc cagcacacct gccgtcttca ctccccaca ggtggtgctc cggctccacc
3721 ccagggccag cttttcctca ccaggagccc ggcttccact cccacatag gaatagtcca
3781 tccccagatt cgccattggt caccctcgc cctgccctcc tttgcttcc acccccacca
3841 tccaggtgga gaccctgaga aggaccctgg gagctctggg aatttgaggt gaccaaaggt
3901 gtgccctgta cacaggcgag gaccctgcac ctggatgggg gtcctgtggt gtcaaattgg
3961 ggggaggtgc tgtgggagta aaatactgaa tatatgagtt tttcagtttt gaaaaaaa

```

**Figure 2.2:** Human TERT cDNA. The position of the PCR primers used in this study are indicated in red.

### **2.2.5 Quantitative real time PCR (qRT-PCR)**

In this study, qRT-PCR was conducted to quantify the expression of the target genes (which include NEIL3, hTERT, POT1 and Gapdh) on cDNA from different paediatric cell lines using the Sensi Fast SYBR Lo-ROX Kit (Bioline) according to the manufacturer's instructions. The reference gene for normalisation was Gapdh and melting curves were used to confirm the specificity of the PCR primers.

Each 5 µl of cDNA from the reverse transcription reaction (20 µl) was mixed with 45 µl of TE to obtain a final volume of 50 µl and then a standard curve was obtained by a 10-fold serial dilution which was made as follows: 100%, 10%, 1%, 0.1% and 0% cDNA by the following steps:

10%: 8 µl from 100% of cDNA sample was added to 72 µl RNase free water.

1%: 8 µl from 10% was added to 72 µl RNase free water.

0.1%: 8 µl from 1% was added to 72 µl RNase free water.

0%: 72 µl RNase free water.

Triplicate aliquots of 5 µl cDNA template were then added to the wells of a 96-well reaction plate as detailed in Table 2.9. The PCR primers were prepared by diluting 1 µl (100 pmol) with 9 µl TE to give a final concentration of 10 pmol/ µl. For each PCR reaction mix, 18.5 µl forward primer, 18.5 µl reverse primer, 230 µl 2x SensiFast SYBR Lo-ROX (containing SYBR Green I dye and dNTPs) and 78 µl RNase free water were

mixed in a 1.5 ml microcentrifuge tube and then 15  $\mu$ l was distributed in each well as appropriate (see Table 2.10). Negative control wells have forward primer, reverse primer, 2x SensiFast SYBR Lo-ROX and RNase free water. The qRT-PCR was prepared in triplicate in a 96-well plate and the wells were loaded as revealed in Table 2.10.

**Table 2.9: Loading of the 10-fold serially diluted cDNA in triplicate in a 96-well plate**

100%	10%	1%	0.1%	0%
B1,B6,B11, C4,C9,D2, D7,D12,E5, E10,F3,F8	B2,B7,B12, C5,C10,D3, D8,E1,E6, E11,F4,F9	B3,B8,C1, C6,C11,D4, D9,E2,E7, E12,F5,F10	B4,B9,C2, C7,C12,D5, D10,E3,E8, F1,F6,F11	B5,B10,C3, C8,D1,D6, D11,E4,E9, F2,F7,F12

**Table 2.10: Loading of a 96-well plate**

Primer	Sample	Standard	Negative Control
TERT	A1,A2,A3	B1,B2,B3,B4,B5 C9,C10,C11,C12,D1 E5,E6,E7,E8,E9	G1,G2,G3
POT1	A4,A5,A6	B6,B7,B8,B9,B10 D2,D3,D4,D5,D6 E10,E11,E12,F1,F2	G4,G5,G6
NEIL3	A7,A8,A9	B11,B12,C1,C2,C3 D7,D8,D9,D10,D11 F3,F4,F5,F6,F7	G7,G8,G9
Gapdh	A10,A11,A12	C4,C5,C6,C7,C8 D12,E1,E2,E3,E4 F8,F9,F10,F11,F12	G10,G11,G12

Two-step cycling was used for the PCR reaction and the conditions are given in Table 2.11

**Table 2.11: qRT-PCR conditions**

Cycles	Temperature	Time	PCR phase
1	95°C	2 min	Denaturation
40	95°C	5 s	Denaturation
	60°C	30 s	Annealing/ Extention

Melting curve from 72°C to 90°C, reading every 1°C, hold at 30 s.

Analysis of the results was conducted through MJ Optocon Monitor version 3.1 software and the relative expression of the target gene in each cell line was calculated via normalization of its mRNA quantitative values with the values of Gapdh using the following equation:

$$\text{Relative mRNA level of the target gene} = \frac{\text{Numerical value of target gene expression}}{\text{Numerical value of Gapdh expression}}$$

## **2.2.6 Cytotoxicity assays**

Two experiments; MTS assay and MTT assay were conducted to analyse the cell proliferation in presence of the cytotoxic drugs: cisplatin, doxorubicin and *tert*-butyl hydroperoxide.

### **2.2.6.1 MTS assay (cell Titer 96 AQueous Non-Radioactive Cell Proliferation)**

This tetrazolium dye; [3-(4,5-dimethylthiazol-2-yl)-5-(3-carboxymethoxyphenol)-2-(4-sulfophenyl)-2H-tetrazolium, inner salt] in the presence of an electron coupling reagent (phenazinemethosulfate; PMS) is characterized by its ability to be reduced via NAD or NADP dependent dehydrogenase enzymes to a water-soluble formazan. Therefore, there is no need to wash the cells or extracting the dye after adding (Buttke *et al*, 1993; Dunigan *et al*, 1995). The MTS assay was conducted on the suspension cells CEM-7-14

and CEM-1-15 to determine the concentration of a drug required to inhibit the growth by 50% (IC<sub>50</sub>). The preparation was carried out as detailed in Table 2.12.

**Table 2.12: Preparation of MTS solution**

Reagent	Composition
MTS	21 ml PBS+ 0.042 g
PMS	5 ml PBS + 0.0046 g

Finally 3 ml MTS was added to 150 µl PMS.

The drugs examined by this assay were: cisplatin, doxorubicin and *tert*-butyl hydroperoxide. Each well of a U-shaped 96-well plate was loaded with 2000 cells in 100 µl of RPMI complete medium. Seven, 2-fold serially diluted drug solutions were prepared as follows:

Eight, 1.5 ml microcentrifuge tubes were labelled from 1 to 8. Tube number 8 was the control (it does not have drug). Two millilitres of complete medium was put into tube 1, while 1 ml of medium was put into the remaining tubes. The desired amount of the drug was added to tube 1 as detailed in Table 2.13 and mixed. Then, 1 ml from this tube was taken and mixed with the medium in tube 2. This step was repeated for the remainder of the tubes until tube 7. Then triplicate aliquots of 100 µl were added to the wells of a 96-well plate as shown in Table 2.14. Finally, the 96-well plate was incubated for 72 h at 37°C in a humidified, 5% CO<sub>2</sub> atmosphere. After this incubation period, 40 µl of combined MTS / PMS solution was added to each well and incubated again for 3 h at 37°C in a humidified, 5% CO<sub>2</sub> atmosphere. Finally, the absorbance at 490nm was recorded using Multiscan Ascent/Thermo lab system ELISA reader and Ascent software. Then MTT template was used to analyze the results obtained.

**Table 2.13: Drug preparation**

Drug	Drug preparation	The amount of drug which was added to tube 1	Final Drug Concentration ( <i>i.e.2x</i> )
Cisplatin	1 mg + 1 ml NaCl 0.9% (w/v) (3.3 mM)	30 $\mu$ l (3.3 mM) + 1970 $\mu$ l medium	<b>50 <math>\mu</math>M</b>
Doxorubicin	17.2 ml PBS added to 10 mg (1 mM), then 10 $\mu$ l + 990 $\mu$ l PBS (10 $\mu$ M)	40 $\mu$ l (10 $\mu$ M) + 1960 $\mu$ l medium	<b>200 nM</b>
<i>tert</i> -Butyl hydroperoxide solution 70% (w/v)	10 $\mu$ l (7.77 M) + 67.7 $\mu$ l d-H <sub>2</sub> O = 1 M, then 10 $\mu$ l (1 M) + 990 $\mu$ l de-H <sub>2</sub> O = 10 mM	100 $\mu$ l (10 mM) + 1900 $\mu$ l medium	<b>500 <math>\mu</math>M</b>

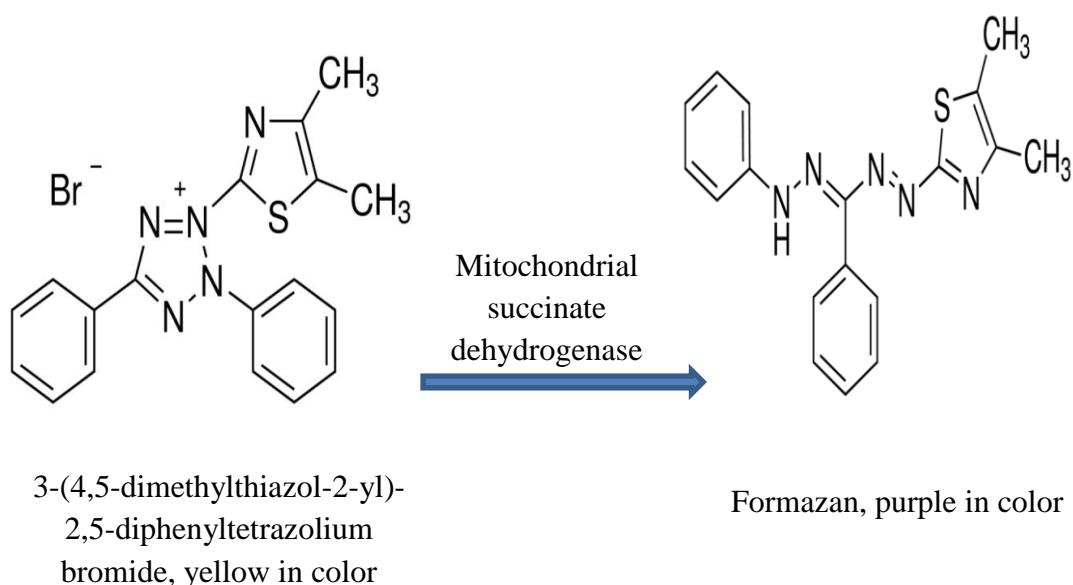
**Table 2.14: Loading of the 96-well plate**

Row of the 96-well plate	Tube contains the drug
Row A	Tube 8
Row B	Tube 7
Row C	Tube 6
Row D	Tube 5
Row E	Tube 4
Row F	Tube 3
Row G	Tube 2
Row H	Tube 1



### 2.2.6.1 MTT assay

MTT assay is a colorimetric test, used to assess the cells viability to cytotoxic compounds via using Tetrazolium salt (MTT solution); 3-(4,5-dimethylthiazol-2-yl)-2,5-diphenyltetrazolium bromide. This yellow water soluble reagent is metabolized in the dividing cells by mitochondrial succinate dehydrogenase to a purple water insoluble formazan, which accumulates in the cells and is dissolved by adding DMSO. Through a microplate reader, the absorbance of the produced formazan is measured at 570 nm (Figure 2.3) (Talorete *et al*, 2006; Massignan *et al*, 2011).



**Figure 2.3:** Reaction of thiazolyl blue tetrazolium blue with mitochondrial succinate dehydrogenase.

This method was carried out on adherent cells; HepG2 cell line. A density of  $2 \times 10^3$  cells was plated in each well of a flat-shaped 96-well plate containing 100  $\mu$ l of complete DMEM medium and incubated in a humidified atmosphere in 5%  $\text{CO}_2$  at  $37^\circ\text{C}$  for 24 h. After the incubation period was completed, the cells were treated with one of the cytotoxic drugs; cisplatin, doxorubicin or *tert*-butyl hydroperoxide (Table 2.12) and the plates prepared as described for the MTS assay. Then the plate was incubated at  $37^\circ\text{C}$ , 5%  $\text{CO}_2$  with a humidified atmosphere for 72 h. On third day of incubation, 50  $\mu$ l of MTT reagent (made by dissolving 3 mg of MTT in 1 ml PBS) was added to each

well of the 96-well plate. Again, the plate was incubated in 5% CO<sub>2</sub> at 37°C in a humidified atmosphere for 3 h.

The supernatant was aspirated and 200 µl DMSO was added to each well. After that, the difference in the optical density between the sample absorption wavelength (570 nm) and the reference wavelength (650 nm) was calculated through Ascent software and Multiscan Ascent/Thermo lab system ELISA reader. Then MTT template was used to analyze the data obtained.

### **2.2.7 qRT-PCR on treated HepG2 cells**

The HepG2 cell line was used as a model to evaluate the influence of oxidative stress on NEIL3, hTERT and POT1 by qRT-PCR. 5 x10<sup>4</sup> cells were seeded per well in 2 ml of complete DMEM medium in a 6-well plate, which was then incubated for 24 h at 37°C in a humidified, 5% CO<sub>2</sub> atmosphere. After 24 h, the cells were treated with, 2.5 µM or 5 µM of *tert*-butyl hydroperoxide solution (prepared as described below) and incubated for 72 h at 37°C in a humidified, 5% CO<sub>2</sub> atmosphere.

After 72 h, the cells were trypsinised, counted and pellets prepared for RNA extraction. Following the extraction of RNA, reverse transcription PCR was carried out. Triplicate aliquots of 5 µl cDNA template HepG2 were used to run qRT-PCR reaction with NEIL3, hTERT and POT1 using the Sensi Fast SYBR Lo-ROX Kit. The reference gene was Gapdh and the fluorescent dye was SYBR Green I.

#### **2.2.7.1 Preparation of 2.5 µM and 5 µM *tert*-butyl hydroperoxide solution**

Ten microliters of the 70% (w/v) stock solution of *tert*-butyl hydroperoxide solution was added to 66.7 µl of d-H<sub>2</sub>O to produce a 1 M solution then 10 µl of the 1 M solution was added to 990 µl of d-H<sub>2</sub>O to produce a 10 mM solution. Finally, 10 µl of the 10 mM solution was added to 990 µl of DMEM medium to produce a 100 µM solution. For 2.5 µM, 200 µl of the 100 µM stock solution was mixed with 3.8 ml of cell culture medium and 2 ml transferred to each of two wells. While 5 µM was prepared by mixing 400 µl of the 100 µM stock solution with 3.6 ml of cell culture medium and 2 ml transferred to each of two wells. The 6-well plate was loaded as showed in Table 2.15.

**Table 2.15: Loading of the 6-well plate**

Row	Content
Row A	Control
Row B	2.5 $\mu$ M drug concentration
Row C	5 $\mu$ M drug concentration

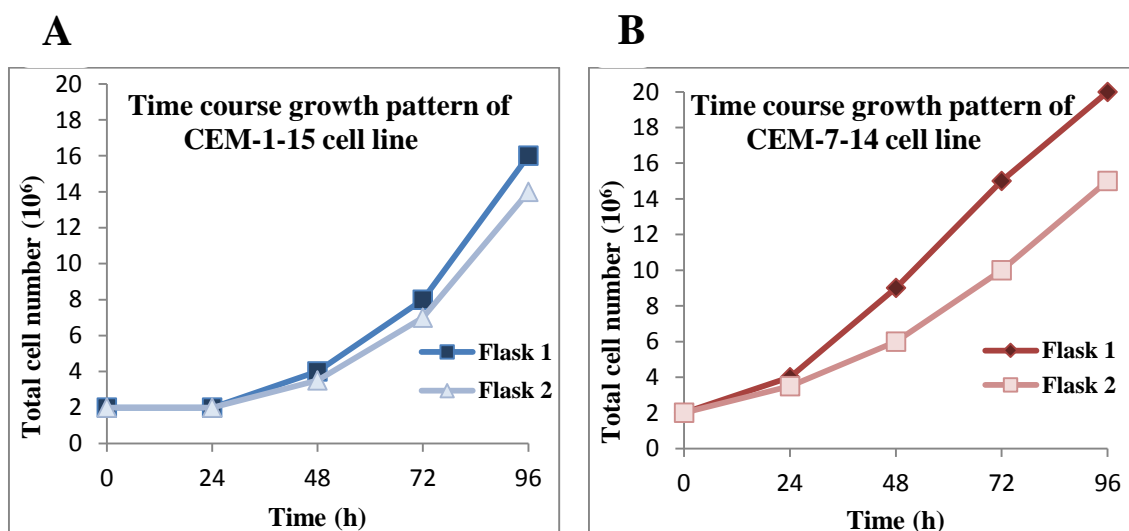
## Chapter 3: Results

Statistical analysis of data was carried out by ANOVA and t-test. Results were expressed by average and standard deviation. In addition, the relation between different parameters were assessed by *P* value.  $P < 0.05$  was considered as statistical significance.

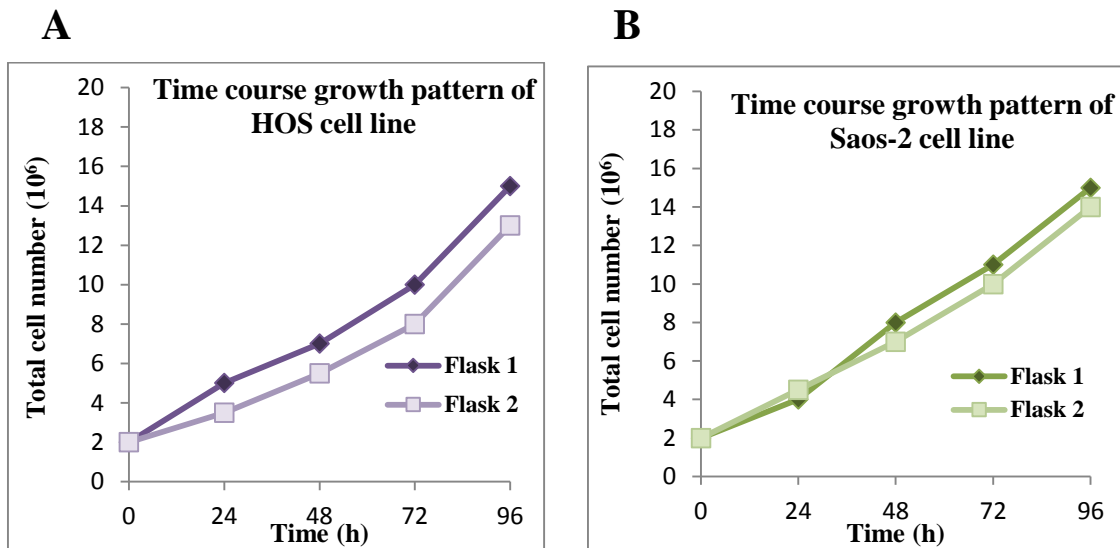
### 3.1 Identification of the exponential growth phase of each cell line

The cell growth curve is divided into three phases; lag, exponential and stationary phase. During the lag phase, the cells adjust to the new environmental conditions before starting to grow in the exponential phase. Here, cellular proliferation increases significantly in relation to time in the exponential phase, while the stationary phase is characterized by inert cell division and this phase has a mixed of dying and living cells as all the nutrients have been consumed by the growing cells. Therefore, the target growth phase for conducting the gene expression analyses is the exponential phase (Rolfe *et al*, 2012).

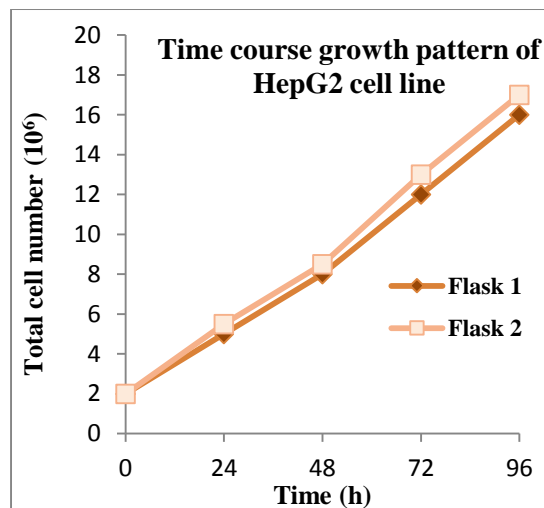
The growth of the CEM-1-15, CEM-7-14, HOS, Saos2, TC-32 and HepG2 cell lines was examined for 96 h and plotted against time in a line graph (Figures 3.1 to 3.4).



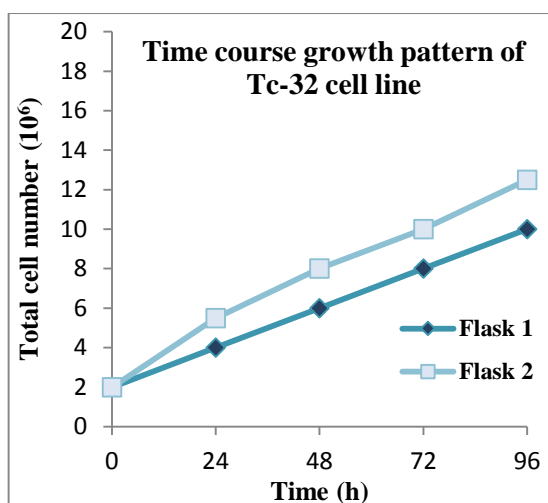
**Figure 3.1:** Growth curve of ALL cells over a period of 96 h. (A) Each flask represents CEM-1-15 cells. (B) Each flask represents CEM-7-14 cells.  $2 \times 10^6$  cells were used as a total cell number per flask. Cell counting was carried out every 24 h for a period of 96 h.



**Figure 3.2:** Growth curve of osteosarcoma cell lines over a period of 96 h. (A) Each flask represents HOS cells. (B) Each flask represents Saos-2 cells.  $2 \times 10^6$  cells were used as a total cell number per flask. Cell counting was carried out every 24 h for a period of 96 h.



**Figure 3.3:** Growth curve of hepatoblastoma cells over a period of 96 h. Each flask represents HepG2 cells.  $2 \times 10^6$  cells were used as a total cell number per flask. Cell counting was carried out every 24 h for a period of 96 h.



**Figure 3.4:** Growth curve of medulloblastoma cells over a period of 96 h. Each flask represents Tc-32 cells.  $2 \times 10^6$  cells were used as a total cell number per flask. Cell counting was carried out every 24 h for a period of 96 h.

The results showed that the growth pattern for CEM-1-15 cell line remained in a plateau phase in the first 24 h as the cell number of this cell line is constant (Figure 3.1). After this period, the cells show a robust activity of cellular proliferation with a doubling time of 24 h. On the other hand, CEM-7-14, Saos2, HOS, HepG2 and TC-32 cell lines displayed a faster growth rate entering the exponential growth with a doubling time in the initial 24 h (Figures 3.1 to 3.4).

### **3.2 RNA extraction from the cancer cell lines**

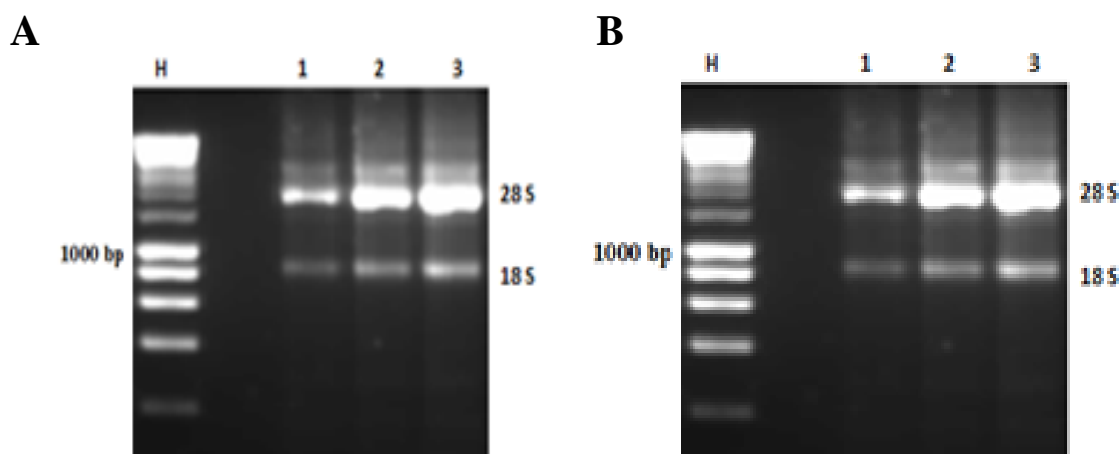
Total RNA was extracted from the different cell lines using ISOLATE II RNA Mini Kit (Section 2.2.2). The concentration of the extracted RNA was determined by spectrophotometry using a Nanodrop 2000. As well as the  $OD_{260}$ , the 260/280 ratio was determined to check the level of protein contamination and the 260/230 ratio was determined to assess the carryover of organic materials during RNA extraction (Table 3.1).

The purified RNA was then subjected to 1% agarose gel electrophoresis to check for degradation of the RNA by visualising the two principal rRNA species; 28 S and 18 S (Figures 3.5 to 3.8).

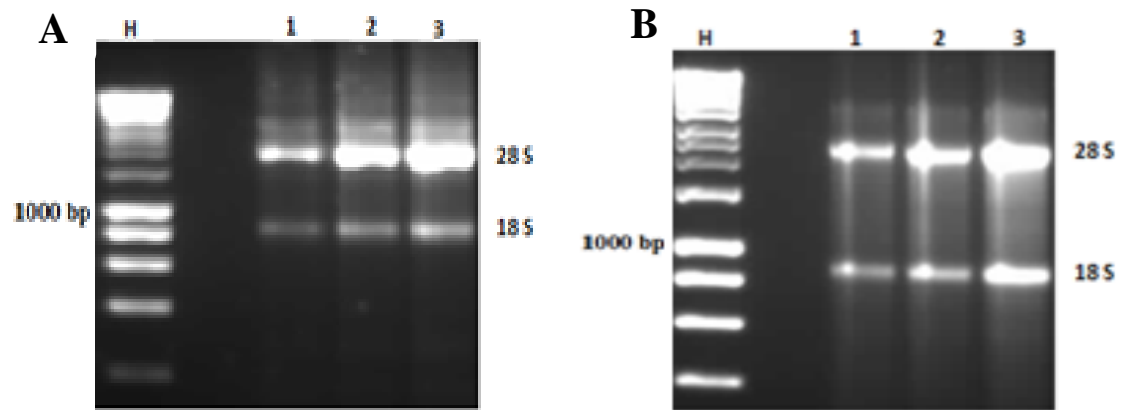
**Table 3.1: The concentration and the purity of RNA**

Cell lines	Concentration	260/280	260/230
CEM-1-15	400 ng/ $\mu$ l	2.07	2.09
CEM-7-14	327 ng/ $\mu$ l	2.07	2.1
HOS	308 ng/ $\mu$ l	2.04	2.07
TC-32	621 ng/ $\mu$ l	2.19	2.2
HEPG-2	800 ng/ $\mu$ l	2.02	2.04
Saos-2	267 ng/ $\mu$ l	2.07	2.1

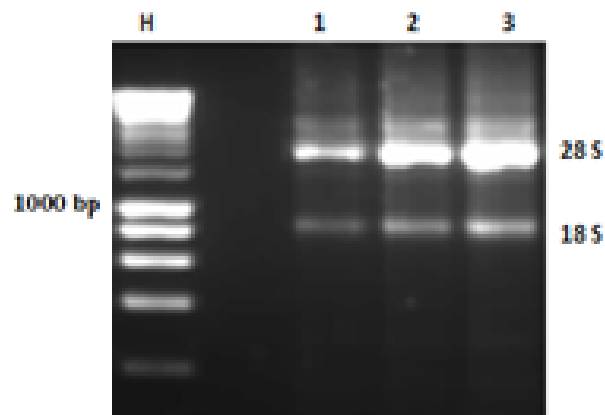
Comparing the RNA concentration in six different cell lines, HepG2 cells have the highest RNA concentration. On the other hand, Saos-2 cells have the lowest concentration. In terms of RNA purity, TC-32 cells have the maximum 260/230 ratio of RNA purity, while the 260/230 ratio of RNA purity is lowest in HepG2 (Table 3.1).



**Figure 3.5:** Agarose gel electrophoresis of extracted total RNA from the ALL cell lines. (A) CEM-1-15 cell line. (B) CEM-7-14 cell line. Lane H contains Hyperladder I, while sample 1, 2 and 3 are shown in lanes 1, 2 and 3 respectively. 5  $\mu$ l from each RNA sample was mixed with 3  $\mu$ l loading buffer and the final volume of 11  $\mu$ l was achieved via adding d-H<sub>2</sub>O then 2  $\mu$ l, 4  $\mu$ l and 5  $\mu$ l were loaded as sample 1, 2 and 3 respectively in 1 % agarose gel along with 6  $\mu$ l Hyperladder I.

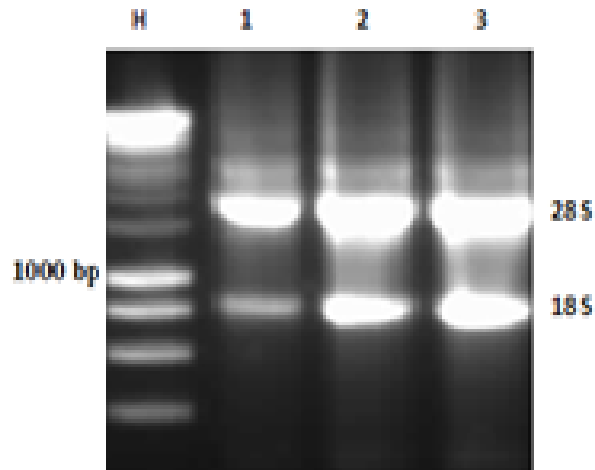


**Figure 3.6:** Agarose gel electrophoresis of extracted total RNA from the osteosarcoma cell lines. (A) HOS cell line. (B) Saos2 cell line. Lane H contains Hyperladder I, while sample 1, 2 and 3 are shown in lanes 1, 2 and 3 respectively. 5  $\mu$ l from each RNA sample was mixed with 3  $\mu$ l loading buffer and the final volume of 11  $\mu$ l was achieved via adding d-H<sub>2</sub>O then 2  $\mu$ l, 4  $\mu$ l and 5  $\mu$ l were loaded as sample 1, 2 and 3 respectively in 1 % agarose gel along with 6  $\mu$ l Hyperladder I.



**Figure 3.7:** Agarose gel electrophoresis of extracted total RNA from the medulloblastoma cell lines (TC-32 cells). Lane H contains Hyperladder I, while sample 1, 2 and 3 are shown in lanes 1, 2 and 3 respectively. 5  $\mu$ l from each RNA sample was mixed with 3  $\mu$ l loading buffer and the final volume of 11  $\mu$ l was achieved via adding d-H<sub>2</sub>O then 2  $\mu$ l, 4  $\mu$ l and 5  $\mu$ l were loaded as sample 1, 2 and 3 respectively in 1 % agarose gel along with 6  $\mu$ l Hyperladder I.





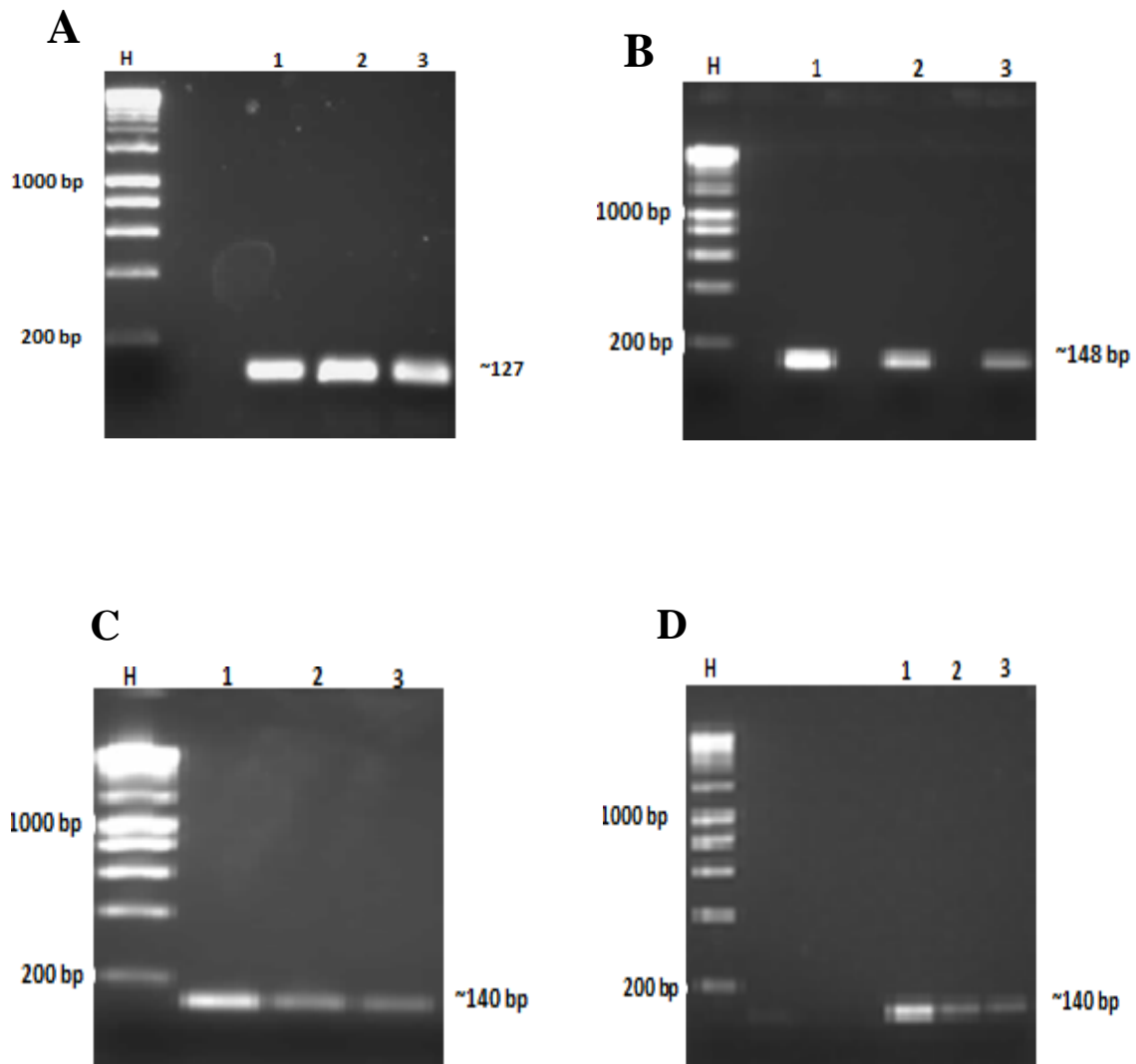
**Figure 3.8:** Agarose gel electrophoresis of extracted total RNA from the hepatoblastoma cell lines (HepG2). Lane H contains Hyperladder I, while sample 1, 2 and 3 are shown in lanes 1, 2 and 3 respectively. 5  $\mu$ l from each RNA sample was mixed with 3  $\mu$ l loading buffer and the final volume of 11  $\mu$ l was achieved via adding d-H<sub>2</sub>O then 2  $\mu$ l, 4  $\mu$ l and 5  $\mu$ l were loaded as sample 1, 2 and 3 respectively in 1 % agarose gel along with 6  $\mu$ l Hyperladder I.

The results reveal the thickness of 28 S in all cell lines is almost twice larger than that in 18 S. In addition, there is no genomic DNA contamination and all RNA samples show very little degradation (Figures 3.5 to 3.8).

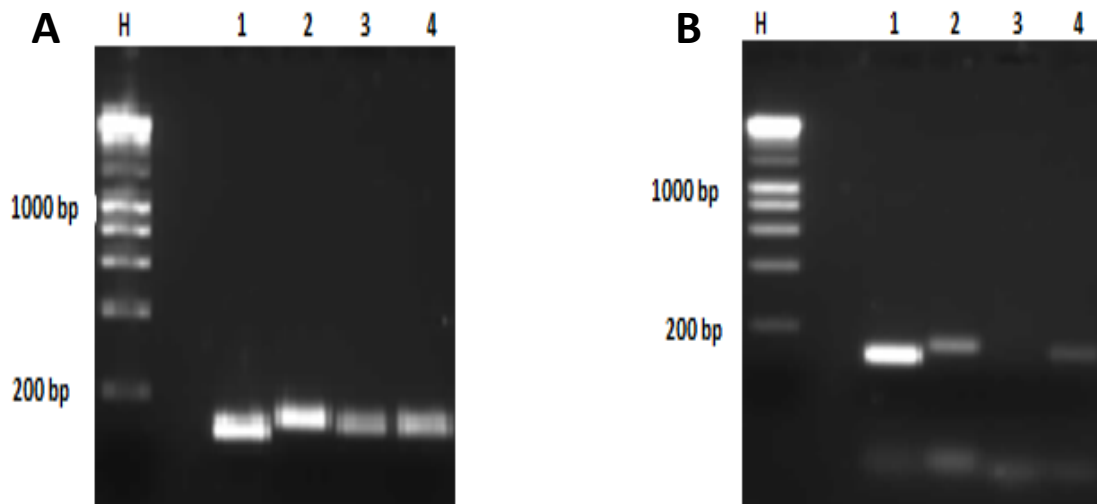
### **3.3 Specificity of the PCR primers**

It is common for PCR primers to amplify more than one target DNA sequence due to incorrect annealing temperature or just binding to non-specific DNA sequences. Therefore, a careful assessment of primer specificity is necessary and is a mandatory step before conducting any qRT-PCR.

To test the specificity of Gapdh, NEIL3, hTERT and POT1 primers, a 1.5% agarose gel was loaded with PCR products amplified from cDNA from CEM-1-15 cells (Figure 3.9), Saos-2 and HepG2 cell lines (Figure 3.10).



**Figure 3.9:** Agarose gel electrophoresis with Gapdh, NEIL3, hTERT and POT1 on cDNA template from CEM-1-15 cells. (A) cDNA in PCR reaction with Gapdh primers. (B) cDNA in PCR reaction with NEIL3 primers. (C) cDNA in PCR reaction with hTERT primers (D) cDNA in PCR reaction with POT1 primers. Lane H represents Hyperladder I, while lanes 1, 2 and 3 contain sample 1, 2 and 3 respectively. Sample 1, 2 and 3 represents three different concentrations of cDNA CEM-1-15 cells, 100 %, 1:5 and 1:10 respectively.



**Figure 3.10:** Agarose gel with PCR primers on cDNA from HepG2 and cDNA Saos-2 cell lines. (A) PCR products with cDNA template of HepG2 cell line as the template material. (B) PCR products with cDNA template of Saos-2 cells as the template material. Lane H represents Hyperladder I, while lanes 1, 2, 3 and 4 contain Gapdh, NEIL3, hTERT and POT1 respectively.

The results confirm that, the primers for Gapdh, NEIL3, hTERT and POT1 amplify a single band of 127 bp, 148 bp, 140 bp and 140 bp respectively in cDNA of CEM-1-15 cell line (Figure 3.9). Thus, these primers are successfully suitable for qRT-PCR to quantify the expression of the target genes. Importantly, PCR on cDNA from the Saos-2 cells confirms the hypothesis; Saos-2 cells does not express telomerase gene compared with HepG2 cells. As revealed by Figure 3.10 (A) and (B) the absence of amplifying cDNA fragments with hTERT on Saos-2 cells.

### **3.4 Quantification of gene expression by qRT-PCR**

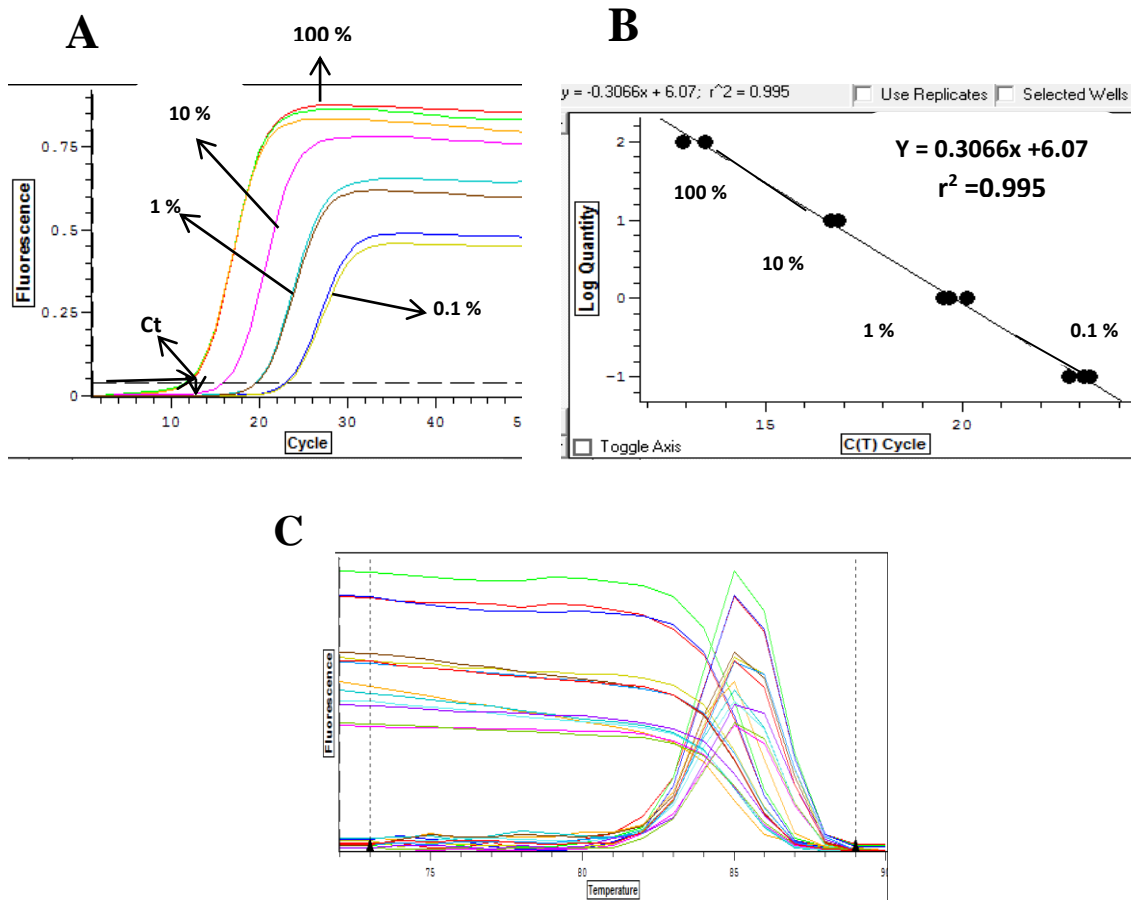
qRT-PCR, the fluorescent based technique commonly used in molecular medicine and in biotechnology to measure the level of the mRNA of target genes in biological samples through the usage of fluorescent dye such as SYBR Green I. In each amplification cycle, the fluorescent signal, which reflects the accumulation of the PCR product is detected (Cikos *et al*, 2007).

In qRT-PCR appropriate normalisation is required to sort out the experimental errors arising from RNA extraction and cDNA generation. Gapdh (glyceraldehyde-3-phosphate dehydrogenase) is identified as a reference gene as it is assumed that its

expression level is constant in the cells. The level of the target gene mRNA is normalised to the reference gene and it is quantified relative to the reference gene. Therefore, the measurement of the gene expression is a numerical value, which allows studying the patterns of gene expression between different cell lines. Importantly, each run of qRT-PCR has a standard curve, which was generated through serial dilution of cDNA (Bustin, 2002).

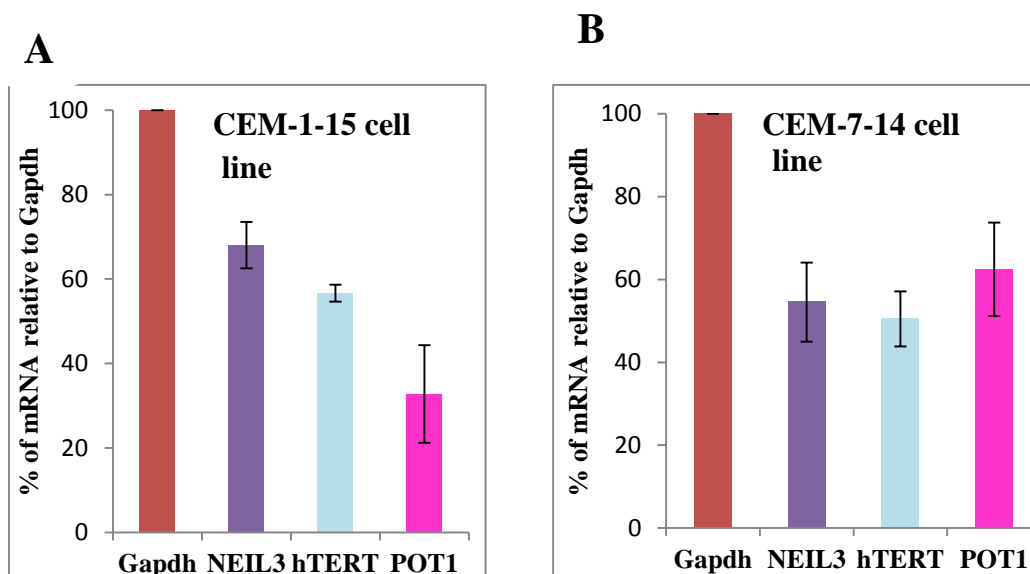
There are several methods to analyse the obtained fluorescent data from qRT-PCR in order to obtain the relative measurement of mRNA target gene. Most of these are analyse the data from the exponential phase of the PCR amplification. The most predominant analytic way is the threshold-based method in which threshold cycle (Ct) represents the number of the amplification cycles required for reaching the threshold fluorescence. The amplification curve is a graph of the fluorescent PCR product against the number of the amplification cycle and the threshold fluorescence represents a point in the amplification curve that has the similar amounts of PCR product in each amplification cycle (Cikos *et al*, 2007). Subsequently, analysis of the linear regression (correlation coefficient,  $r^2$ ) is calculated by plotting the log concentration versus the Ct. However, the validity of  $r^2$  should be more than 0.99 (Peirson *et al*, 2003).

The mRNA level of Gapdh, NEIL3, hTERT and POT1 was assessed in CEM-1-15, CEM-7-14, HOS, Saos2, TC-32 and HepG2 cell lines by qRT-PCR. Using Gapdh and the CEM-1-15 cell line as an example for each primer pair (Figure 3.11), the standards were made from 10-fold serial dilutions of the cDNA and the standard curve was applied to optimise the threshold cycle (Figure 3.11 A). The Ct was adjusted where the  $\text{Log}_{10}$  quantity against the Ct cycle became linear. At the same time,  $r^2$  was set at a value higher than 0.97 as revealed in Figure 3.9 B. In addition, the melting curve was assessed carefully to ensure that a single sharp peak was obtained, which represented a single PCR product (Figure 3.11 C).

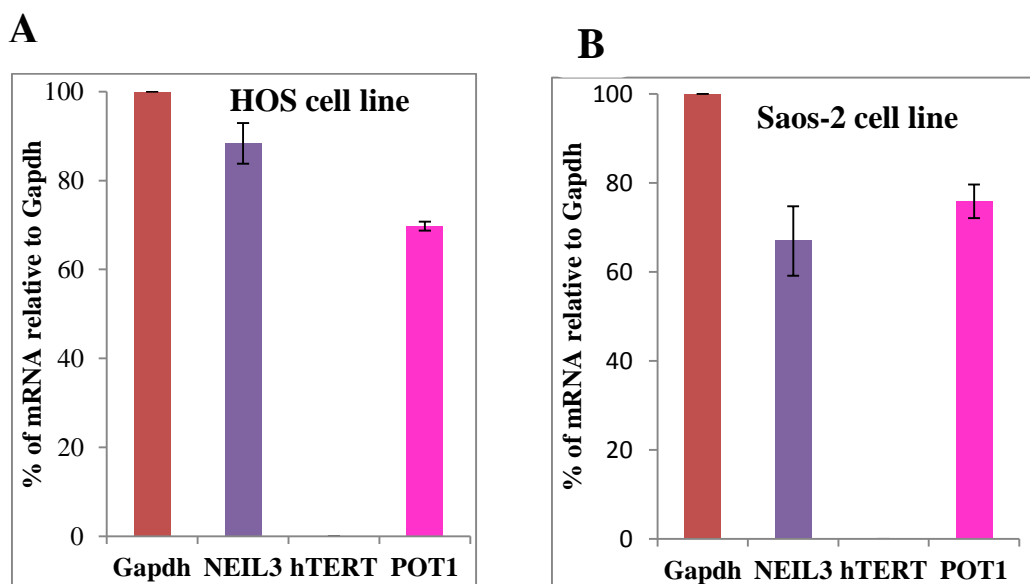


**Figure 3.11:** Analysis of the result for Gapdh expression in CEM-1-15 cells. Each coloured line represents a single PCR reaction with serial dilution of cDNA. (A) Amplification curve shows 10-fold serial dilution of cDNA. Ct was set on the graph at a point where the Ct cycle and the log quantity became linear. In this example, the sample reaches the Ct value at 13 cycles. (B) The linear regression curve (the standard curve for use with Gapdh) represents the relation between the Ct cycle and the log quantity and  $r^2$  showing a value of 0.995. (C) Melting curve with single sharp peak.

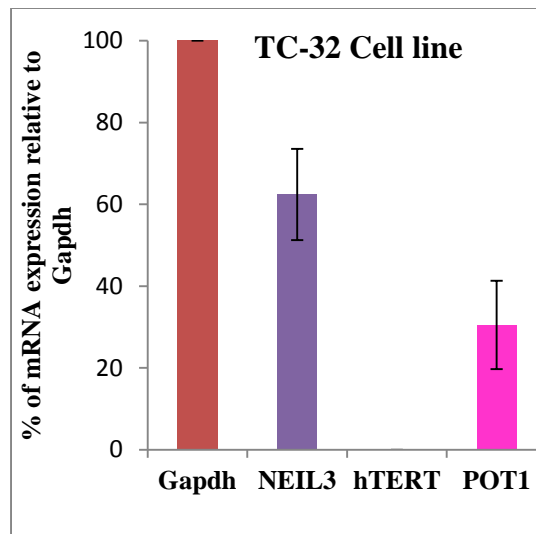
Following the expression of the target gene was determined in every of the six cell lines. The raw data is presented in the appendix (Figures 5.1 to 5.6) and the normalised data is shown in Figures 3.12 to 3.18.



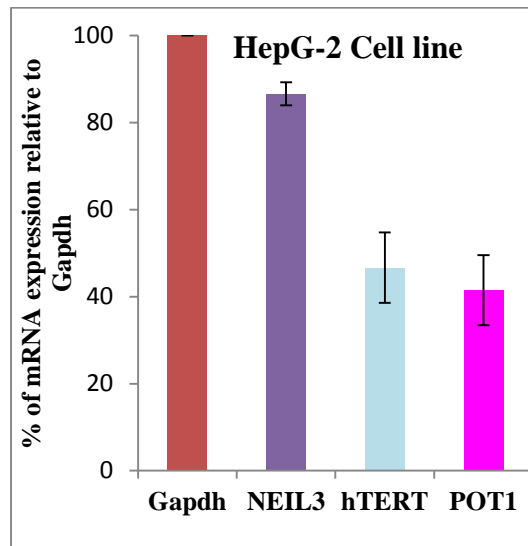
**Figure 3.12:** Quantification of the expression level of NEIL3, hTERT and POT1 in ALL cell lines by qRT-PCR. (A) The expression levels of the target genes in the CEM-1-15 cell line with the data expressed relative to Gapdh. (B) The expression levels of the target genes in the CEM-7-14 cell line with the data expressed relative to Gapdh. The results are presented as averages of two independent experiments, which were performed in triplicate and the standard deviation of these experiments is illustrated as error bars.



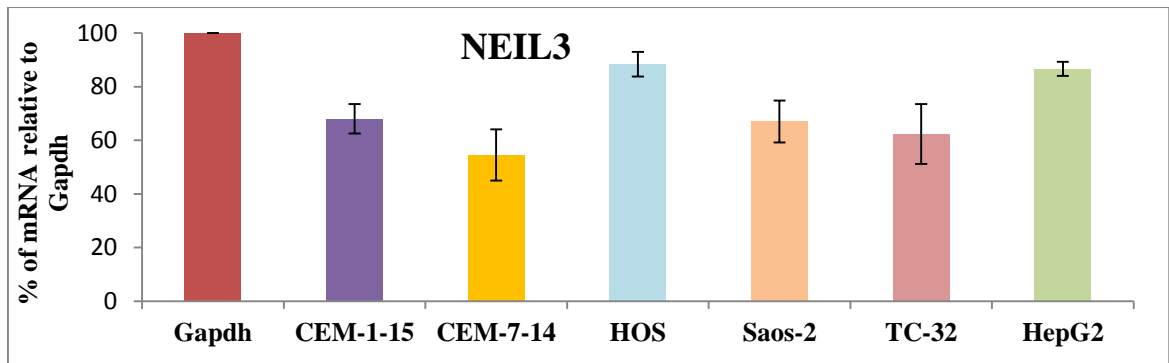
**Figure 3.13:** Quantification of the expression level of NEIL3, hTERT and POT1 in osteosarcoma cell lines by qRT-PCR. (A) The expression levels of the target genes in the HOS cell line with the data expressed relative to Gapdh. (B) The expression levels of the target genes in the Saos-2 cell line with the data expressed relative to Gapdh. The results are presented as averages of two independent experiments, which were performed in triplicate, and the standard deviation of these experiments is illustrated as error bars.



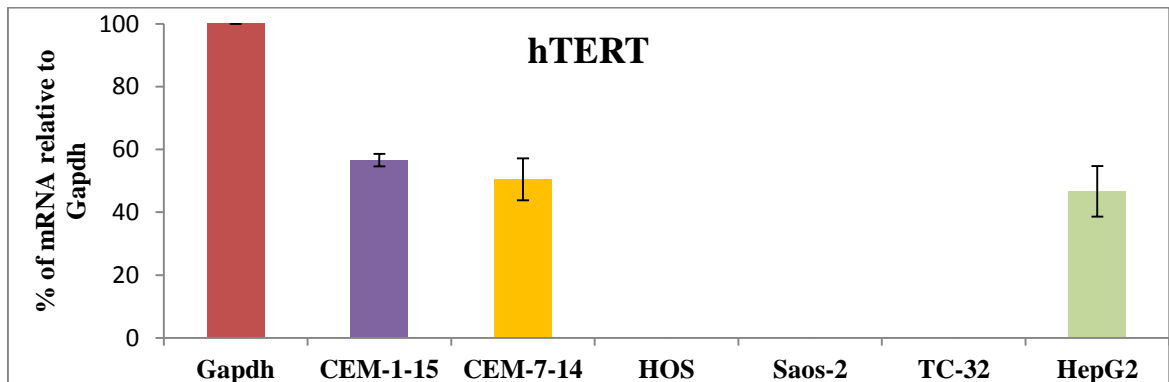
**Figure 3.14:** Quantification of the expression level of NEIL3, hTERT and POT1 in medulloblastoma cell line by qRT-PCR. The expression levels of the target genes in the TC-32 cell line with the data expressed relative to Gapdh. The results are presented as averages of two independent experiments, which were performed in triplicate and the standard deviation of these experiments is illustrated as error bars.



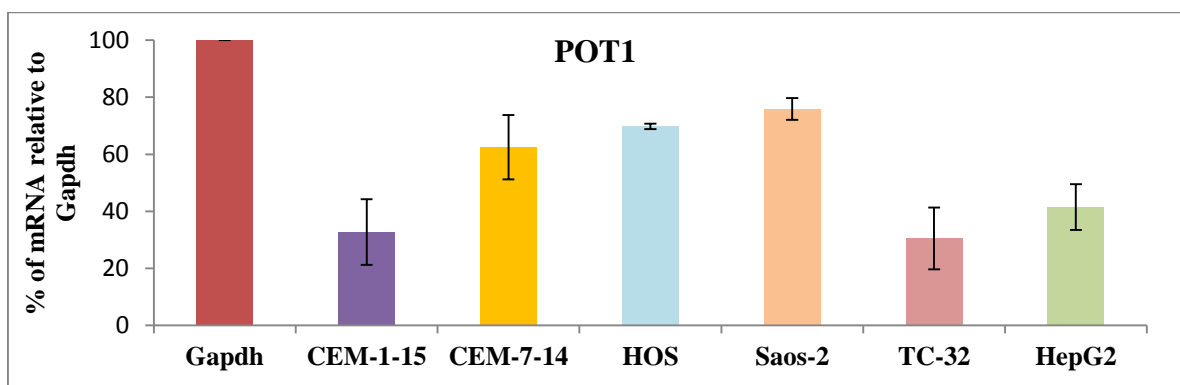
**Figure 3.15:** Quantification of the expression level of NEIL3, hTERT and POT1 in hepatoblastoma cell line by qRT-PCR. The expression levels of the target genes in the HepG2cell line with the data expressed relative to Gapdh. The results are presented as averages of two independent experiments, which were performed in triplicate and the standard deviation of these experiments is illustrated as error bars.



**Figure 3.16:** The relative level of NEIL3 mRNA in different cell lines. The relative expression of NEIL3 mRNA was calculated via normalization with Gapdh. Data are representative averages of two independent PCR reactions carried out in triplicate. Error bars represent standard deviation.



**Figure 3.17:** The relative level of hTERT mRNA in different cell lines. The relative expression of hTERT mRNA was calculated via normalization with Gapdh. Data are representative averages of two independent PCR reactions carried out in triplicate. Error bars represent standard deviation.



**Figure 3.18:** The relative level of POT1 mRNA in different cell lines. The relative expression of POT1 mRNA was calculated via normalization with Gapdh. Data are representative averages of two independent PCR reactions carried out in triplicate. Error bars represent standard deviation.



Analysis of the qRT-PCR data in ALL cells showed, the relative expression level of NEIL3 gene was significantly higher than that of hTERT ( $P < 0.01$ ) and of POT1 ( $P < 0.01$ ) in the CEM-1-15 cell line. However, there was no significant correlation between the relative expression of NEIL3, hTERT and POT1 in CEM-7-14 cell line.

Interestingly, the relative level of NEIL3 mRNA in CEM-1-15 cells was significantly higher than that in CEM-7-14 cells ( $P < 0.01$ ). Furthermore, the increase in the relative expression level of hTERT in CEM-1-15 cells when compared to CEM-7-14 cells was also highly significant ( $P < 0.01$ ). However, there was no significant change in the relative level of POT1 mRNA between both cell lines (Figures 3.12 and 3.16 to 3.18).

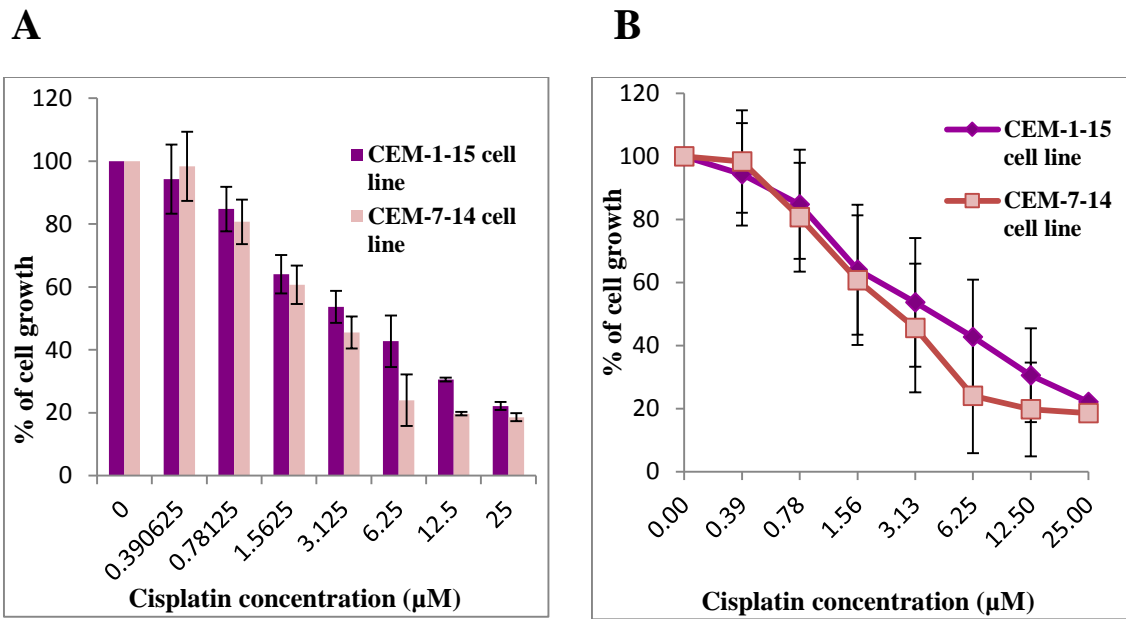
Studying the expression of the target genes in osteosarcoma cell lines revealed that the relative expression level of NEIL3 gene was significantly higher ( $P < 0.01$ ) than that of POT1 in HOS cell line. While, in Saos-2 cells the relative level of POT1 mRNA was significantly ( $P < 0.01$ ) higher than that of NEIL3. In addition, NEIL3 expression in HOS cells was significantly increased over that seen in Saos-2 cells ( $P < 0.01$ ). On the other hand, HOS cells have a significantly lower relative level of POT1 mRNA compared with Saos-2 cells ( $P < 0.01$ ) (Figure 3.13, 3.16 and 3.18).

In TC-32 and HepG2 cell lines, NEIL3 was again highly expressed, significantly more than POT1 in both cell lines ( $P < 0.01$ ). Moreover, the relative expression of NEIL3 was much higher than that of hTERT in HepG2 cells ( $P < 0.01$ ) (Figures 3.14 and 3.15).

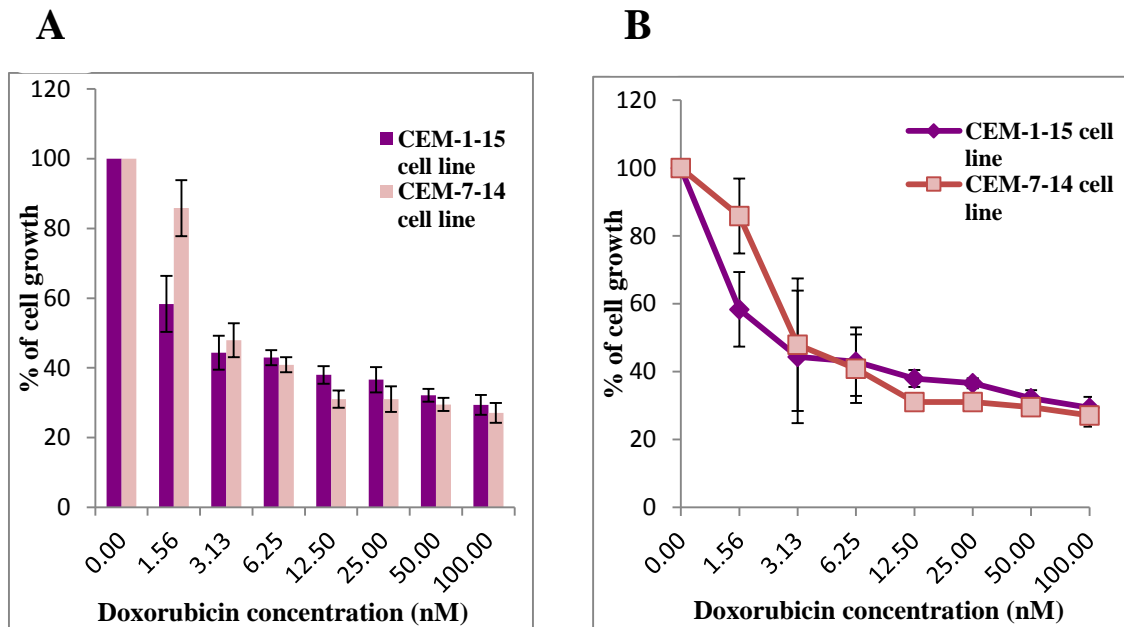
These experiments also confirm that, HOS, Saos-2 and TC-32 cells do not express the hTERT gene (Figure 3.17). The data indicate that, there is no correlation between the expression of NEIL3 and the presence or absence of hTERT. Importantly, NEIL3 mRNA was expressed in all the cell lines tested.

### **3.5 Determination the cell growth inhibitory effect of genotoxic agents using the MTS assay**

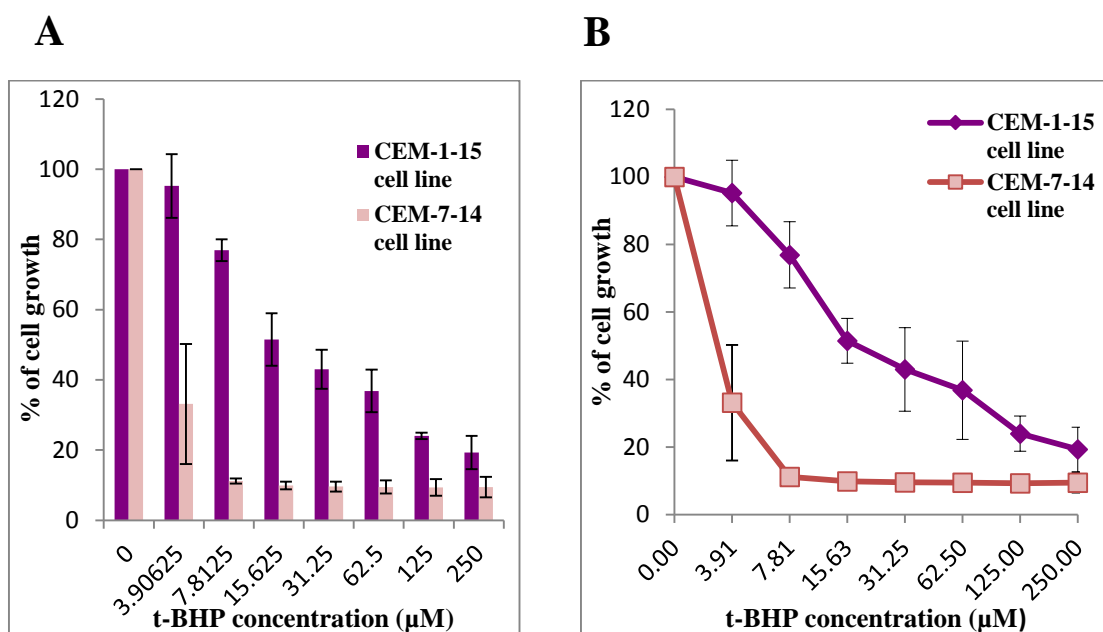
CEM-1-15 and CEM-7-14 cell lines were treated with cisplatin, doxorubicin and *tert*-butyl hydroperoxide for 72 h. Then the cell growth was examined using the MTS assay (Figures 3.19 to 3.21).



**Figure 3.19:** Growth curves for ALL cell lines treated with cisplatin for 72 h. (A) The percent survival of CEM-1-15 and CEM-7-14 cells after treatment with 0-25 μM cisplatin. (B) The IC<sub>50</sub> value of CEM-1-15 cells to cisplatin is 4.18 μM, while the IC<sub>50</sub> value of CEM-7-14 cells to cisplatin is 2.67 μM. Data are representative averages of two independent experiments carried out in triplicate. Error bars represent standard deviation.



**Figure 3.20:** Growth curves for ALL cell lines treated with doxorubicin for 72 h. (A) The percent survival of CEM-1-15 and CEM-7-14 cells after treatment with 0-100 nM doxorubicin. (B) The IC<sub>50</sub> value of CEM-1-15 cells to doxorubicin is 2.5 nM, while the IC<sub>50</sub> value of CEM-7-14 cells to doxorubicin is 3.04 nM. Data are representative averages of two independent experiments carried out in triplicate. Error bars represent standard deviation.



**Figure 3.21:** Growth curves for ALL cell lines treated with *t*-BHP for 72 h. (A) The percent survival of CEM-1-15 and CEM-7-14 cells after treatment with 0-250 µM *t*-BHP. (B) The IC<sub>50</sub> value of CEM-1-15 cells to *t*-BHP is 18.35 µM, while the IC<sub>50</sub> value of CEM-7-14 cells to *t*-BHP is 2.92 µM. Data are representative averages of two independent experiments carried out in triplicate. Error bars represent standard deviation.

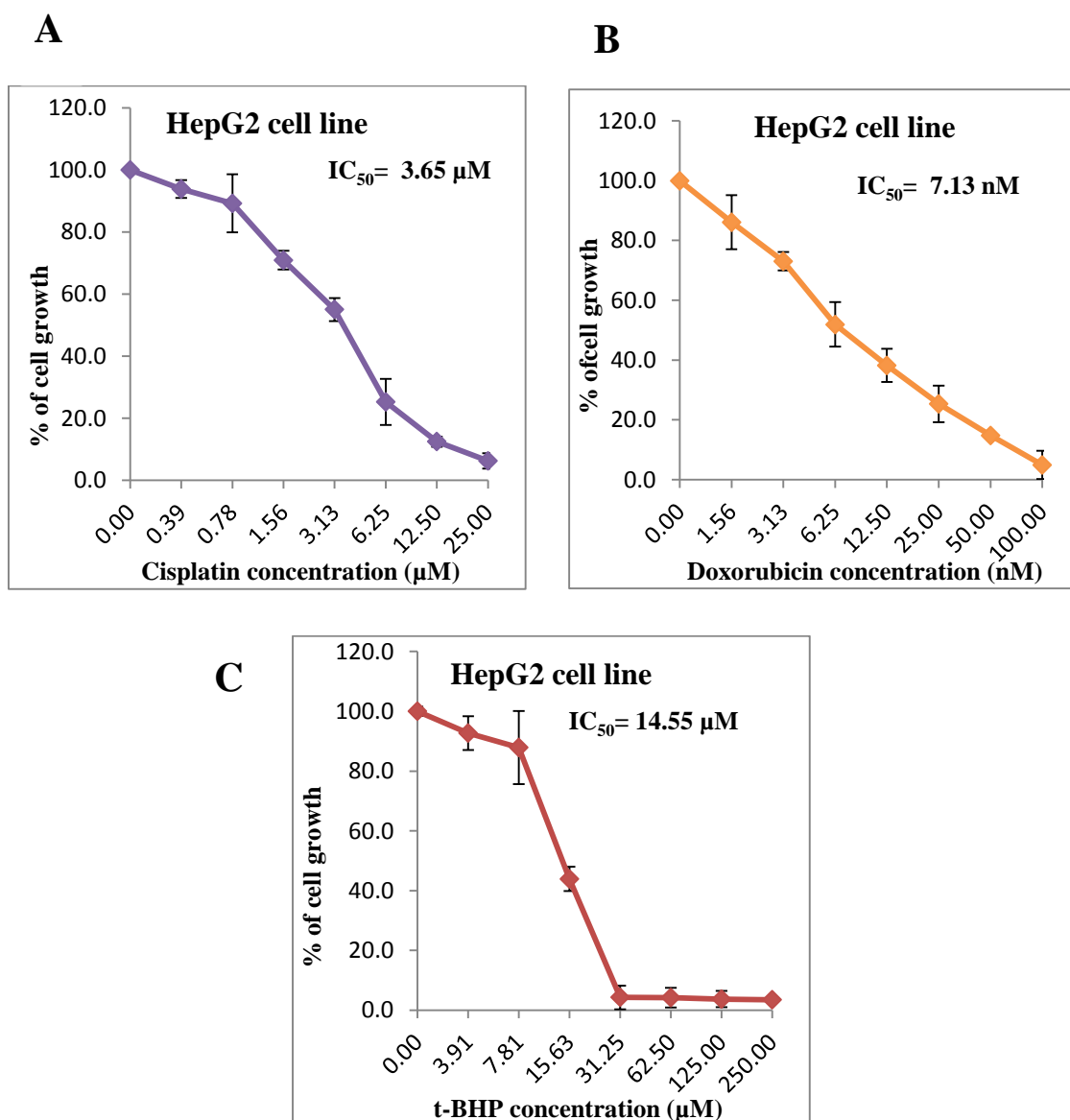
The growth of both CEM-1-15 and CEM-7-14 cells was inhibited at every concentration of cisplatin examined (Figure 3.19). Although no significant differences was observed between the cell lines, the IC<sub>50</sub> for CEM-7-14 cells was lower (2.67 µM) than that of the CEM-1-15 cells (4.18 µM).

Similarly, with increasing concentration of doxorubicin, a substantial decrease in the growth of ALL cells was observed. At only one concentration (1.56 nM), CEM-1-15 cells showed greater inhibition of growth than CEM-7-14 cells ( $P < 0.05$ ). Therefore, the value of IC<sub>50</sub> in CEM-1-15 cells treated with doxorubicin is 2.5 nM and the value of IC<sub>50</sub> in CEM-7-14 cells treated with doxorubicin is 3.04 nM (Figure 3.20).

Interestingly, treatment with *t*-BHP elicited a marked difference in response between the CEM-1-15 and CEM-7-14 cells. Growth of the CEM-7-14 cell line was significantly ( $P < 0.01$ ) more inhibited following treatment with *t*-BHP, an IC<sub>50</sub> of 2.92 µM, compared with an IC<sub>50</sub> of 18.35 µM for the CEM-1-15 cells (Figure 3.21).

### 3.6 Determination the cell growth inhibitory effect of genotoxic agents using the MTT assay

In order to examine the effect of a non-toxic dose of *t*-BHP on the expression of NEIL3, TERT and POT1, the sensitivity of HepG2 cells to this agent and, as controls, cisplatin and doxorubicin was examined using the MTT assay (Figure 3.22).

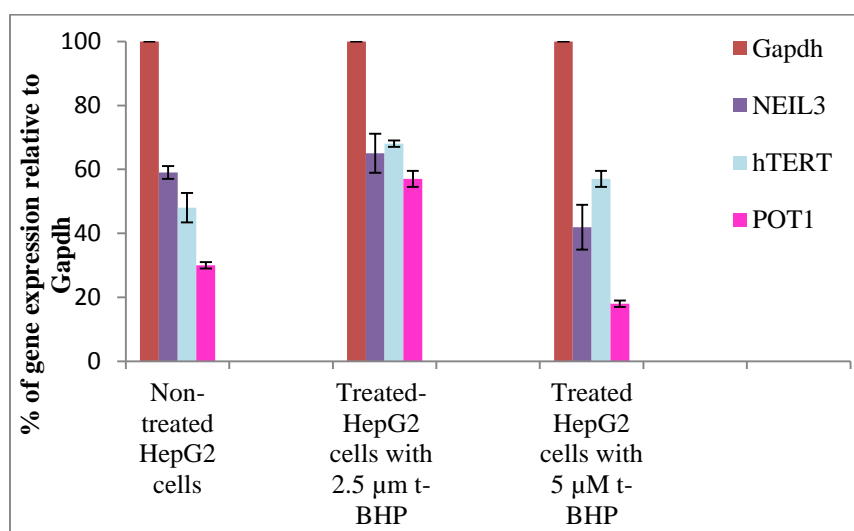


**Figure 3.22:** Growth curves for HepG2 cell line. (A) The percent of HepG2 survival cells after treatment with 0-25 μM cisplatin, IC<sub>50</sub> = 3.65 μM. (B) The percent of HepG2 survival cells after treatment with 0-100 nM doxorubicin, IC<sub>50</sub> = 7.13 nM. (C) The percent of HepG2 survival cells after treatment with 0-250 μM *t*-BHP, IC<sub>50</sub> = 14.55 μM. Data are representative averages of two independent experiments carried out in triplicate. Error bars represent standard deviation.

As shown in Figure 3.22, HepG2 cells were sensitive to cisplatin, doxorubicin and *t*-BHP as a decline in cell growth was observed at each concentrations of the compounds tested. A 50% reduction in the cells growth was obtained with 3.65  $\mu\text{M}$  cisplatin, 7.13 nM doxorubicin and 14.55  $\mu\text{M}$  *t*-BHP.

### **3.7 Estimation of the effect of *tert*-butyl hydroperoxide on HepG2 cells on target gene expression by qRT-PCR**

To examine the influence of oxidative stress on the expression levels of Gapdh, NEIL3, hTERT and POT1 genes in hepatoblastoma cells, the HepG2 cells were treated with 2.5  $\mu\text{M}$  or 5  $\mu\text{M}$  *t*-BHP for 72 h, then RNA extracted and reverse transcription PCR was carried out. The levels of mRNA target genes were measured via qRT-PCR. The raw data is presented in the appendix (Figures 5.7 to 5.9) and the normalised data with the reference gene is shown in Figure 3.23.



**Figure 3.23:** Measurement of the level of mRNA NEIL3, hTERT and POT1 on cDNA of hepatoblastoma cells treated with *t*-BHP using qRT-PCR. The first three columns represent the control samples, which illustrates the levels of target gene expression in the HepG2 cells relative to Gapdh. The second three columns represent HepG2 cells treated with 2.5  $\mu\text{M}$  *t*-BHP, while the third set of columns represent HepG2 cells treated with 5  $\mu\text{M}$  *t*-BHP. Data are representative averages of two independent PCR reactions carried out in triplicate. Error bars represent standard deviation.

Compared with non-treated HepG2 cells, the relative expression of NEIL3 decreased significantly following 5  $\mu\text{M}$  *t*-BHP treatment ( $P < 0.01$ ), however the relative level of NEIL3 mRNA did not change significantly following treatment with 2.5  $\mu\text{M}$  *t*-BHP. In addition, the relative level of hTERT mRNA increased significantly ( $P < 0.01$ ) after treatment with 2.5  $\mu\text{M}$  and 5  $\mu\text{M}$  *t*-BHP. On the other hand, the relative level of POT1 mRNA appears to increase significantly ( $P < 0.01$ ) following 2.5  $\mu\text{M}$  *t*-BHP, but was reduced significantly ( $P < 0.01$ ) compared with control levels following 5  $\mu\text{M}$  *t*-BHP treatment (Figure 3.23).

## Chapter 4: Discussion

In this thesis, I set out first to determine the gene expression of NEIL3 in a number of different paediatric cancer cell lines. Secondly, I was interested to discover if there was any correlation between the high levels of expression of NEIL3 previously reported in cancer cells and tumours (Hildrestrand *et al*, 2009) with the gene expression of telomerase and POT1, a component of the shelterin proteins that surround the telomere. Telomerase is known to be expressed in 85% of human tumours (Tahtouh *et al*, 2015) and is an important for cell immortality, one of Hanahan and Weinberg's Hallmarks of Cancer (Hanahan and Weinberg, 2011) while NEIL3 has recently been shown to act on telomeric regions of DNA (Zhou *et al*, 2015). Finally, I wanted to determine the effect of different genotoxic compounds on the growth of selected cancer cell lines, particularly the two ALL lines, but also the hepatoblastoma cells, which could more easily be used for future RNAi knockdown studies.

### 4.1 The significant role of NEIL3

While the biological role of NEIL3 has yet to be fully determined, it is known that the N-terminal domains can function as a DNA glycosylase (Liu *et al*, 2013). Recently, it has been shown that NEIL3 may be involved in the repair of telomeric and other G-quadruplex regions in DNA, such as those found in the promoters of certain oncogenes (Zhou *et al*, 2015).

Hildrestrand *et al* (2009) confirmed that NEIL3 was highly expressed in sixteen different cancer tissues compared with normal counterparts (Figure 1.16) and the analysis carried out in this work confirmed that NEIL3 was highly expressed in all of the paediatric cancer cell lines tested, with the highest levels of NEIL3 mRNA detected in the HOS and HepG2 cell lines.

When comparing the two ALL cell lines, the expression of NEIL3 in the glucocorticoid resistant CEM-1-15 cells was significantly higher than that in GC sensitive CEM-7-14 cells ( $P < 0.01$ ). In a microarray analysis, Kauffmann *et al* (2008) found that NEIL3 was the most over-expressed DNA repair gene in metastatic melanoma tumours when compared to primary melanoma tumours where no metastasis had been observed. Thus,

a high level of NEIL3 mRNA was correlated with a high risk of metastasis and low survival rates in patients with primary malignant melanoma. The authors also speculated that the general increase in DNA repair protein expression, including NEIL3, in metastatic melanoma could be the cause of their resistance to genotoxic chemotherapeutic agents and radiotherapy. The results described in this project confirm that NEIL3 is highly expressed in the paediatric cancer cell lines tested and that a higher expression level is correlated with resistance to oxidative stress (Figure 3.21 & Section 4.2).

While, NEIL3 is the largest of the five mammalian DNA glycosylases involved in removing oxidative base damage (Hegde *et al*, 2008; Liu *et al*, 2013), the exact cellular function of its unique protein structure still needs to be determined. It has two GRF zinc finger motifs and a RANbp-like zinc finger motif at the C-terminus and an N-terminal Val2 amino acid instead of Pro2 (Liu *et al*, 2013). Therefore, further studies should be conducted to determine the biological role of these distinct components, as they could be involved with decreasing the sensitivity of paediatric malignant cells to chemo- and radio- therapeutic agents.

Approximately 15% of tumours lack telomerase activity, which include some of sarcomas, brain tumours and certain types of epithelial-derived tumours; however, they can still maintain the length of the telomeric DNA by ALT (Tahtouh *et al*, 2015). The results of this study confirmed that osteosarcoma (HOS and Saos-2 cell lines) and medulloblastoma tumours do not express telomerase (Figure 3.17). Furthermore, the results show that there was no correlation between the expression of NEIL3 and the presence or absence of telomerase (Figures 3.12 to 3.17). POT1, along with TRF1 and TRF2, are part of the shelterin complex that protects the telomeric ends of chromosomes. Zhou *et al* (2013) reported that they were unable to detect any physical correlation between NEIL3 protein and TRF1 or TRF2 using co-immunoprecipitation in HeLa or HEK293 cells, or to colocalise NEIL3 and POT1. The results of this study indicate that the expression of NEIL3 and POT1 do not appear to be linked (Figures 3.12 – 3.15).

Artandi *et al* (2002) stated that high levels of telomerase mRNA was associated with tumourgenesis. Thus, hindering telomere maintenance in tumour cells could be targeted in treatment of neoplasms (Henson *et al*, 2002; Morrish *et al*, 2013). In this work the



results showed that the relative level of telomerase mRNA was significantly higher in steroid resistant ALL cells (CEM-C1-15) than in the steroid sensitive ALL cells (CEM-C7-14) ( $P < 0.01$ ) (Figure 3.12). Kauffmann *et al* (2008) concluded that high levels of the genes responsible for telomere maintenance was correlated with spreading of metastases in patients with melanoma and increased the resistance of these neoplastic cells to chemo- and radiotherapy. Thus, the results reported here confirm that higher levels of telomerase expression was observed in the GC resistant ALL cell line relative to Gapdh, the expression of which was also higher in the GC resistant cell line.

#### **4.2 The effect of oxidative stress on steroid sensitive and steroid resistant acute lymphoblastic leukaemia**

*t*-BHP is commonly used to illustrate the biological effects of oxidative stress in cells (Haidara *et al*, 2008; Tan *et al*, 2011; Jho *et al*, 2013). It has been shown that the action of *t*-BHP is similar to lipid hydroperoxides, which lead to the formation of ROS (Cheng *et al*, 2007). Calderon *et al* (1991) stated that *t*-BHP leads to elevation in the level of intracellular calcium ions and decreases the level of cellular GSH. Moreover, Lin *et al* (2014) reported that *t*-BHP is an oxidative stress-inducing compound that exerts oxidative genomic damage in many cells mainly by its metabolites; alkoxy and alkyl radicals.

ALL is the most common paediatric cancer that arises from lymphoid progenitor cells. GCs are widely used in the treatment protocol of ALL patients. However, some ALL cells develop resistance to GCs, as evidenced by CEM-1-15 cells, while CEM-7-14 cells are steroid sensitive cells (Chen *et al*, 2012). In addition, Cole *et al* (2015) confirmed that oxidative stress leads to poor neurocognitive outcome in ALL patients who received cytotoxic drugs.

Here, the effect of oxidative stress on the growth of ALL cells was assessed; CEM-1-15 and CEM-7-14 cell lines were exposed to various concentrations of *t*-BHP for 72 h. Interestingly, the results showed that the growth of the GC insensitive CEM-1-15 cell line was also significantly ( $P < 0.01$ ) more resistant to *t*-BHP (IC<sub>50</sub> of 18.35  $\mu$ M) than the GC sensitive CEM-7-14 cells (IC<sub>50</sub> of 2.92  $\mu$ M) (Figure 3.21). Therefore, these results confirm the finding of Rasool *et al* (2015) who reported that an increased level

of ROS has been linked with the development of ALL and, furthermore, that it was correlated with emerging chemotherapeutic-resistant ALL cells. Additionally, Beesley *et al* (2010) concluded that ALL cells might develop resistance to DEX and gamma radiation. Another study showed that the disparity between the CEM-1-15 and CEM-7-14 cell lines is mainly related to the difference in the efficacy of the oxidative phosphorylation pathway (Berrou *et al*, 2012).

As mentioned before, the expression levels of NEIL3 in the GC resistant CEM-1-15 cells was significantly higher than that in GC sensitive CEM-7-14 cells (Figure 3.12). This suggests the possibility that a high level of NEIL3 may be one factor in the increased resistance of the CEM-1-15 cells to oxidative stress. NEIL3 acts on oxidised purine and pyrimidine bases in both single – and double-stranded DNA releasing them in the first step of BER (Liu *et al*, 2013). To explore this further, similar expression studies on a range of DNA repair enzymes would be needed.

#### **4.3 The effect of oxidative stress on hepatoblastoma cells**

In the current study, the impact of oxidative stress on the growth of hepatoblastoma cells and on the gene expression levels of NEIL3, hTERT and POT1 was determined. HepG2 cells were treated with *t*-BHP for 72 h and then an MTT assay was carried out to estimate the IC<sub>50</sub> followed by qTR-PCR to measure the relative expression of NEIL3, hTERT and POT1.

A review of the literature indicates that extensive ROS leads to hepatic cell death (Marra *et al*, 2011). The results of this study confirmed that the viability of the HepG2 cells was inhibited following treatment with *t*-BHP and a 50% reduction in the cell growth was obtained with 14.55 µM *t*-BHP (Figure 3.22).

Furthermore, the influence of the oxidative stress on NEIL3 gene expression was investigated. However, the results were difficult to evaluate as opposite trends were observed in the level NEIL3 mRNA following exposure of HepG2 cells to 2.5 µM *t*-BHP and 5 µM *t*-BHP, concentrations that were minimally toxic to the cells. At 2.5 µM *t*-BHP, the level of NEIL3 gene expression was significantly greater than in the untreated cells ( $P < 0.01$ ), while at the higher dose, the level of NEIL3 expression was significantly less than the controls ( $P < 0.01$ ) (Figure 3.23). The MTT results suggest

that at both concentrations of *t*-BHP the oxidative DNA base damage could be repaired by the high levels of NEIL3 and other DNA glycosylases. Therefore, the decrease in NEIL3 mRNA observed at the higher dose may be due to the toxicity of the agent on the cells.

#### **4.4 The effect of cisplatin on steroid sensitive, steroid resistant acute lymphoblastic leukaemia and hepatoblastoma cells**

Cisplatin was used herein as a control for the MTT and MTS assays. Jordan *et al* (2000) reported that cisplatin inhibits DNA synthesis, transcription and replication through DNA cross-links. Subsequently, cisplatin DNA adducts lead to apoptotic cell death. In this work, CEM-1-15, CEM-7-14 and HepG2 cell lines were exposed to various concentrations of cisplatin for 72 h. The results illustrated a decrease in the growth of CEM-1-15, CEM-7-14 and HepG2 cells at each concentration of cisplatin tested. In addition, there was no difference in the response of CEM-1-15, CEM-7-14 cells to cisplatin (Figures 3.19 and 3.22).

#### **4.5 The effect of doxorubicin on steroid sensitive, steroid resistant acute lymphoblastic leukaemia and hepatoblastoma cells**

Doxorubicin belongs to the anthracyclines group of chemotherapeutic drugs (Thorn *et al*, 2011). DOX is commonly used to treat different types of tumours such as sarcoma, lymphoma, leukaemia, bladder, liver, lung, thyroid and breast cancer (O'Brien *et al*, 2004; Smith *et al*, 2010; Girotti *et al*, 2013).

DOX was chosen for this study to obtain insight on its effect on ALL and hepatoblastoma cells, and to correlate this effect with NEIL3. CEM-1-15, CEM-7-14 and HepG2 cell lines were exposed to various concentrations of DOX for 72 h. The statistical analysis showed that the growth of CEM-1-15, CEM-7-14 and HepG2 cells declined at each higher concentration of DOX tested. Interestingly, at only one concentration (1.56 nM), CEM-1-15 cells showed greater inhibition of growth than CEM-7-14 cells ( $P < 0.05$ ) (Figure 3.20). As it was stated by Minotti *et al* (2004) DOX induces ROS through a pathway of one-electron redox cycling. However, NEIL3

belongs to the oxidative DNA glycosylases, which initiate BER to eliminate oxidative damaged DNA bases (Liu *et al*, 2013). Therefore, the influence of 1.56 nM DOX on CEM-1-15 cells should be evaluated and it is of great value to explore the effect of this dose on oxidative DNA repair genes.

## **Conclusion**

The results confirmed that NEIL3 is highly expressed in paediatric ALL, osteosarcoma, medulloblastoma and hepatoblastoma cells. Thus, NEIL3 could provide novel insights for the improved treatment of paediatric cancers. Studying the relation between NEIL3 and telomerase in paediatric tumour cells illustrated that there was no correlation between the expression of NEIL3 and the presence or absence of telomerase.

Hepatoblastoma cells, steroid sensitive and steroid resistant acute lymphoblastic leukaemia (ALL) cells were sensitive to cisplatin, doxorubicin and *tert*-butyl hydroperoxide as a decline in the growth of these cells was observed at each concentration of the compounds tested. However, GC resistant ALL cells were also more resistant to the cytotoxic effects of *t*-BHP when compared to the GC sensitive ALL cell line. This was associated with a higher expression of NEIL3 in the GC resistant cell line. Therefore, high levels of NEIL3 may have a role in decreasing the sensitivity of paediatric tumour cells to genotoxic chemotherapeutic drugs.

## **Future perspectives**

Unpublished work in our laboratory has indicated that siRNA induced knockdown of NEIL3 sensitizes colorectal cancer cells to a clinically relevant chemotherapy drug. Therefore, based on the results described herein, further research to decrease the levels of NEIL3 mRNA (siRNA) or to delete the NEIL3 gene (CRISPR) in paediatric cancer cells are warranted.

## References

- Adams, JD Jr., Klaidman, LK., Huang, YM. *et al.* (1994) The neuropathology of intracerebroventricular-butylhydroperoxide. *Molecular and Chemical Neuropathology*, **22**, 123-142.
- Akman, SA., Forrest, G., Chu, FF., Esworthy, RS. & Doroshow, JH. (1990) Antioxidant and xenobiotic-metabolizing enzyme gene expression in doxorubicin-resistant MCF-7 breast cancer cells. *Cancer Research*, **50**, 1397-1402.
- Aller, P., Ye, Y., Wallace, SS., Burrows, CJ. & Doublié, S. (2010) Crystal structure of a replicative DNA polymerase bound to the oxidized guanine lesion guanidinohydantoin. *Biochemistry*, **49**, 2502-2509.
- Alter, BP., Rosenberg, PS., Giri, N. *et al.* (2012) Telomere length is associated with disease severity and declines with age in dyskeratosis congenita. *Haematologica*, **97**, 353-359.
- Amable, L., Fain, J., Gavin, E. & Reed, E. (2014) Gli1 contributes to cellular resistance to cisplatin through altered cellular accumulation of the drug. *Oncology Reports*, **32**, 469-474.
- Armenian, SH., Kremer, LC. & Sklar, C. (2015) Approaches to reduce the long-term burden of treatment-related complications in survivors of childhood cancer. *American Society of Clinical Oncology*, **35**, 196-204.
- Andrew, T., Aviv, A., Falchi, M. *et al.* (2006) Mapping genetic loci that determine leukocyte telomere length in a large sample of unselected female sibling pairs. *American Journal of Human Genetics*, **78**, 480-486.
- Aquilina, G. & Bignami, M. (2001) Mismatch repair in correction of replication errors and processing of DNA damage. *Journal of Cellular Physiology*, **187**, 145-154.
- Artandi, SE., Alson, S., Tietze, MK. *et al.* (2002) Constitutive telomerase expression promotes mammary carcinomas in aging mice. *Proceedings of the National Academy of Sciences USA*, **99**, 8191-8196.

- Asamitsu, K., Hirokawa, T., Hibi, Y. & Okamoto, T. (2015) Molecular Dynamics Simulation and Experimental Verification of the Interaction between Cyclin T1 and HIV-1 Tat Proteins. *PloS One*, **10**, 1-17.
- Asghar, M., Bensch, S., Tarka, M., Hansson, B. & Hasselquist, D. (2015) Maternal and genetic factors determine early life telomere length. *Proceedings of the Royal Society of London B: Biological Sciences*, **282**, 20.
- Athas, WF., Hedayati, MA., Matanoski, GM., Farmer, ER. & Grossman, L. (1991) Development and field-test validation of an assay for DNA repair in circulating human lymphocytes. *Cancer Research*, **51**, 5786-5793.
- Aviv, A. (2002) Chronology versus biology telomeres, essential hypertension, and vascular aging. *Hypertension*, **40**, 229-232.
- Bai, X., Meng, H., Ma, L. & Guo, A. (2015) Inhibitory effects of evodiamine on human osteosarcoma cell proliferation and apoptosis. *Oncology Letters*, **9**, 801-805.
- Barrow Neurological Institute (2013) About brain tumours.  
[http://www.thebarrow.org/Neurological\\_Services/Brain\\_Tumor\\_Center/203343](http://www.thebarrow.org/Neurological_Services/Brain_Tumor_Center/203343).  
[Accessed 10 March 2015].
- Baumann, P. & Cech, TR. (2001) Pot1, the putative telomere end-binding protein in fission yeast and humans. *Science*, **292**, 1171-1175.
- Beach, JA., Nary, LJ., Hirakawa, Y. *et al.* (2011) E4BP4 facilitates glucocorticoid-evoked apoptosis of human leukemic CEM cells via upregulation of Bim. *Journal of Molecular Signalling*, **6**, 13.
- Beesley, AH., Rampellini JL., Palmer ML. *et al.* (2010) Influence of wild-type MLL on glucocorticoid sensitivity and response to DNA-damage in pediatric acute lymphoblastic leukemia. *Molecular Cancer*, **9**, 284.
- Bekker-Méndez, V.C., Miranda-Peralta, E., Núñez-Enríquez, J.C. *et al.* (2014) Prevalence of Gene Rearrangements in Mexican Children with Acute Lymphoblastic Leukemia: A Population Study—Report from the Mexican Interinstitutional Group for the Identification of the Causes of Childhood Leukemia. *BioMed Research International*, **2014**, 8.

- Benhamou, S. & Sarasin, A. (2000) Variability in nucleotide excision repair and cancer risk: a review. *Mutation Research/Reviews in Mutation Research*, **462**, 149-158.
- Ben-Porath, I. & Weinberg, RA. (2004) When cells get stressed: an integrative view of cellular senescence. *Journal of Clinical Investigation*, **113**, 8-13.
- Berrou, I., Krstic-Demonacos, M. & Demonacos, C. (2012) Molecular Mechanisms Conferring Resistance/Sensitivity to Glucocorticoid-Induced Apoptosis. *In: Glucocorticoids - New Recognition of Our Familiar Friend*. (Ed. Qian, X), pp. 151-174. Intech, Rijeka, Croatia
- Biffi, G., Tannahill, D., McCafferty, J. & Balasubramanian, S. (2013) Quantitative visualization of DNA G-quadruplex structures in human cells. *Nature Chemistry*, **5**, 182-186.
- Bindreither, D., Ecker, S., Gschirr, B. *et al.* (2014) The synthetic glucocorticoids prednisolone and dexamethasone regulate the same genes in acute lymphoblastic leukemia cells. *BioMed Central Genomics*, **15**, 662.
- Biron-Shental, T., Sukenik-Halevy, R., Naboani, H. *et al.* (2015) Telomeres are shorter in placentas from pregnancies with uncontrolled diabetes. *Placenta*, **36**, 199-203.
- Brabec, V. & Kasparkova, J. (2005) Modifications of DNA by platinum complexes: relation to resistance of tumors to platinum antitumor drugs. *Drug Resistance Updates*, **8**, 131-146.
- Brooks, SC., Adhikary, S., Rubinson, EH. & Eichman, BF. (2013) Recent advances in the structural mechanisms of DNA glycosylases. *Biochimica Biophysica Acta-Proteins and Proteomics*, **1834**, 247-271.
- Bryan, TM., Englezou, A., Gupta, J., Bacchetti, S. & Reddel, RR. (1995) Telomere elongation in immortal human cells without detectable telomerase activity. *EMBO J*, **14**, 4240-4248.
- Bryce, LA., Morrison, N., Hoare, SF., Muir, S. & Keith, WN. (2000) Mapping of the gene for the human telomerase reverse transcriptase, hTERT, to chromosome 5p15.33 by fluorescence in situ hybridization. *Neoplasia*, **2**, 197-201.

- Buc-Calderon, P., Latour, I. & Roberfroid M. (1991) Biochemical changes in isolated hepatocytes exposed to tert-butyl hydroperoxide. implications for its cytotoxicity. *Cell Biology and Toxicology*, **7**, 129-143.
- Burger, H., Zoumaro-Djayoon, A., Boersma, AW. *et al.* (2010) Differential transport of platinum compounds by the human organic cation transporter hOCT2 (hSLC22A2). *British Journal of Pharmacology*, **159**, 898-908.
- Bustin, S. A. (2002) Quantification of mRNA using real-time reverse transcription PCR (RT-PCR): trends and problems. *Journal of Molecular Endocrinology*, **29**, 23-39.
- Bustin, SA., Benes, V., Garson, JA. *et al.* (2009) The MIQE guidelines: minimum information for publication of quantitative real-time PCR experiments. *Clinical Chemistry*, **55**, 611-622.
- Buttke, TM., McCubrey, JA. & Owen, TC. (1993) Use of an aqueous soluble tetrazolium/formazan assay to measure viability and proliferation of lymphokine-dependent cell lines. *Journal of Immunological Methods*, **157**, 233-240.
- Cacciatore, I., Cornacchia, C., Pinnen, F., Mollica, A. & Di Stefano, A. (2010) Prodrug approach for increasing cellular glutathione levels. *Molecules*, **15**, 1242-1264.
- Cancer Research UK (2014) How cancer starts. <http://www.cancerresearchuk.org/about-cancer/what-is-cancer/how-cancer-starts>. [Accessed 15 February 2015].
- Chen, B., Liang, J., Tian, X. & Liu, X. (2008) G-quadruplex structure: a target for anticancer therapy and a probe for detection of potassium. *Biochemistry (Moscow)*, **73**, 853-861.
- Chen, DW., Krstic-Demonacos, M. & Schwartz, JM. (2012) Modeling the Mechanism of GR/c-Jun/Erg Crosstalk in Apoptosis of AcuteLymphoblastic Leukemia. *Frontiers in Physiology*, **3**, 410.
- Chen, P., Wang, H., Duan, Z. *et al.* (2014) Estrogen-related receptor alpha confers methotrexate resistance via attenuation of reactive oxygen species production and p53 mediated apoptosis in osteosarcoma cells. *BioMed Research International*, **2014**, 9.



Cheng, Q., Nguyen, T., Song, H. & Bonanno, J. (2007) Hypoxia protects human corneal endothelium from tertiary butyl hydroperoxide and paraquat-induced cell death *in vitro*. *Experimental Biology and Medicine*, **232**, 445-453.

Choi, MK., Kim, HG., Han, JM. *et al.* (2015) Hepatoprotective Effect of Terminalia chebula against t-BHP-Induced Acute Liver Injury in C57/BL6 Mice. *Evidence-Based Complementary and Alternative Medicine*, **2015**, 11.

Čikoš, Š., Bukovská, A. & Koppel, J. (2007) Relative quantification of mRNA: comparison of methods currently used for real-time PCR data analysis. *Molecular Biology*, **8**, 113.

Cole, PD., Finkelstein, Y., Stevenson, KE. *et al.* (2015) Polymorphisms in Genes Related to Oxidative Stress Are Associated With Inferior Cognitive Function After Therapy for Childhood Acute Lymphoblastic Leukemia. *Journal of Clinical Oncology*, **33**, 2205-2211.

Collins, AR. (1999) Oxidative DNA damage, antioxidants, and cancer. *Bioessays*, **21**, 238-246.

Coluzzi, E., Colamartino, M., Cozzi, R. *et al.* (2014) Oxidative stress induces persistent telomeric DNA damage responsible for nuclear morphology change in mammalian cells. *PloS One*, **9**, 12.

Cuevas, EP., Escribano, O., Chiloeches, A. *et al.* (2007) Role of insulin receptor substrate-4 in IGF-I-stimulated HEPG2 proliferation. *Journal of Hepatology*, **46**, 1089-1098.

Czauderna, P., Lopez-Terrada, D., Hiyama, E. *et al.* (2014) Hepatoblastoma state of the art: pathology, genetics, risk stratification, and chemotherapy. *Current Opinion in Paediatrics*, **26**, 19-28.

Dahmen, RP., Koch, A., Denkhau, D. *et al.* (2001) Deletions of AXIN1, a component of the WNT/wingless pathway, in sporadic medulloblastomas. *Cancer Research*, **61**, 7039-7043.

- De Biasi, AR., Villena-Vargas, J. & Adusumilli, PS. (2014) Cisplatin-Induced Antitumor Immunomodulation: A Review of Preclinical and Clinical Evidence. *Clinical Cancer Research*, **20**, 5384-5391.
- De Boer, J. & Hoeijmakers, JH . (2000) Nucleotide excision repair and human syndromes. *Carcinogenesis*, **21**, 453-460.
- De Lange, T. (2005) Shelterin: the protein complex that shapes and safeguards human telomeres. *Genes & Development*, **19**, 2100-2110.
- Degerman, S., Domellöf, M., Landfors, M. *et al.* (2014) Long Leukocyte Telomere Length at Diagnosis Is a Risk Factor for Dementia Progression in Idiopathic Parkinsonism. *PloS One*, **9**, 1-14.
- Dinger, ME., Pang KC, Mercer TR. *et al.* (2009) NRED: a database of long noncoding RNA expression. *Nucleic Acids Research*, **37**, 122-126.
- D'Mello, MJ., Ross, SA., Briel, M. *et al.* (2015) Association Between Shortened Leukocyte Telomere Length and Cardiometabolic Outcomes Systematic Review and Meta-Analysis. *Circulation: Cardiovascular Genetics*, **8**, 82-90.
- Dominguez, PM. & Shakhovich, R. (2014) Epigenetic function of activation-induced cytidine deaminase and its link to lymphomagenesis. *Frontiers in Immunology*, **5** , 642.
- Dong, J., Gailani, MR., Pomeroy, SL., Reardon, D. & Bale AE. (2000) Identification of PATCHED mutations in medulloblastomas by direct sequencing. *Human Mutation*, **16**, 89-90.
- Dong, R.,Jia, D., Xue, P. *et al.* (2014) Genome-wide analysis of long noncoding RNA (lncRNA) expression in hepatoblastoma tissues. *PloS One*, **9**, 1-9.
- Doublié, S., Bandaru, V., Bond, JP. & Wallace, SS. (2004) The crystal structure of human endonuclease VIII-like 1 (NEIL1) reveals a zincless finger motif required for glycosylase activity. *Proceedings of the National Academy of Sciences USA*, **101**, 10284-10289.
- Duffner, PK., Horowitz, ME., Krischer, JP. *et al.* (1993) Postoperative chemotherapy and delayed radiation in children less than three years of age with malignant brain tumors. *New England Journal of Medicine*, **328**, 1725-1731.

- Dunigan, DD., Waters, SB. & Owen, TC. (1995) Aqueous soluble tetrazolium/formazan MTS as an indicator of NADH-and NADPH-dependent dehydrogenase activity. *Biotechniques*, **19**, 640-649.
- Eberhart, CG., Kepner, JL., Goldthwaite, PT. *et al.* (2002) Histopathologic grading of medulloblastomas. *Cancer*, **94**, 552-560.
- Edmonds, MJ. & Parsons, JL. (2014) Regulation of base excision repair proteins by ubiquitylation. *Experimental Cell Research*, **329**, 132-138.
- Elbashir, SM., Harborth, J., Lendeckel, W. *et al.* (2001) Duplexes of 21-nucleotide RNAs mediate RNA interference in cultured mammalian cells. *Nature*, **411**, 494-498.
- Faderl, S., Jeha, S. & Kantarjian, HM. (2003) The biology and therapy of adult acute lymphoblastic leukemia. *Cancer*, **98**, 1337-1354.
- Faderl, S., Talpaz, M., Estrov Z. *et al.* (1999) The biology of chronic myeloid leukemia. *New England Journal of Medicine*, **341**, 164-172.
- Ferrari, S., Bertoni, F., Zanella, L. *et al.* (2004) Evaluation of P-glycoprotein, HER-2/ErbB-2, p53, and Bcl-2 in primary tumor and metachronous lung metastases in patients with high-grade osteosarcoma. *Cancer*, **100**, 1936-1942.
- Ferry, KV., Hamilton, TC. & Johnson, SW. (2000) Increased nucleotide excision repair in cisplatin-resistant ovarian cancer cells: role of ERCC1–XPF. *Biochemical Pharmacology*, **60**, 1305-1313.
- Finn, NA., Findley, HW. & Kemp, ML. A switching mechanism in doxorubicin bioactivation can be exploited to control doxorubicin toxicity. *PLoS Comput Biol*, **7**, 1-16.
- Flintoff, WF., Sadlish, H., Gorlick, R., Yang, R. & Williams, FM. (2004) Functional analysis of altered reduced folate carrier sequence changes identified in osteosarcomas. *Biochimica Biophysica Acta*, **1690**, 110-117.
- Forrest, RA., Swift, LP., Rephaeli, A. *et al.* (2012) Activation of DNA damage response pathways as a consequence of anthracycline-DNA adduct formation. *Biochemical Pharmacology*, **83**, 1602-1612.

- Fuller, GN., Su, X., Price, RE. *et al.* (2005) Many human medulloblastoma tumors overexpress repressor element-1 silencing transcription (REST)/neuron-restrictive silencer factor, which can be functionally countered by REST-VP16. *Molecular Cancer Therapeutics*, **4**, 343-349.
- Gardner, JP., Li, S., Srinivasan, SR. *et al.* (2005) Rise in insulin resistance is associated with escalated telomere attrition. *Circulation*, **111**, 2171-2177.
- Garza-Veloz, I., Martinez-Fierro, ML., Jaime-Perez JC. *et al.* (2015) Identification of Differentially Expressed Genes Associated with Prognosis of B Acute Lymphoblastic Leukemia. *Disease Markers*, **15**, 11.
- Ge, X., Chen, Y., Liao, X. *et al.* (2013) Overexpression of long noncoding RNA PCAT-1 is a novel biomarker of poor prognosis in patients with colorectal cancer. *Medical Oncology*, **30**, 1-6.
- Gewirtz, DA. (1999) A critical evaluation of the mechanisms of action proposed for the antitumor effects of the anthracycline antibiotics adriamycin and daunorubicin. *Biochemical Pharmacology*, **57**, 727-741.
- Giardini, MA., Segatto, M., da Silva, MS., Nunes, VS. & Cano, MI. (2014) Telomere and telomerase biology. *Progress in Molecular Biology and Translational Science*, **125**, 1-40.
- Girotti, Albert W., and Giorgio Minotti. (2013) Development of a Tumor-Specific Photoactivatable Doxorubicin Prodrug. *Photochemistry and Photobiology*, **89**, 1009-1010.
- Goff, SP. (2007) Host factors exploited by retroviruses. *Nature Reviews Microbiology*, **5**, 253-263.
- Goode, EL., Ulrich, CM. & Potter, JD. (2002) Polymorphisms in DNA repair genes and associations with cancer risk. *Cancer Epidemiology Biomarkers & Prevention*, **11**, 1513-1530.
- Greider, CW. & Blackburn, EH. (1985) Identification of a specific telomere terminal transferase activity in Tetrahymena extracts. *Cell*, **43**, 405-413.

- Grotzer, MA., Hogarty, MD., Janss, AJ. *et al.* (2001) MYC messenger RNA expression predicts survival outcome in childhood primitive neuroectodermal tumor/medulloblastoma. *Clinical Cancer Research*, **7**, 2425-2433.
- Guidarelli, A., Cattabeni, F. & Cantoni, O. (1997) Alternative mechanisms for hydroperoxide-induced DNA single strand breakage. *Free Radical Research*, **26**, 537-547.
- Guo, W., Healey, JH., Meyers PA. *et al.* (1999) Mechanisms of methotrexate resistance in osteosarcoma. *Clinical Cancer Research*, **5**, 621-627.
- Hagag, AA. & Nosair, NA. (2015) Prognostic Impact of Neuropilin-1 Expression in Egyptian Children with B-lineage Acute Lymphoblastic Leukemia. *Mediterranean Journal of Hematology and Infectious Diseases*, **7**, 1.
- Haidara, K., Marion, M., Gascon-Barré, M., Denizeau, F. & Averill-Bates, DA. (2008) Implication of caspases and subcellular compartments in tert-butylhydroperoxide induced apoptosis. *Toxicology and Applied Pharmacology*, **229**, 65-76.
- Haidara, K., Morel, I., Abalea, V., Gascon Barre, M. & Denizeau, F. (2002) Mechanism of tert-butylhydroperoxide induced apoptosis in rat hepatocytes: involvement of mitochondria and endoplasmic reticulum. *Biochimica Biophysica Acta -Molecular Cell Research*, **1542**, 173-185.
- Hakem, R. (2008) DNA-damage repair; the good, the bad, and the ugly. *EMBO J*, **27**, 589-605.
- Hall, MD., Okabe, M., Shen, DW., Liang, XJ. & Gottesman, MM. (2008) The role of cellular accumulation in determining sensitivity to platinum-based chemotherapy. *Annual Reviews Pharmacology Toxicology*, **48**, 495-535.
- Hanahan, D. & Weinberg, RA. (2011) Hallmarks of cancer: the next generation. *Cell*, **144**, 646-674.
- Hato, SV., Khong, A., de Vries, IJ. & Lesterhuis, WJ. (2014) Molecular pathways: the immunogenic effects of platinum-based chemotherapeutics. *Clinical Cancer Research*, **20**, 2831-2837.

Hattinger, CM., Reverter-Branchat, G., Remondini, D. *et al.* (2003) Genomic imbalances associated with methotrexate resistance in human osteosarcoma cell lines detected by comparative genomic hybridization-based techniques. *European Journal of Cell Biology*, **82**, 483-493.

Hazra, TK., Kow, YW., Hatahet, Z. *et al.* (2002) Identification and characterization of a novel human DNA glycosylase for repair of cytosine-derived lesions. *Journal of Biological Chemistry*, **277**, 30417-30420.

He, H., Ni, J. & Huang J. (2014) Molecular mechanisms of chemoresistance in osteosarcoma (Review). *Oncology Letters*, **7**, 1352-1362.

Hegde, ML., Hazra, TK. & Mitra, S. (2008) Early steps in the DNA base excision/single-strand interruption repair pathway in mammalian cells. *Cell Research*, **18**, 27-47.

Henson, JD., Neumann, AA., Yeager, TR. & Reddel, RR. (2002) Alternative lengthening of telomeres in mammalian cells. *Oncogene*, **21**, 598-610.

Herzog, CE., Andrassy, RJ. & Eftekhari, F. (2000) Childhood cancers: hepatoblastoma. *The Oncologist*, **5**, 445-453.

Heywood, G., Burgart, LJ. & Nagorney, DM. (2002) Ossifying malignant mixed epithelial and stromal tumor of the liver. *Cancer*, **94**, 1018-1022.

Hilden, JM., Dinndorf, PA. & Meerbaum, SO. (2006) Analysis of prognostic factors of acute lymphoblastic leukemia in infants: report on CCG 1953 from the Children's Oncology Group. *Blood*, **108**, 441-451.

Hildrestrand, GA., Neurauter, CG., Diep, DB. *et al.* (2009) Expression patterns of Neil3 during embryonic brain development and neoplasia. *BMC Neuroscience*, **10**, 45.

Holden, JA. (1997) Human deoxyribonucleic acid topoisomerases: molecular targets of anticancer drugs. *Annals of Clinical & Laboratory Science*, **27**, 402-412.

Honda, S., Hjelmeland, LM. & Handa, JT. (2001) Oxidative stress-induced single-strand breaks in chromosomal telomeres of human retinal pigment epithelial cells in vitro. *Investigative Ophthalmology and Visual Science*, **42**, 2139-2144.

- Huang, G., Mills, L. & Worth LL. (2007) Expression of human glutathione S-transferase P1 mediates the chemosensitivity of osteosarcoma cells. *Molecular Cancer Therapeutics*, **6**, 1610-1619.
- Hug, N. & Lingner, J. (2006) Telomere length homeostasis. *Chromosoma*, **115**, 413-425.
- Iacobucci, I., Storlazzi, CT., Cilloni, D. *et al.* (2009) Identification and molecular characterization of recurrent genomic deletions on 7p12 in the IKZF1 gene in a large cohort of BCR-ABL1-positive acute lymphoblastic leukemia patients: on behalf of Gruppo Italiano Malattie Ematologiche dell'Adulto Acute Leukemia Working Party (GIMEMA AL WP). *Blood*, **114**, 2159-2167.
- Ifergan, I., Meller, I., Issakov, J. & Assaraf, YG. (2003) Reduced folate carrier protein expression in osteosarcoma. *Cancer*, **98**, 1958-1966.
- Itoh, M., Kitano, T., Watanabe, M. *et al.* (2003) Possible role of ceramide as an indicator of chemoresistance decrease of the ceramide content via activation of glucosylceramide synthase and sphingomyelin synthase in chemoresistant leukemia. *Clinical Cancer Research*, **9**, 415-423.
- Jakacki, RI. (2005) Treatment strategies for high-risk medulloblastoma and supratentorial primitive neuroectodermal tumors: review of the literature. *Journal of Neurosurgery. Pediatrics*, **102**, 44-52.
- Jho, EH., Kang, K., Oidovsambuu, S. *et al.* (2013) Gymnaster koraiensis and its major components, 3, 5-di-O-caffeoylquinic acid and gymnasterkoreayne B, reduce oxidative damage induced by tert-butyl hydroperoxide or acetaminophen in HepG2 cells. *BMB Reports*, **46**, 513.
- Jordan, P. & Carmo-Fonseca, M. (2000) Molecular mechanisms involved in cisplatin cytotoxicity. *Cellular and Molecular Life Sciences*, **57**, 1229-1235.
- Kang, K., Jho, EH., Lee, HJ. *et al.* (2011) *Youngia denticulata* protects against oxidative damage induced by tert-butylhydroperoxide in HepG2 cells. *Journal of Medicinal Food*, **14**, 1198-1207.

- Kaspers, GJ., Pieters, R., Klumper, E., De Waal, FC. & Veerman, AJ. (1994) Glucocorticoid resistance in childhood leukemia. *Leukemia & lymphoma*, **13**, 187-201.
- Kauffmann, A., Rosselli, F., Lazar, V. *et al.* (2008) High expression of DNA repair pathways is associated with metastasis in melanoma patients. *Oncogene*, **27**, 565-573.
- Kavazis, AN., Smuder, AJ. & Powers, SK. (2014) Effects of short-term endurance exercise training on acute doxorubicin-induced FoxO transcription in cardiac and skeletal muscle. *Journal of Applied Physiology*, **117**, 223-230.
- Kawanishi, Shosuke, and Shinji Oikawa. (2004) Mechanism of telomere shortening by oxidative stress. *Annals of the New York Academy of Sciences* **1019**, 278-284.
- Kawase, M., Watanabe, M., Kondo, T. *et al.* (2002) Increase of ceramide in adriamycin-induced HL-60 cell apoptosis: detection by a novel anti-ceramide antibody. *Biochimica Biophysica Acta-Molecular and Cell Biology of Lipids*, **1584**, 104-114.
- Kelman, Z. (1997) PCNA: structure, functions and interactions. *Oncogene*, **14**, 629-640.
- Kenney, AM., Cole, MD. & Rowitch DH. (2003) Nmyc upregulation by sonic hedgehog signaling promotes proliferation in developing cerebellar granule neuron precursors. *Development*, **130**, 15-28.
- Khanna, C., Khan, J., Nguyen, P. *et al.* (2001) Metastasis-associated differences in gene expression in a murine model of osteosarcoma. *Cancer Research*, **61**, 3750-3759.
- Kheirollahi, M., Dashti, S., Khalaj, Z., Nazemroaia, F. & Mahzouni P. (2015). Brain tumors: Special characters for research and banking. *Advanced Biomedical Research*, **4**, 4.
- Koch, A., Waha, A., Tonn, JC. *et al.* (2001) Somatic mutations of WNT/wingless signaling pathway components in primitive neuroectodermal tumors. *International Journal of Cancer*, **93**, 445-449.
- Kostrzewa-Nowak, D., Paine, MJ., Wolf, CR. & Tarasiuk, J. (2005) The role of bioreductive activation of doxorubicin in cytotoxic activity against leukaemia HL60-sensitive cell line and its multidrug-resistant sublines. *British Journal of Cancer*, **93**, 89-97.



- Kreutzer, Deborah A. & John M, Essigmann. (1998) Oxidized, deaminated cytosines are a source of C→ T transitions in vivo. *Proceedings of the National Academy of Sciences USA*, **95**, 3578-3582.
- Krokan, HE., Nilsen, H., Skorpen, F., Otterlei, M. & Slupphaug, G. (2000) Base excision repair of DNA in mammalian cells. *FEBS Letters*, **476**, 73-77.
- Kučera, O., Endlicher, R., Roušar, T. *et al.* (2014) The effect of tert-butyl hydroperoxide-induced oxidative stress on lean and steatotic rat hepatocytes *in vitro*. *Oxidative Medicine and Cellular Longevity*, **2014**, 12.
- Lama, J. & Planelles, V. (2007) Host factors influencing susceptibility to HIV infection and AIDS progression. *Retrovirology*, **4**, 52.
- Lawinger, P., Venugopal, R., Guo, ZS. *et al.* (2000) The neuronal repressor REST/NRSF is an essential regulator in medulloblastoma cells. *Nature Medicine*, **6**, 826-831.
- Li, KK., Lau, KM. & Ng, HK. (2013) Signaling pathway and molecular subgroups of medulloblastoma. *International Journal of Clinical and Experimental Pathology*, **6**, 1211-1222.
- Lin, WL., Wang, SM., Ho, YJ. *et al.* (2014) Ethyl acetate extract of *Wedelia chinensis* inhibits tert-butyl hydroperoxide-induced damage in PC12 cells and D-galactose-induced neuronal cell loss in mice. *BMC Complementary and Alternative medicine*, **14**, 491.
- Lindahl, T. (1993) Instability and decay of the primary structure of DNA. *Nature*, **362**, 709-715.
- Lipps, HJ. & Rhodes, D. (2009) G-quadruplex structures: *in vivo* evidence and function. *Trends in Cell Biology*, **19**, 414-422.
- Litten, JB. & Tomlinson, GE. (2008) Liver tumors in children. *The Oncologist*, **13**, 812-820.
- Liu, M., Doublie S. & Wallace, SS. (2013) Neil3, the final frontier for the DNA glycosylases that recognize oxidative damage. *Mutation Research/Fundamental and Molecular Mechanisms of Mutagenesis*, **743**, 4-11.

- Liu, M., Bandaru, V., Bond, JP. *et al.* (2010) The mouse ortholog of NEIL3 is a functional DNA glycosylase *in vitro* and *in vivo*. *Proceedings of the National Academy of Sciences USA*, **107**, 4925-4930.
- Lopez-Terrada, D. (2006) Integrating the diagnosis of childhood malignancies. *New Trends in Cancer for the 21st Century*, **587**, 121-137.
- López-Terrada, D., Gunaratne, PH., Adesina, AM. *et al.* (2009) Histologic subtypes of hepatoblastoma are characterized by differential canonical Wnt and Notch pathway activation in DLK+ precursors. *Human Pathology*, **40**, 783-794.
- Lu, AL., Li, X., Gu, Y., Wright, PM. & Chang, DY. (2001) Repair of oxidative DNA damage. *Cell Biochemistry and Biophysics*, **35**, 141-170.
- Macpherson, IRJ. & Evans, TRJ. New approaches in the management of advanced breast cancer—role of combination treatment with liposomal doxorubicin. *Breast Cancer. Targets and Therapy*, **1**, 1-18.
- Mandic, A., Hansson, J., Linder, S. & Shoshan, MC. (2003) Cisplatin induces endoplasmic reticulum stress and nucleus-independent apoptotic signaling. *Journal of Biological Chemistry*, **278**, 9100-9106.
- Marra, M., Sordelli, IM., Lombardi, A. *et al.* (2011) Molecular targets and oxidative stress biomarkers in hepatocellular carcinoma: an overview. *Journal of Translational Medicine*, **9**, 171.
- Massignan, T., Biasini, E. & Harris, DA. A Drug-Based Cellular Assay (DBCA) for studying cytotoxic and cytoprotective activities of the prion protein: A practical guide. *Methods*, **53**, 214-219.
- McEachern, MJ., Krauskopf A. & Blackburn, EH. (2000) Telomeres and their control. *Annual Review of Genetics*, **34**, 331-358.
- Medh, RD., Webb, MS., Miller, AL. *et al.* (2003) Gene expression profile of human lymphoid CEM cells sensitive and resistant to glucocorticoid-evoked apoptosis. *Genomics*, **81**, 543-555.

- Meijerink, JP., den Boer, ML. & Pieters, R. (2009) New genetic abnormalities and treatment response in acute lymphoblastic leukemia. *Seminars in Hematology*, **46**, 16-23.
- Min, K., Kwon, OS., Smuder, AJ. *et al.* (2015) Increased mitochondrial emission of reactive oxygen species and calpain activation are required for doxorubicin-induced cardiac and skeletal muscle myopathy. *Journal of Physiology*, **593**, 2017-2036.
- Minotti, G., Menna, P., Salvatorelli, E., Cairo, G. & Gianni, L. (2004) Anthracyclines: molecular advances and pharmacologic developments in antitumor activity and cardiotoxicity. *Pharmacological Reviews*, **56**, 185-229.
- Mori, H., Ouchida, R., Hijikata A. *et al.* (2009) Deficiency of the oxidative damage-specific DNA glycosylase NEIL1 leads to reduced germinal center B cell expansion. *DNA Repair*, **8**, 1328-1332.
- Morin, GB. (1989) The human telomere terminal transferase enzyme is a ribonucleoprotein that synthesizes TTAGGG repeats. *Cell*, **59**, 521-529.
- Morland, I., Rolseth, V., Luna, L. *et al.* (2002) Human DNA glycosylases of the bacterial Fpg/MutM superfamily: an alternative pathway for the repair of 8-oxoguanine and other oxidation products in DNA. *Nucleic Acids Research*, **30**, 4926-4936.
- Morrish, TA., Bekbolysnov, D., Velliquette, D. *et al.* (2013) Multiple Mechanisms Contribute To Telomere Maintenance. *Journal of Cancer Biology & Research*, **1**, 1012.
- Mulhern, RK., Palmer, SL., Merchant, TE. *et al.* (2005) Neurocognitive consequences of risk-adapted therapy for childhood medulloblastoma. *Journal of Clinical Oncology*, **23**, 5511-5519.
- Mullighan, CG., Goorha, S., Radtke I. *et al.* (2007) Genome-wide analysis of genetic alterations in acute lymphoblastic leukaemia. *Nature*, **446**, 758-764.
- Mullighan, CG., Miller, CB., Radtke, I. *et al.* (2008) BCR–ABL1 lymphoblastic leukaemia is characterized by the deletion of Ikaros. *Nature*, **453**, 110-114.
- Mullighan, CG., Zhang, J., Harvey, RC. *et al.* (2009) JAK mutations in high-risk childhood acute lymphoblastic leukemia. *Proceedings of the National Academy of Sciences USA*, **106**, 9414-9418.

Nakanishi, S., Prasad, R., Wilson, SH. & Smerdon, M. (2007) Different structural states in oligonucleosomes are required for early versus late steps of base excision repair. *Nucleic Acids Research*, **35**, 4313-4321.

Nathrath, M., Kremer, M., Letzel H. *et al.* (2001) Expression of genes of potential importance in the response to chemotherapy in osteosarcoma patients. *Klinische Padiatrie*, **214**, 230-235.

Nawrot, TS., Staessen, JA., Gardner, JP. & Aviv, A. (2004) Telomere length and possible link to X chromosome. *The Lancet*, **363**, 507-510.

Neidle, S. & Read, MA. (2000) G-quadruplexes as therapeutic targets. *Biopolymers*, **56**, 195-208.

Neurauter, CG., Luna, L. & Bjørås, M. (2012) Release from quiescence stimulates the expression of human NEIL3 under the control of the Ras dependent ERK–MAP kinase pathway. *DNA Repair*, **11**, 401-409.

Newbold, RF. (2002) The significance of telomerase activation and cellular immortalization in human cancer. *Mutagenesis*, **17**, 539-550.

Nishioka, K., Ohtsubo, T., Oda, H. *et al.* (1999) Expression and differential intracellular localization of two major forms of human 8-oxoguanine DNA glycosylase encoded by alternatively spliced OGG1 mRNAs. *Molecular Biology of the Cell*, **10**, 1637-1652.

Njajou, OT., Cawthon, RM., Damcott, CM. *et al.* (2007) Telomere length is paternally inherited and is associated with parental lifespan. *Proceedings of the National Academy of Sciences USA*, **104**, 12135-12139.

Nordfjäll, K., Larefalk, A., Lindgren, P., Holmberg, D. & Roos, G. (2005) Telomere length and heredity: Indications of paternal inheritance. *Proceedings of the National Academy of Sciences USA*, **102**, 16374-16378.

Oakman, C., Moretti, E., Galardi, F., Santarpia, L. & Di Leo, A. *et al.* (2009) The role of topoisomerase II $\alpha$  and HER-2 in predicting sensitivity to anthracyclines in breast cancer patients. *Cancer Treatment Reviews*, **35**, 662-667.

O'Brien, ME., Wigler, N., Inbar, M. *et al.* (2004) Reduced cardiotoxicity and comparable efficacy in a phase III trial of pegylated liposomal doxorubicin HCl

(CAELYX™/Doxil®) versus conventional doxorubicin for first-line treatment of metastatic breast cancer. *Annals of Oncology*, **15**, 440-449.

Oganesian, L. & Karlseder, J. (2011) Mammalian 5' C-rich telomeric overhangs are a mark of recombination-dependent telomere maintenance. *Molecular Cell*, **42**, 224-236.

Oikawa, S., Tada-Oikawa, S. & Kawanishi, S. (2001) Site-specific DNA damage at the GGG sequence by UVA involves acceleration of telomere shortening. *Biochemistry*, **40**, 4763-4768.

Okuda, K., Bardeguet, A., Gardner, JP. *et al.* (2002) Telomere length in the newborn. *Pediatric Research*, **52**, 377-381.

Onciu, M. (2009) Acute lymphoblastic leukemia. *Hematology/Oncology Clinics of North America*, **23**, 655-674.

Opresko, PL., Fan, J., Danzy, S., Wilson, DM 3<sup>rd</sup> & Bohr, VA. (2005) Oxidative damage in telomeric DNA disrupts recognition by TRF1 and TRF2. *Nucleic Acids Research*, **33**, 1230-1239.

Palm, W. & de Lange, T. (2008) How shelterin protects mammalian telomeres. *Annual Review of Genetics*, **42**, 301-334.

Pang, B., Qiao, X., Janssen, L. *et al.* (2013) Drug-induced histone eviction from open chromatin contributes to the chemotherapeutic effects of doxorubicin. *Nature Communications*, **4**, 1908.

Pasello, M., Michelacci, F., Scionti, I. *et al.* (2008) Overcoming glutathione S-transferase P1-related cisplatin resistance in osteosarcoma. *Cancer Research*, **68**, 6661-6668.

Peirson, SN., Butler, JN. & Foster, RG. (2003) Experimental validation of novel and conventional approaches to quantitative real-time PCR data analysis. *Nucleic Acids Research*, **31**, 73.

Perilongo, G., Malogolowkin, M. & Feusner, J. (2012) Hepatoblastoma clinical research: Lessons learned and future challenges. *Pediatric Blood & Cancer*, **59**, 818-821.

- Pfister, DG., Su, YB., Kraus, DH. *et al.* (2006) Concurrent cetuximab, cisplatin, and concomitant boost radiotherapy for locoregionally advanced, squamous cell head and neck cancer: a pilot phase II study of a new combined-modality paradigm. *Journal of Clinical Oncology*, **24**, 1072-1078.
- Pinato, O., Musetti, C., Farrell, NP. & Sissi, C. (2013) Platinum-based drugs and proteins: Reactivity and relevance to DNA adduct formation. *Journal of Inorganic Biochemistry*, **122**, 27-37.
- Ploner, C., Schmidt, S., Presul, E. *et al.* (2005) Glucocorticoid-induced apoptosis and glucocorticoid resistance in acute lymphoblastic leukemia. *Journal of Steroid Biochemistry and Molecular Biology*, **93**, 153-160.
- Ponting, CP., Oliver, PL. & Reik W. (2009) Evolution and functions of long noncoding RNAs. *Cell*, **136**, 629-641.
- Preti, HA., O'Brien, S., Giralt, S. *et al.* (1994) Philadelphia-chromosome-positive adult acute lymphocytic leukaemia: characteristics, treatment results, and prognosis in 41 patients. *American Journal of Medicine*, **97**, 60-65.
- Pui, CH & Evans, WE. (1999) Acute lymphoblastic leukemia in infants. *Journal of Clinical Oncology*, **17**, 438.
- Pui, CH., Carroll, WL., Meshinchi, S. & Arceci, RJ. (2011) Biology, risk stratification, and therapy of pediatric acute leukemias: an update. *Journal of Clinical Oncology*, **29**, 551-565.
- Pui, CH., Mullighan, CG., Evans, WE. & Relling MV. (2012) Pediatric acute lymphoblastic leukemia: where are we going and how do we get there? *Blood*, **120**, 1165-1174.
- Pui, CH., Relling, MV. & Downing, JR. (2004) Acute lymphoblastic leukemia. *New England Journal of Medicine*, **350**, 1535-1548.
- Pui, CH., Robison, LL. & Look, AT. (2008) Acute lymphoblastic leukaemia. *The Lancet*, **371**, 1030-1043.

- Quintanilla, RA., Orellana, JA. & von Bernhardt, R. (2012) Understanding risk factors for Alzheimer's disease: interplay of neuroinflammation, connexin-based communication and oxidative stress. *Archives of Medical Research*, **43**, 632-644.
- Rada, C., Di Noia, JM. & Neuberger, MS. (2004) Mismatch recognition and uracil excision provide complementary paths to both Ig switching and the A/T-focused phase of somatic mutation. *Molecular Cell*, **16**, 163-171.
- Rai, P., Wemmer, DE. & Linn, S. (2005) Preferential binding and structural distortion by Fe<sup>2+</sup> at RGGG-containing DNA sequences correlates with enhanced oxidative cleavage at such sequences. *Nucleic Acids Research*, **33**, 497-510.
- Rasool, M., Farooq, S., Malik, A. *et al.* (2015) Assessment of circulating biochemical markers and antioxidative status in acute lymphoblastic leukemia (ALL) and acute myeloid leukemia (AML) patients. *Journal of Clinical Oncology*, **22**, 106-111.
- Raynaud, CM., Sabatier, L., Philipot, O., Olaussen, KA. & Soria, JC. (2008) Telomere length, telomeric proteins and genomic instability during the multistep carcinogenic process. *Critical Reviews in Oncology/Hematology*, **66**, 99-117.
- Reed, JC. (1997) Double identity for proteins of the Bcl-2 family. *Nature*, **387**, 773-776.
- Rhee, DB., Ghosh, A., Lu, J., Bohr, VA. & Liu, Y. (2011) Factors that influence telomeric oxidative base damage and repair by DNA glycosylase OGG1. *DNA Repair*, **10**, 34-44.
- Richardson, RB. (2014) Age-specific bone tumour incidence rates are governed by stem cell exhaustion influencing the supply and demand of progenitor cells. *Mechanisms of Ageing and Development*, **139**, 31-40.
- Roco, A., Cayún, J., Contreras, S., Stojanova, J. & Quiñones, L. (2014) Can pharmacogenetics explain efficacy and safety of cisplatin pharmacotherapy? *Frontiers in Genetics*, **5**, 391.
- Rolfe, MD., Rice, CJ., Lucchini, S. *et al.* (2012) Lag phase is a distinct growth phase that prepares bacteria for exponential growth and involves transient metal accumulation. *Journal of Bacteriology*, **194**, 686-701.

- Rosenberg, B., VanCamp, L. & Krigas, T. (1965) Inhibition of cell division in *Escherichia coli* by electrolysis products from a platinum electrode. *Nature*, **205**, 698-699.
- Rosenquist, TA., Zaika, E., Fernandes, AS. *et al.* (2003) The novel DNA glycosylase, NEIL1, protects mammalian cells from radiation-mediated cell death. *DNA Repair*, **2**, 581-591.
- Ryu, RJ., Eyal, S., Kaplan, HG. *et al.* (2014) Pharmacokinetics of doxorubicin in pregnant women. *Cancer Chemotherapy and Pharmacology*, **73**, 789-797.
- Sakanaka, C., Sun, TQ. & Williams LT. (1999) New steps in the Wnt/beta-catenin signal transduction pathway. *Recent Progress in Hormone Research*, **55**, 225-236.
- Saldanha, SN., Andrews, LG. & Tollefsbol TO. (2003) Assessment of telomere length and factors that contribute to its stability. *European Journal of Biochemistry*, **270**, 389-403.
- Samuels, AL., Beesley, AH., Yadav, BD. *et al.* (2014) A pre-clinical model of resistance to induction therapy in pediatric acute lymphoblastic leukemia. *Blood Cancer Journal*, **4**, 232.
- Santhana Kumar, K., Tripolitsioti, D., Ma ,M. *et al.* (2015) The Ser/Thr kinase MAP4K4 drives c-Met-induced motility and invasiveness in a cell-based model of SHH medulloblastoma. *SpringerPlus*, **4**, 19.
- Saretzki, G. & Zglinicki, T. (2002) Replicative aging, telomeres, and oxidative stress. *Annals of the New York Academy of Sciences*, **959**, 24-29.
- Schmidt, S., Rainer, J., Riml, S. *et al.* (2006) Identification of glucocorticoid-response genes in children with acute lymphoblastic leukemia. *Blood*, **107**, 2061-2069.
- Schnellmann, RG. (1988) Mechanisms of t-butyl hydroperoxide-induced toxicity to rabbit renal proximal tubules. *American Journal of Physiology-Cell Physiology*, **255**, 28-33.
- Senchenkov, A., Litvak, DA. & Cabot, MC. (2001) Targeting ceramide metabolism—a strategy for overcoming drug resistance. *Journal of the National Cancer Institute*, **93**, 347-357.



- Shah, DS. & Kumar, R. (2013) Steroid resistance in leukemia. *World Journal of Experimental Medicine*, **3**, 21.
- Shiraishi, F., Curtis, LM., Truong, L. *et al.* (2000) Heme oxygenase-1 gene ablation or expression modulates cisplatin-induced renal tubular apoptosis. *American Journal of Physiology-Renal Physiology*, **278**, 726-736.
- Školáková, P., Foldynová-Trantírková, S., Bednářová, K. *et al.* (2015) Unique *C. elegans* telomeric overhang structures reveal the evolutionarily conserved properties of telomeric DNA. *Nucleic Acids Research*, **43**, 4733-4745.
- Slijepcevic, P. (2006) The role of DNA damage response proteins at telomeres—an “integrative” model. *DNA Repair*, **5**, 1299-1306.
- Smith, FW. & Feigon, J. (1992) Quadruplex structure of *Oxytricha* telomeric DNA oligonucleotides. *Nature*, **356**, 164-168.
- Smith, LA., Cornelius, VR., Plummer, CJ. *et al.* (2010) Cardiotoxicity of anthracycline agents for the treatment of cancer: systematic review and meta-analysis of randomised controlled trials. *BioMed Central Cancer*, **10**, 337.
- Stanulla, M. & Schrappe, M. (2009) Treatment of childhood acute lymphoblastic leukemia. *Seminars in Hematology*, **46**, 52-63.
- Su, X., Gopalakrishnan, V., Stearns, D. *et al.* (2006) Abnormal expression of REST/NRSF and Myc in neural stem/progenitor cells causes cerebellar tumors by blocking neuronal differentiation. *Molecular and Cellular Biology*, **26**, 1666-1678.
- Sullivan, LB. & Chandel, NS. (2014) Mitochondrial reactive oxygen species and cancer. *Cancer & Metabolism*, **2**, 17.
- Sun, W., Wu, Y., Yu, X. *et al.* (2013) Decreased expression of long noncoding RNA AC096655. 1-002 in gastric cancer and its clinical significance. *Tumour Biology*, **34**, 2697-2701.
- Susa, M., Iyer, AK., Ryu, K. *et al.* (2010) Inhibition of ABCB1 (MDR1) expression by a siRNA nanoparticulate delivery system to overcome drug resistance in osteosarcoma. *Cancer Research*, **70**, 3526-3526.

- Swartling, FJ. (2012) Myc proteins in brain tumor development and maintenance. *Upsala Journal of Medical Sciences*, **117**, 122-131.
- Szalai, VA., Singer, MJ. & Thorp, MM. (2002) Site-specific probing of oxidative reactivity and telomerase function using 7, 8-dihydro-8-oxoguanine in telomeric DNA. *Journal of the American Chemical Society*, **124**, 1625-1631.
- Tahtouh, R., Azzi, AS., Alaaeddine, N. *et al.* (2015) Telomerase Inhibition Decreases Alpha-Fetoprotein Expression and Secretion by Hepatocellular Carcinoma Cell Lines: *in vitro* and *in vivo* Study. *PloS One*, **10**, 1-14.
- Takao, M., Kanno, S., Kobayashi, K. *et al.* (2002) A back-up glycosylase in Nth1 knock-out mice is a functional Nei (endonuclease VIII) homologue. *Journal of Biological Chemistry*, **277**, 42205-42213.
- Takao, M., Oohata, Y., Kitadokoro, K. *et al.* (2009) Human Nei-like protein NEIL3 has AP lyase activity specific for single-stranded DNA and confers oxidative stress resistance in Escherichia coli mutant. *Genes to Cells*, **14**, 261-270.
- Takubo, K., Izumiyama-Shimomura, N., Honma, N. *et al.* (2002) Telomere lengths are characteristic in each human individual. *Experimental Gerontology*, **37**, 523-531.
- Talorete, TP., Bouaziz, M., Sayadi, S. & Isoda, H. (2006) Influence of medium type and serum on MTT reduction by flavonoids in the absence of cells. *Cytotechnology*, **52**, 189-198.
- Tan, EC., van Goor, H., Bahrami, S. *et al.* (2011) Intra-arterial tert-Butyl-Hydroperoxide Infusion Induces an Exacerbated Sensory Response in the Rat Hind Limb and is Associated with an Impaired Tissue Oxygen Uptake. *Inflammation*, **34**, 49-57.
- Taniguchi, K., Wada, M., Kohno, K. *et al.* (1996) A human canalicular multispecific organic anion transporter (cMOAT) gene is overexpressed in cisplatin-resistant human cancer cell lines with decreased drug accumulation. *Cancer Research*, **56**, 4124-4129.
- Taylor, MD., Northcott, PA., Korshunov A. *et al.* (2012) Molecular subgroups of medulloblastoma: the current consensus. *Acta Neuropathologica*, **123**, 465-472.

- Thompson, MC., Fuller, C., Hogg, TL. *et al.* (2006) Genomics identifies medulloblastoma subgroups that are enriched for specific genetic alterations. *Journal of Clinical Oncology*, **24**, 1924-1931.
- Thorn, CF., Oshiro, C., Marsh, S. *et al.* (2011) Doxorubicin pathways: pharmacodynamics and adverse effects. *Pharmacogenetics and Genomics*, **21**, 440.
- Torisu, K., Tsuchimoto, D., Ohnishi, Y. & Nakabeppu, Y. (2005) Hematopoietic Tissue-Specific Expression of Mouse Neil3 for Endonuclease VIII-Like Protein. *Journal of Biochemistry*, **138**, 763-772.
- Uchida, Y., Itoh, M., Taguchi, Y. *et al.* (2004) Ceramide reduction and transcriptional up-regulation of glucosylceramide synthase through doxorubicin-activated Sp1 in drug-resistant HL-60/ADR cells. *Cancer Research*, **64**, 6271-6279.
- Ueda, K., Cardarelli, C., Gottesman, MM. & Pastan, I. (1987) Expression of a full-length cDNA for the human "MDR1" gene confers resistance to colchicine, doxorubicin, and vinblastine. *Proceedings of the National Academy of Sciences USA*, **84**, 3004-3008.
- Uozaki, H., Horiuchi, H., Ishida, T. *et al.* (1997) Overexpression of resistance-related proteins (metallothioneins, glutathione-S-transferase  $\pi$ , heat shock protein 27, and lung resistance-related protein) in osteosarcoma. *Cancer*, **79**, 2336-2344.
- Valdes, AM., Andrew, T., Gardner, JP. *et al.* (2005) Obesity, cigarette smoking, and telomere length in women. *The Lancet*, **366**, 662-664.
- Vanel, D., Ruggieri, P., Ferrari, S. *et al.* (2009) The incidental skeletal lesion: ignore or explore? *Cancer Imaging*, **9**, 38-43.
- Vasa-Nicotera, M., Brouillette, S., Mangino, M. *et al.* (2005) Mapping of a major locus that determines telomere length in humans. *American Journal of Human Genetics*, **76**, 147-151.
- Vavrova, A., Jansova, H., Mackova, E. *et al.* (2013) Catalytic inhibitors of topoisomerase II differently modulate the toxicity of anthracyclines in cardiac and cancer cells. *PloS One*, **8**, 1-13.

- Vaziri, H., Schächter, F., Uchida, I. *et al.* (1993) Loss of telomeric DNA during aging of normal and trisomy 21 human lymphocytes. *American Journal of Human Genetics*, **52**, 661.
- Venkitaraman, AR. (2002) Cancer susceptibility and the functions of BRCA1 and BRCA2. *Cell*, **108**, 171-182.
- Von Zglinicki, T., Pilger, R. & Sitte, N. (2000) Accumulation of single-strand breaks is the major cause of telomere shortening in human fibroblasts. *Free Radical Biology and Medicine*, **28**, 64-74.
- Wang, C., Zhao, L. & Lu, S. (2015) Role of TERRA in the Regulation of Telomere Length. *International Journal of Biological Sciences*, **11**, 316-323.
- Wang, D., Luo, M. & Kelley, MR. (2004) Human apurinic endonuclease 1 (APE1) expression and prognostic significance in osteosarcoma: enhanced sensitivity of osteosarcoma to DNA damaging agents using silencing RNA APE1 expression inhibition. *Molecular Cancer Therapeutics*, **3**, 679-686.
- Wang, F., Remke, M., Bhat, K. *et al.* (2015) A microRNA-1280/JAG2 network comprises a novel biological target in high-risk medulloblastoma. *Oncotarget*, **6**, 2709.
- Wang, X. & Guo, Z. (2007) The role of sulfur in platinum anticancer chemotherapy. *Anti-Cancer Agents in Medicinal Chemistry*, **7**, 19-34.
- Weidmann, AG., Komor, AC. & Barton, JK. (2014) Targeted Chemotherapy with Metal Complexes. *Comments on Inorganic Chemistry*, **34**, 114-123.
- Wong, RP., Tsang, WP., Chau, PY. *et al.* (2007) p53-R273H gains new function in induction of drug resistance through down-regulation of procaspase-3. *Molecular Cancer Therapeutics*, **6**, 1054-1061.
- Wu, X., Fan, W., Xu, S. & Zhou, Y. (2003) Sensitization to the cytotoxicity of cisplatin by transfection with nucleotide excision repair gene xeroderma pigmentosum group A antisense RNA in human lung adenocarcinoma cells. *Clinical Cancer Research*, **9**, 5874-5879.
- Wu, Y. & Brosh, RM. (2010) G-quadruplex nucleic acids and human disease. *FEBS Journal*, **277**, 3470-3488.

- Xia, Z., Zhang, N. & Ding, D. (2014) Proliferation and migration of hepatoblastoma cells are mediated by IRS-4 via PI3K/Akt pathways. *International Journal of Clinical and Experimental Medicine*, **7**, 3763.
- Yakes, FM. & Van Houten, B. (1997) Mitochondrial DNA damage is more extensive and persists longer than nuclear DNA damage in human cells following oxidative stress. *Proceedings of the National Academy of Sciences USA*, **94**, 514-519.
- Yamamoto, R., Ohshiro, Y., Shimotani, T. *et al.* (2014) Hypersensitivity of mouse NEIL1-knockdown cells to hydrogen peroxide during S phase. *Journal of Radiation Research*, **55**, 707-712.
- Yang, F., Kemp, CJ. & Henikoff, S. (2015) Anthracyclines induce double-strand DNA breaks at active gene promoters. *Mutation Research/Fundamental and Molecular Mechanisms of Mutagenesis*, **773**, 9-15.
- Yang, F., Teves, SS., Kemp, CJ. & Henikoff, S. (2014) Doxorubicin, DNA torsion, and chromatin dynamics. *Biochimica Biophysica Acta- Reviews on Cancer*, **1845**, 84-89.
- Yang, Q., Xiang, J., Yang, S. *et al.* (2009) Verification of specific G-quadruplex structure by using a novel cyanine dye supramolecular assembly: I. Recognizing mixed G-quadruplex in human telomeres. *Chemical Communications*, **9**, 1103-1105.
- Ye, D., Li, H., Qian, S. *et al.* (1998) bcl-2/bax expression and p53 gene status in human bladder cancer: relationship to early recurrence with intravesical chemotherapy after resection. *The Journal of Urology*, **160**, 2025-2029.
- Zhang, R., Niu, Y. & Zhou, Y. (2010) Increase the cisplatin cytotoxicity and cisplatin-induced DNA damage in HepG2 cells by XRCC1 abrogation related mechanisms. *Toxicology letters*, **192**, 108-114.
- Zhang, S., Liu, X., Bawa-Khalfe, T. *et al.* (2012) Identification of the molecular basis of doxorubicin-induced cardiotoxicity. *Nature Medicine*, **18**, 1639-1642.
- Zhang, SL., Mao, NF., Sun, JY. *et al.* (2012) Predictive potential of glutathione S-transferase polymorphisms for prognosis of osteosarcoma patients on chemotherapy. *Asian Pacific Journal of Cancer Prevention*, **13**, 2705-2709.

Zhao, Y., Zhang, CL., Zeng, BF. *et al.* (2009) Enhanced chemosensitivity of drug-resistant osteosarcoma cells by lentivirus-mediated Bcl-2 silencing. *Biochemical and Biophysical Research Communications*, **390**, 642-647.

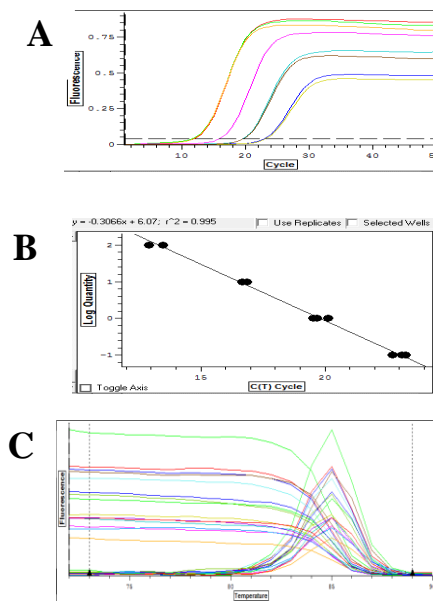
Zhou, H., Xu, M., Huang, Q. *et al.* (2008) Genome-scale RNAi screen for host factors required for HIV replication. *Cell Host & Microbe*, **4**, 495-504.

Zhou, J., Fleming, AM., Averill, AM., Burrows, CJ. & Wallace, SS. (2015) The NEIL glycosylases remove oxidized guanine lesions from telomeric and promoter quadruplex DNA structures. *Nucleic Acids Research*, **43**, 4039-4054.

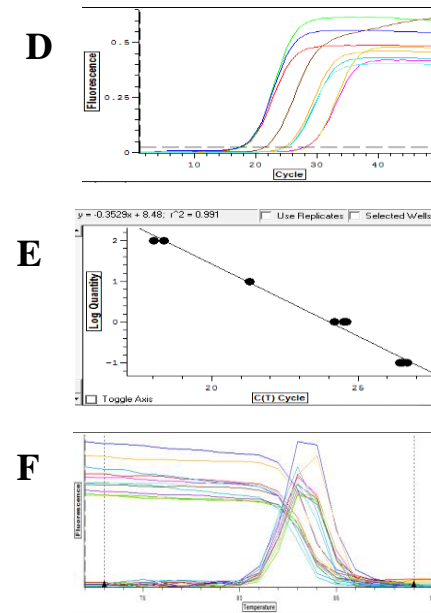
Zhou, J., Liu, M., Fleming, AM., Burrows, CJ. & Wallace, SS. (2013) Neil3 and NEIL1 DNA glycosylases remove oxidative damages from quadruplex DNA and exhibit preferences for lesions in the telomeric sequence context. *Journal of Biological Chemistry*, **288**, 27263-27272.

## Chapter 5: Appendix

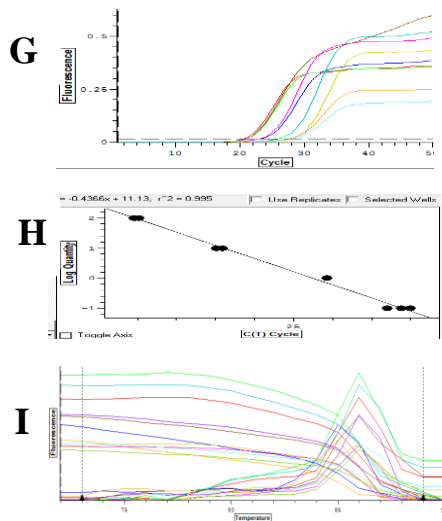
### Gapdh standard curve data



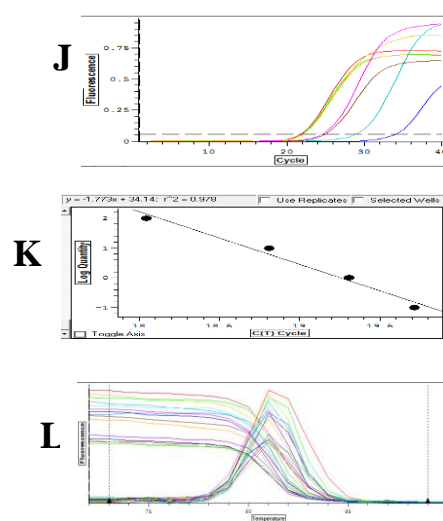
### NEIL3 standard curve data



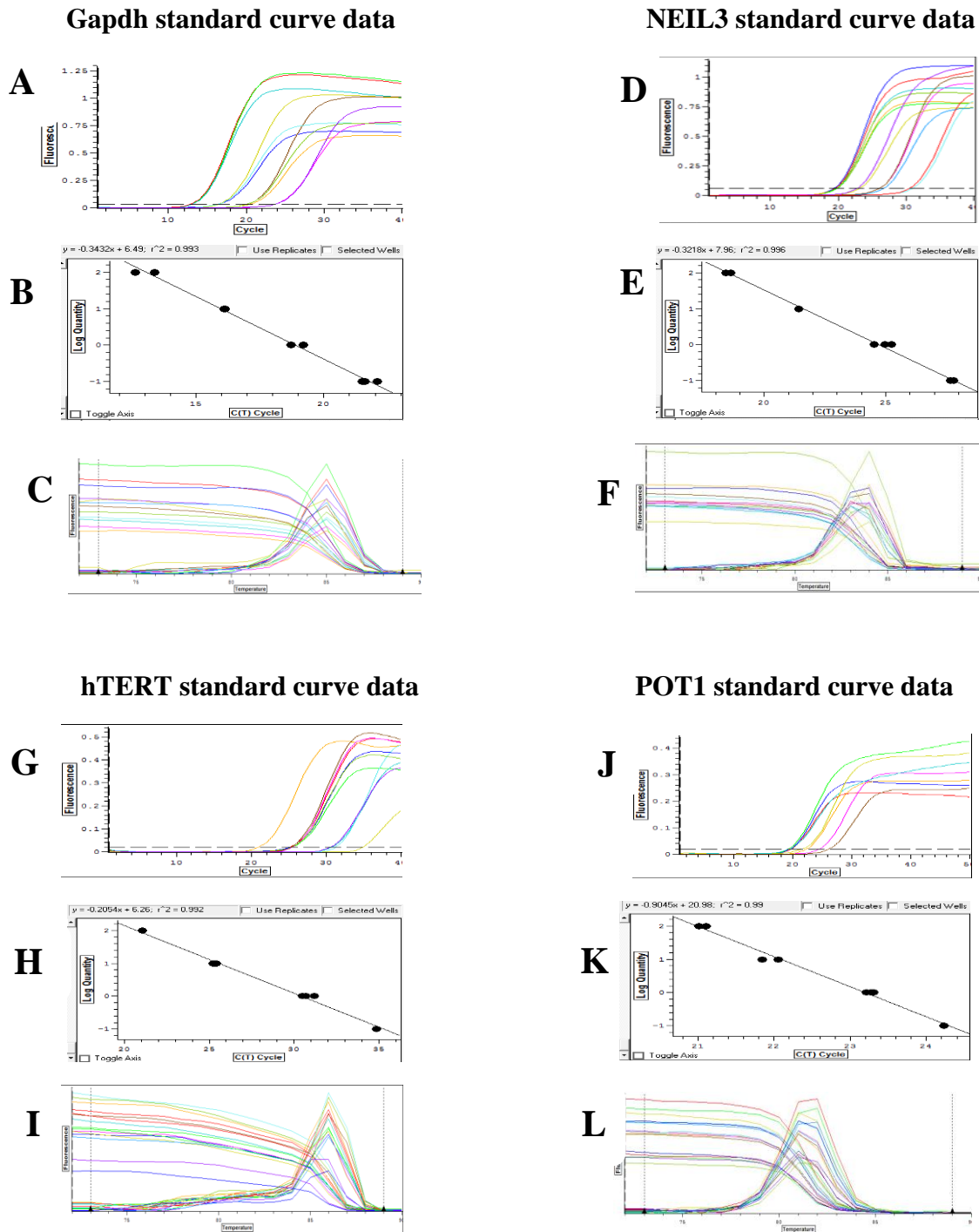
### hTERT standard curve data



### POT1 standard curve data

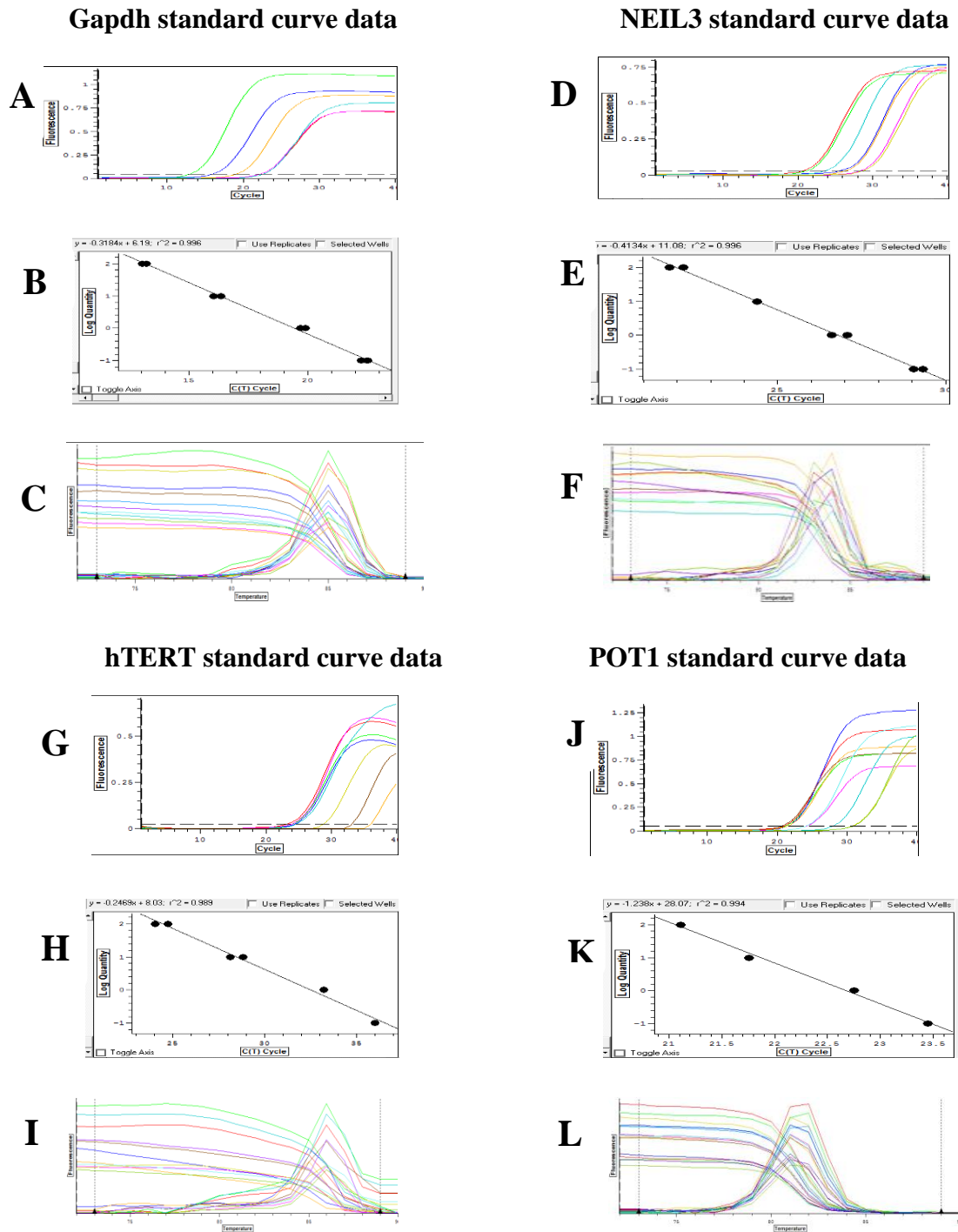


**Figure 5.1:** qRT-PCR on cDNA of CEM-1-15 cells. qRT-PCR reaction was carried out with triplicate aliquots of 5  $\mu$ l cDNA CEM-1-15 cells, NEIL3, hTERT and POT1 primers. The reference gene was Gapdh. (A) Amplification curve with Gapdh primers. (B) The linear regression curve with Gapdh primers. (C) The melting curve for Gapdh primers. (D) Amplification curve with NEIL3 primers. (E) The linear regression curve with NEIL3 primers. (F) The melting curve for NEIL3 primers. (G) Amplification curve with hTERT primers. (H) The linear regression curve with hTERT primers. (I) The melting curve for hTERT primers. (J) Amplification curve with POT1 primers. (K) The linear regression curve with POT1 primers (L) The melting curve for POT1 primers. qRT-PCR was carried out twice on each cell line and these figures represent one of the experiments.

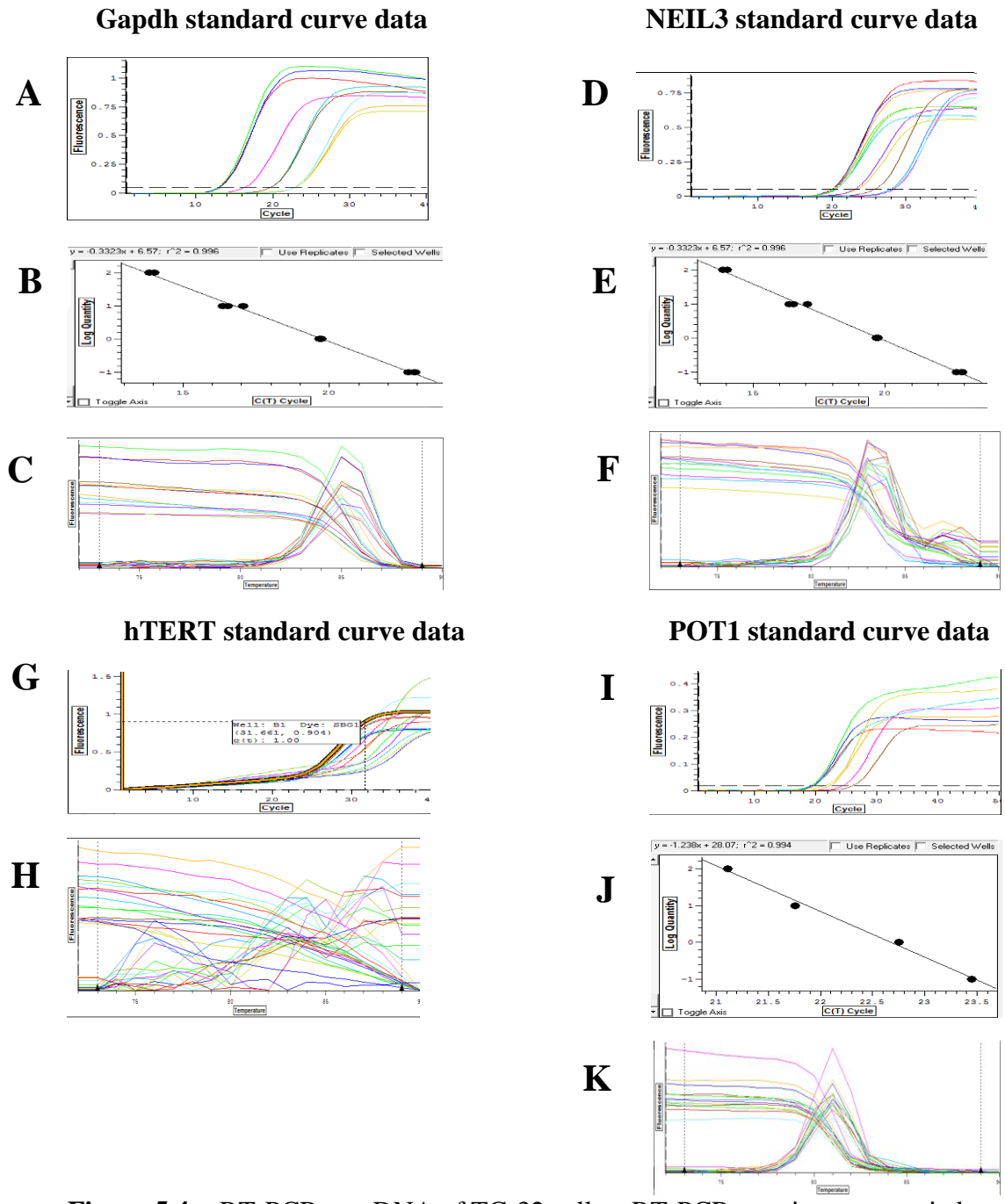


**Figure 5.2:** qRT-PCR on cDNA of CEM-7-14 cells. qRT-PCR reaction was carried out with triplicate aliquots of 5  $\mu$ l cDNA CEM-7-14 cells, NEIL3, hTERT and POT1 primers. The reference gene was Gapdh. (A) Amplification curve with Gapdh primers. (B) The linear regression curve with Gapdh primers. (C) The melting curve for Gapdh primers. (D) Amplification curve with NEIL3 primers. (E) The linear regression curve with NEIL3 primers. (F) The melting curve for NEIL3 primers. (G) Amplification curve with hTERT primers. (H) The linear regression curve with hTERT primers. (I) The melting curve for hTERT primers. (J) Amplification curve with POT1 primers. (K) The linear regression curve with POT1 primers (L) The melting curve for POT1 primers. qRT-PCR was carried out twice on each cell line and these figures represent one of the experiments.

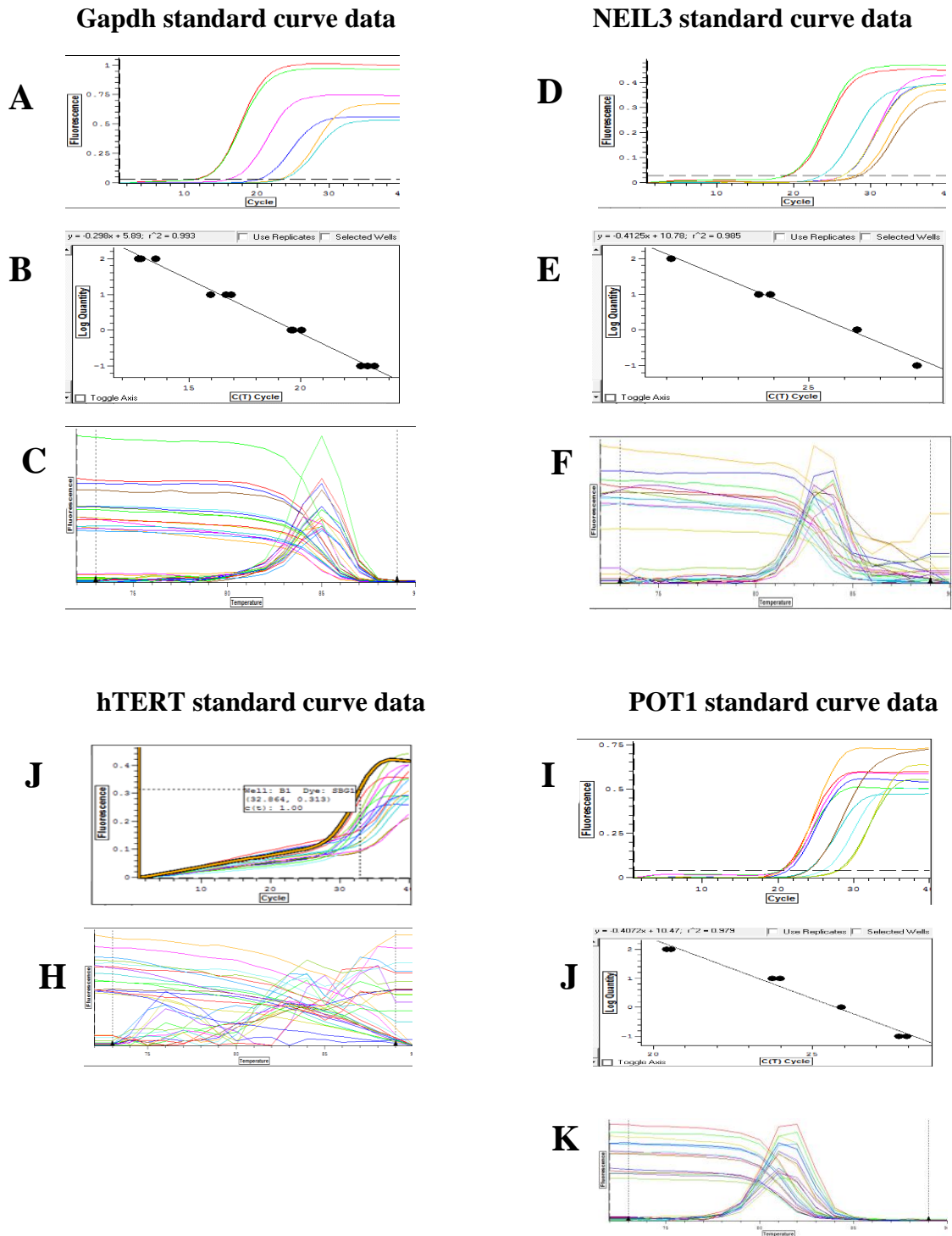




**Figure 5.3:** qRT-PCR on cDNA of HepG2 cells. qRT-PCR reaction was carried out with triplicate aliquots of 5  $\mu$ l cDNA HepG2 cells, NEIL3, hTERT and POT1 primers. The reference gene was Gapdh. (A) Amplification curve with Gapdh primers. (B) The linear regression curve with Gapdh primers. (C) The melting curve for Gapdh primers. (D) Amplification curve with NEIL3 primers. (E) The linear regression curve with NEIL3 primers. (F) The melting curve for NEIL3 primers. (G) Amplification curve with hTERT primers. (H) The linear regression curve with hTERT primers (I) The melting curve for hTERT primers. (J) Amplification curve with POT1 primers. (K) The linear regression curve with POT1 primers (L) The melting curve for POT1 primers. qRT-PCR was carried out twice on each cell line and these figures represent one of the experiments.

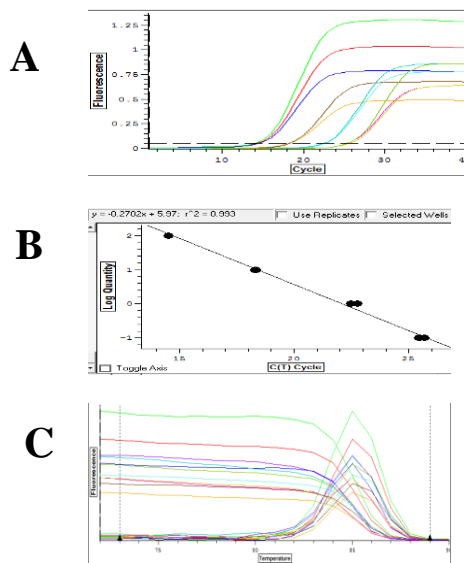


**Figure 5.4:** qRT-PCR on cDNA of TC-32 cells. qRT-PCR reaction was carried out with triplicate aliquots of 5  $\mu$ l cDNA TC-32 cells, NEIL3, hTERT and POT1 primers. The reference gene was Gapdh. (A) Amplification curve with Gapdh primers. (B) The linear regression curve with Gapdh primers. (C) The melting curve for Gapdh primers. (D) Amplification curve with NEIL3 primers. (E) The linear regression curve with NEIL3 primers. (F) The melting curve for NEIL3 primers. (G) Amplification curve with hTERT primers. (H) The melting curve for hTERT primers. (I) Amplification curve with POT1 primers. (J) The linear regression curve with POT1 primers (K) The melting curve for POT1 primers. qRT-PCR was carried out twice on each cell line and these figures represent one of the experiments.

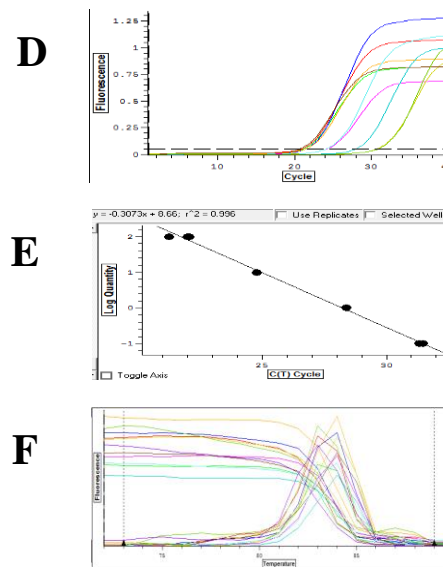


**Figure 5.5:** qRT-PCR on cDNA of Saos-2 cells. qRT-PCR reaction was carried out with triplicate aliquots of 5  $\mu$ l cDNA Saos-2 cells, NEIL3, hTERT and POT1 primers. The reference gene was Gapdh. (A) Amplification curve with Gapdh primers. (B) The linear regression curve with Gapdh primers. (C) The melting curve for Gapdh primers. (D) Amplification curve with NEIL3 primers. (E) The linear regression curve with NEIL3 primers. (F) The melting curve for NEIL3 primers. (G) Amplification curve with hTERT primers. (H) The melting curve for hTERT primers. (I) Amplification curve with POT1 primers. (J) The linear regression curve with POT1 primers (K) The melting curve for POT1 primers. qRT-PCR was carried out twice on each cell line and these figures represent one of the experiments.

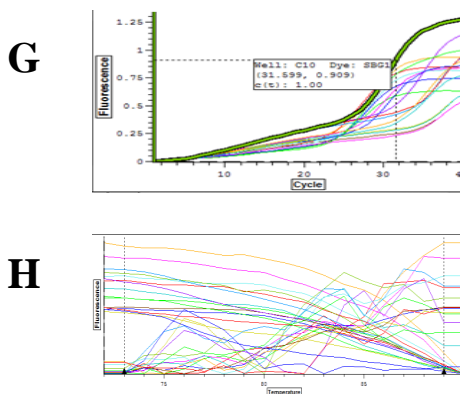
### Gapdh standard curve data



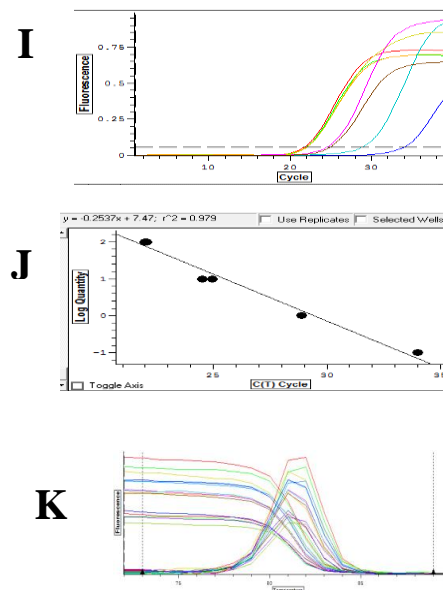
### NEIL3 standard curve data



### hTERT standard curve data

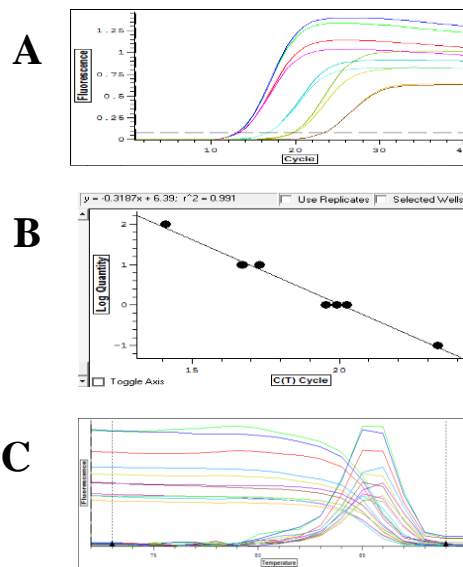


### POT1 standard curve data

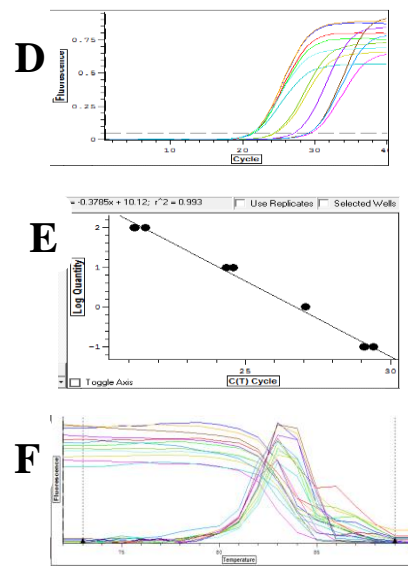


**Figure 5.6:** qRT-PCR on cDNA of HOS cells. qRT-PCR reaction was carried out with triplicate aliquots of 5  $\mu$ l cDNA HOS cells, NEIL3, hTERT and POT1 primers. The reference gene was Gapdh. (A) Amplification curve with Gapdh primers. (B) The linear regression curve with Gapdh primers. (C) The melting curve for Gapdh primers. (D) Amplification curve with NEIL3 primers. (E) The linear regression curve with NEIL3 primers. (F) The melting curve for NEIL3 primers. (G) Amplification curve with hTERT primers. (H) The melting curve for hTERT primers. (I) Amplification curve with POT1 primers. (J) The linear regression curve with POT1 primers (K) The melting curve for POT1 primers. qRT-PCR was carried out twice on each cell line and these figures represent one of the experiments.

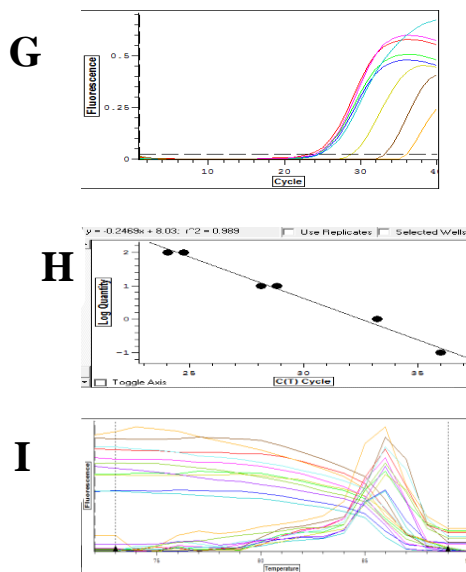
### Gapdh standard curve data



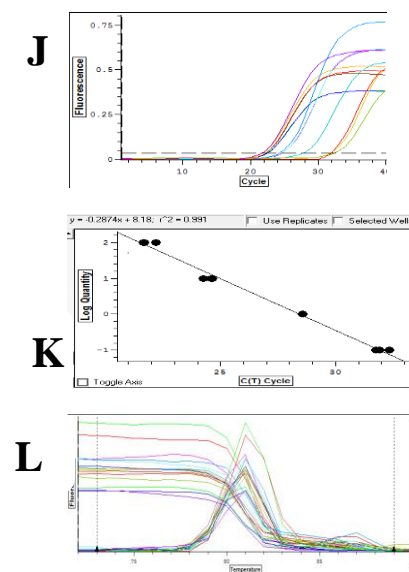
### NEIL3 standard curve data



### hTERT standard curve data

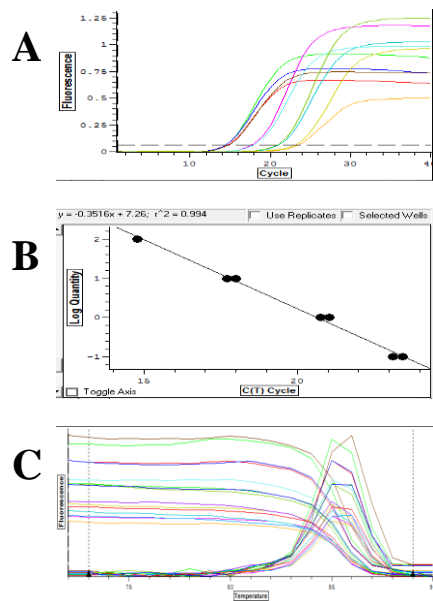


### POT1 standard curve data

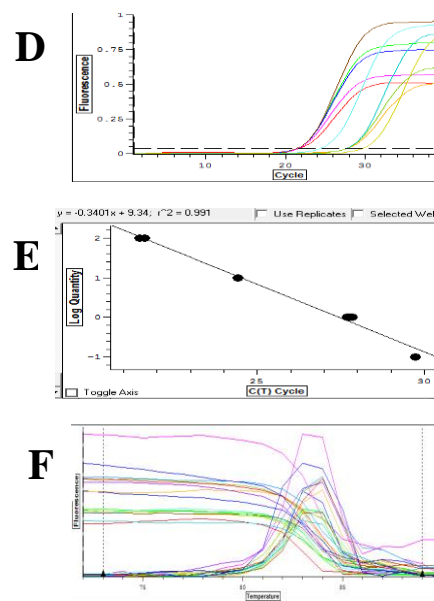


**Figure 5.7:** qRT-PCR on HepG2 cells. qRT-PCR reaction was carried out with triplicate aliquots of 5  $\mu$ l cDNA HepG2 cells, NEIL3, hTERT and POT1 primers. The reference gene was Gapdh. (A) Amplification curve with Gapdh primers. (B) The linear regression curve with Gapdh primers. (C) The melting curve for Gapdh primers. (D) Amplification curve with NEIL3 primers. (E) The linear regression curve with NEIL3 primers. (F) The melting curve for NEIL3 primers. (G) Amplification curve with hTERT primers. (H) The linear regression curve with hTERT primers (I) The melting curve for hTERT primers. (J) Amplification curve with POT1 primers. (K) The linear regression curve with POT1 primers (L) The melting curve for POT1 primers. qRT-PCR was carried out twice on each cell line and these figures represent one of the experiments.

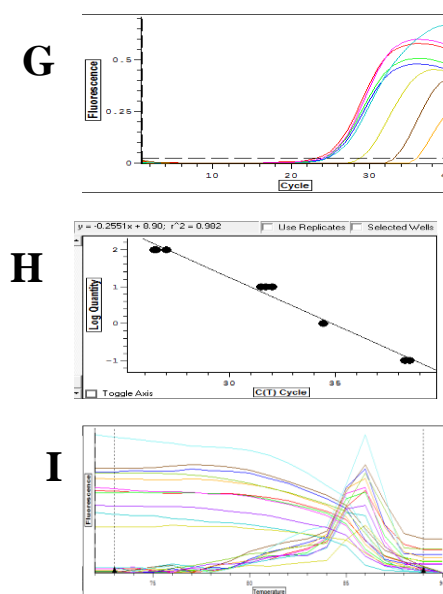
### Gapdh standard curve data



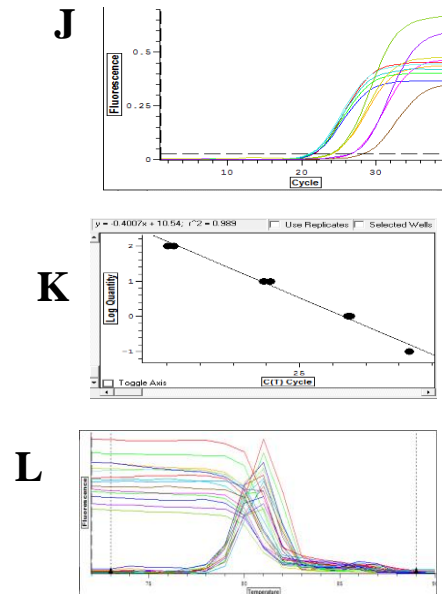
### NEIL3 standard curve data



### hTERT standard curve data

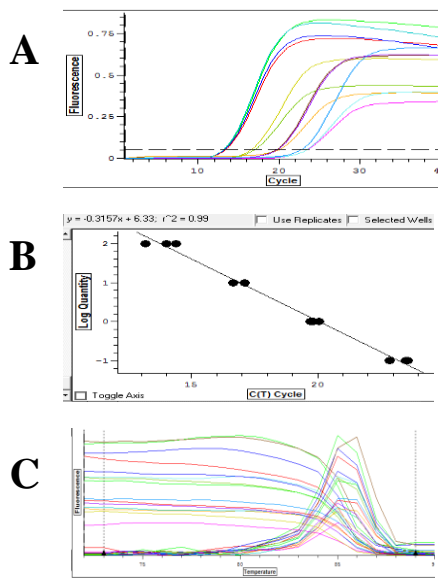


### POT1 standard curve data

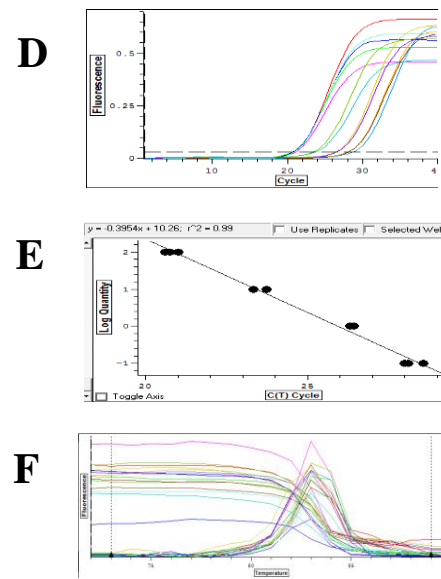


**Figure 5.8:** qRT-PCR on HepG2 cells treated with 2.5  $\mu$ M t-BHP. qRT-PCR reaction was carried out with triplicate aliquots of 5  $\mu$ l cDNA HepG2 cells, NEIL3, hTERT and POT1 primers. The reference gene was Gapdh. (A) Amplification curve with Gapdh primers. (B) The linear regression curve with Gapdh primers. (C) The melting curve for Gapdh primers. (D) Amplification curve with NEIL3 primers. (E) The linear regression curve with NEIL3 primers. (F) The melting curve for NEIL3 primers. (G) Amplification curve with hTERT primers. (H) The linear regression curve with hTERT primers (I) The melting curve for hTERT primers. (J) Amplification curve with POT1 primers. (K) The linear regression curve with POT1 primers (L) The melting curve for POT1 primers. qRT-PCR was carried out twice on each cell line and these figures represent one of the experiments.

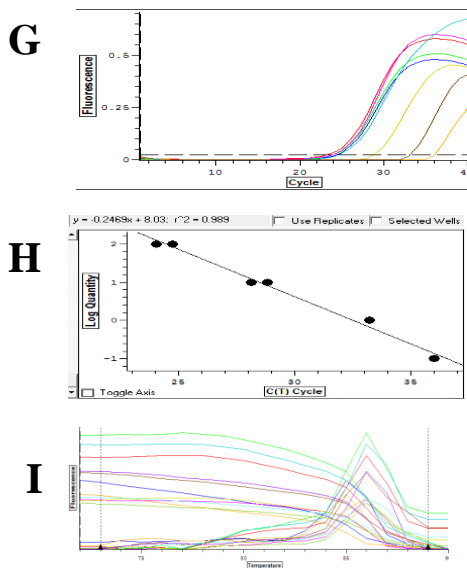
### Gapdh standard curve data



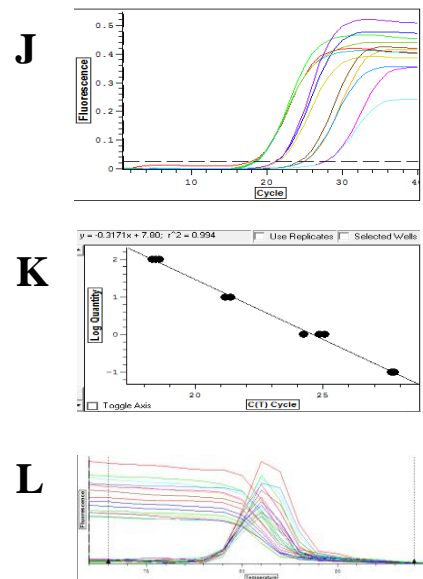
### NEIL3 standard curve data



### hTERT standard curve data



### POT1 standard curve data



**Figure 5.9:** qRT-PCR on HepG2 cells treated with 5  $\mu$ M t-BHP. qRT-PCR reaction was carried out with triplicate aliquots of 5  $\mu$ l cDNA HepG2 cells, NEIL3, hTERT and POT1 primers. The reference gene was Gapdh. (A) Amplification curve with Gapdh primers. (B) The linear regression curve with Gapdh primers. (C) The melting curve for Gapdh primers. (D) Amplification curve with NEIL3 primers. (E) The linear regression curve with NEIL3 primers. (F) The melting curve for NEIL3 primers. (G) Amplification curve with hTERT primers. (H) The linear regression curve with hTERT primers (I) The melting curve for hTERT primers. (J) Amplification curve with POT1 primers. (K) The linear regression curve with POT1 primers (L) The melting curve for POT1 primers. qRT-PCR was carried out twice on each cell line and these figures represent one of the experiments.

**Table 5.1:** Anova: Two-Factor Without Replication for NEIL3 and hTERT in CEM-1-15 cell line

<i>SUMMARY</i>	<i>Count</i>	<i>Sum</i>	<i>Average</i>	<i>Variance</i>
NEIL3	6	706	117.6667	25.46667
hTERT	6	588	98	4.4
Column 1	2	212	106	98
Column 2	2	224	112	242
Column 3	2	209	104.5	180.5
Column 4	2	222	111	392
Column 5	2	212	106	162
Column 6	2	215	107.5	144.5

ANOVA

<i>Source of Variation</i>	<i>SS</i>	<i>df</i>	<i>MS</i>	<i>F</i>	<i>P-value</i>	<i>F crit</i>
Rows	1160.333	1	1160.333	98.89205	0.000176	6.607891
Columns	90.66667	5	18.13333	1.545455	0.322256	5.050329
Error	58.66667	5	11.73333			
Total	1309.667	11				

t-Test: Paired Two Sample for Means of NEIL3 and hTERT in CEM-1-15 cell line

	<i>NEIL3</i>	<i>hTERT</i>
Mean	117.6666667	98
Variance	25.46666667	4.4
Observations	6	6
Pearson Correlation	0.302299611	
Hypothesized Mean Difference		0
Df		5
t Stat	9.944447971	
P(T<=t) one-tail	8.77874E-05	
t Critical one-tail	2.015048373	
P(T<=t) two-tail	0.000176	
t Critical two-tail	2.570581836	



**Table 5.2:** Anova: Two-Factor Without Replication for NEIL3 and POT1 in CEM-1-15 cell line

<i>SUMMARY</i>	<i>Count</i>	<i>Sum</i>	<i>Average</i>	<i>Variance</i>
NEIL3	6	706	117.6667	25.46667
POT1	6	340	56.66667	107.8667
Column 1	2	182	91	968
Column 2	2	194	97	1352
Column 3	2	163	81.5	2112.5
Column 4	2	176	88	2738
Column 5	2	166	83	2048
Column 6	2	165	82.5	2244.5

ANOVA

<i>Source of Variation</i>	<i>SS</i>	<i>df</i>	<i>MS</i>	<i>F</i>	<i>P-value</i>	<i>F crit</i>
Rows	11163	1	11163	186.05	0.00037	6.607891
Columns	366.6667	5	73.33333	1.222222	0.415541	5.050329
Error	300	5	60			
Total	11829.67	11				

t-Test: Paired Two Sample for Means of NEIL3 and POT1 in CEM-1-15 cell line

	<i>NEIL3</i>	<i>POT1</i>
Mean	117.6667	56.66667
Variance	25.46667	107.8667
Observations	6	6
Pearson Correlation	0.127198	
Hypothesized Mean Difference	0	
Df	5	
t Stat	13.64001	
P(T<=t) one-tail	1.9E-05	
t Critical one-tail	2.015048	
P(T<=t) two-tail	0.00037	
t Critical two-tail	2.570582	

**Table 5.3:** Anova: Two-Factor Without Replication for NEIL3 in CEM-1-15 and CEM-7-14 cells

<i>SUMMARY</i>	<i>Count</i>	<i>Sum</i>	<i>Average</i>	<i>Variance</i>
NEIL3 in CEM-1-15	6	706	117.6667	25.46667
NEIL3 in CEM-7-14	6	456	76	72.8
Column 1	2	200	100	338
Column 2	2	193	96.5	1404.5
Column 3	2	185	92.5	924.5
Column 4	2	212	106	722
Column 5	2	185	92.5	1012.5
Column 6	2	187	93.5	1012.5

ANOVA

<i>Source of Variation</i>	<i>SS</i>	<i>df</i>	<i>MS</i>	<i>F</i>	<i>P-value</i>	<i>F crit</i>
Rows	5208.333	1	5208.333	126.6207	0.009	6.607891
Columns	285.6667	5	57.13333	1.388979	0.363617	5.050329
Error	205.6667	5	41.13333			
Total	5699.667	11				

t-Test: Paired Two Sample for Means of NEIL3 in CEM-1-15 and CEM-7-14 cell line

	<i>NEIL3 in CEM-1-15</i>	<i>NEIL3 in CEM-7-14</i>
Mean	117.6666667	76
Variance	25.46666667	72.8
Observations	6	6
Pearson Correlation	0.185796807	
Hypothesized Mean Difference	0	
Df	5	
t Stat	11.25258839	
P(T<=t) one-tail	4.84114E-05	
t Critical one-tail	2.015048373	
P(T<=t) two-tail	0.009	
t Critical two-tail	2.570581836	

**Table 5.4:** Anova: Two-Factor Without Replication for hTERT in CEM-1-15 and CEM-7-14 cells

<i>SUMMARY</i>	<i>Count</i>	<i>Sum</i>	<i>Average</i>	<i>Variance</i>
hTERT in CEM-1-15	6	588	98	4.4
hTERT in CEM-7-14	6	422	70.333333	35.46667
Column 1	2	177	88.5	220.5
Column 2	2	168	84	578
Column 3	2	161	80.5	420.5
Column 4	2	175	87.5	180.5
Column 5	2	164	82	450
Column 6	2	165	82.5	544.5

ANOVA

<i>Source of Variation</i>	<i>SS</i>	<i>df</i>	<i>MS</i>	<i>F</i>	<i>P-value</i>	<i>F crit</i>
Rows	2296.333	1	2296.333	117.5597	0.000116	6.607891
Columns	101.6667	5	20.33333	1.040956	0.48297	5.050329
Error	97.66667	5	19.53333			
Total	2495.667	11				

t-Test: Paired Two Sample for Means of hTERT in CEM-1-15 and CEM-7-14 cells

	<i>hTERT in CEM-1-15</i>	<i>hTERT in CEM-7-14</i>
Mean	98	70.33333333
Variance	4.4	35.46666667
Observations	6	6
Pearson Correlation	0.032020158	
Hypothesized Mean Difference	0	
Df	5	
t Stat	10.84249634	
P(T<=t) one-tail	5.79214E-05	
t Critical one-tail	2.015048373	
P(T<=t) two-tail	0.000116	
t Critical two-tail	2.570581836	

**Table 5.5:** Anova: Two-Factor Without Replication for NEIL3 and POT1 in HOS cells

<i>SUMMARY</i>	<i>Count</i>	<i>Sum</i>	<i>Average</i>	<i>Variance</i>
NEIL3	6	456	76	23.6
POT1	6	361	60.16667	0.566667
Column 1	2	133	66.5	60.5
Column 2	2	130	65	50
Column 3	2	139	69.5	220.5
Column 4	2	144	72	242
Column 5	2	135	67.5	112.5
Column 6	2	136	68	128

ANOVA

<i>Source of Variation</i>	<i>SS</i>	<i>df</i>	<i>MS</i>	<i>F</i>	<i>P-value</i>	<i>F crit</i>
Rows	752.0833	1	752.0833	61.22795	0.000547	6.607891
Columns	59.41667	5	11.88333	0.967436	0.514048	5.050329
Error	61.41667	5	12.28333			
Total	872.9167	11				

t-Test: Paired Two Sample for Means of NEIL3 and POT1 in HOS cells

	<i>NEIL3</i>	<i>POT1</i>
Mean	76	60.16667
Variance	23.6	0.566667
Observations	6	6
Pearson Correlation	-0.05469	
Hypothesized Mean Difference	0	
Df	5	
t Stat	7.824829	
P(T<=t) one-tail	0.000273	
t Critical one-tail	2.015048	
P(T<=t) two-tail	0.000547	
t Critical two-tail	2.570582	

**Table 5.6:** Anova: Two-Factor Without Replication for NEIL3 and POT1 in Saos-2 cells.

<i>SUMMARY</i>	<i>Count</i>	<i>Sum</i>	<i>Average</i>	<i>Variance</i>
NEIL3	6	942	157	31.2
POT1	6	1033	172.1667	8.966667
Column 1	2	318	159	162
Column 2	2	326	163	242
Column 3	2	338	169	50
Column 4	2	338	169	98
Column 5	2	329	164.5	60.5
Column 6	2	326	163	128

ANOVA

<i>Source of Variation</i>	<i>SS</i>	<i>df</i>	<i>MS</i>	<i>F</i>	<i>P-value</i>	<i>F crit</i>
Rows	690.0833	1	690.0833	68.43802	0.000421	6.607891
Columns	150.4167	5	30.08333	2.983471	0.127731	5.050329
Error	50.41667	5	10.08333			
Total	890.9167	11				

t-Test: Paired Two Sample for Means of NEIL3 and POT1 in Saos-2 cells.

	<i>NEIL3</i>	<i>POT1</i>
Mean	157	172.166667
Variance	31.2	8.96666667
Observations	6	6
Pearson Correlation	0.597871	
Hypothesized Mean Difference	0	
Df	5	
t Stat	-8.27273	
P(T<=t) one-tail	0.000211	
t Critical one-tail	2.015048	
P(T<=t) two-tail	0.000421	
t Critical two-tail	2.570582	

**Table 5.7:** Anova: Two-Factor Without Replication for NEIL3 in Saos-2 and HOS cells

<i>SUMMARY</i>	<i>Count</i>	<i>Sum</i>	<i>Average</i>	<i>Variance</i>
NEIL3 in Saos-2	6	942	157	31.2
NEIL3 in HOS	6	456	76	23.6
Column 1	2	222	111	3042
Column 2	2	222	111	3362
Column 3	2	244	122	3528
Column 4	2	245	122.5	3120.5
Column 5	2	234	117	3528
Column 6	2	231	115.5	3120.5

ANOVA

<i>Source of Variation</i>	<i>SS</i>	<i>Df</i>	<i>MS</i>	<i>F</i>	<i>P-value</i>	<i>F crit</i>
Rows	19683	1	19683	5467.5	0.00046	6.607891
Columns	256	5	51.2	14.22222	0.005592	5.050329
Error	18	5	3.6			
Total	19957	11				

t-Test: Paired Two Sample for Means of NEIL3 in Saos-2 and HOS cells

	<i>NEIL3 in Saos-2</i>	<i>NEIL3 in HOS</i>
Mean	157	76
Variance	31.2	23.6
Observations	6	6
Pearson Correlation	0.877088988	
Hypothesized Mean Difference	0	
Df	5	
t Stat	73.94254526	
P(T<=t) one-tail	4.285E-09	
t Critical one-tail	2.015048373	
P(T<=t) two-tail	0.00046	
t Critical two-tail	2.570581836	

**Table 5.8:** Anova: Two-Factor Without Replication for POT 1 in Saos-2 and HOS cells

<i>SUMMARY</i>	<i>Count</i>	<i>Sum</i>	<i>Average</i>	<i>Variance</i>
POT1 in Saos-2	6	1033	172.1667	8.966667
POT1 in HOS	6	361	60.16667	0.566667
Column 1	2	229	114.5	5724.5
Column 2	2	234	117	6498
Column 3	2	233	116.5	6612.5
Column 4	2	237	118.5	6612.5
Column 5	2	230	115	6050
Column 6	2	231	115.5	6160.5

ANOVA

<i>Source of Variation</i>	<i>SS</i>	<i>Df</i>	<i>MS</i>	<i>F</i>	<i>P-value</i>	<i>F crit</i>
Rows	37632	1	37632	7236.923	0.00042	6.607891
Columns	21.66667	5	4.333333	0.833333	0.576848	5.050329
Error	26	5	5.2			
Total	37679.67	11				

t-Test: Paired Two Sample for Means of POT1 in Saos-2 and HOS cells

	<i>POT1 in</i>	
	<i>Saos-2</i>	<i>POT1 in HOS</i>
Mean	172.1666667	60.16666667
Variance	8.966666667	0.566666667
Observations	6	6
	-	
Pearson Correlation	0.192239555	
Hypothesized Mean Difference	0	
Df	5	
t Stat	85.07010684	
P(T<=t) one-tail	2.1269E-09	
t Critical one-tail	2.015048373	
P(T<=t) two-tail	0.00042	
t Critical two-tail	2.570581836	

**Table 5.9:** Anova: Two-Factor Without Replication for NEIL3 and POT1 in TC-32 cells

<i>SUMMARY</i>	<i>Count</i>	<i>Sum</i>	<i>Average</i>	<i>Variance</i>
NEIL3	6	650	108.3333	102.6667
POT1	6	318	53	92
Column 1	2	145	72.5	1860.5
Column 2	2	152	76	1800
Column 3	2	187	93.5	1404.5
Column 4	2	184	92	1800
Column 5	2	149	74.5	1200.5
Column 6	2	151	75.5	1200.5

ANOVA

<i>Source of Variation</i>	<i>SS</i>	<i>Df</i>	<i>MS</i>	<i>F</i>	<i>P-value</i>	<i>F crit</i>
Rows	9185.333	1	9185.333	569.3388	0.00024	6.607891
Columns	892.6667	5	178.5333	11.06612	0.009804	5.050329
Error	80.66667	5	16.13333			
Total	10158.67	11				

t-Test: Paired Two Sample for Means of NEIL3 and POT1 in TC-32 cells

	<i>NEIL3</i>	<i>POT1</i>
Mean	108.3333	53
Variance	102.6667	92
Observations	6	6
Pearson Correlation	0.835502	
Hypothesized Mean Difference	0	
Df	5	
t Stat	23.86082	
P(T<=t) one-tail	1.2E-06	
t Critical one-tail	2.015048	
P(T<=t) two-tail	0.00024	
t Critical two-tail	2.570582	



**Table 5.10:** Anova: Two-Factor Without Replication for NEIL3 and POT1 in HepG2 cells

<i>SUMMARY</i>	<i>Count</i>	<i>Sum</i>	<i>Average</i>	<i>Variance</i>
NEIL3	6	1098	183	9.2
POT1	6	526	87.66667	53.86667
Column 1	2	280	140	4050
Column 2	2	285	142.5	4140.5
Column 3	2	267	133.5	4512.5
Column 4	2	268	134	4232
Column 5	2	263	131.5	4900.5
Column 6	2	261	130.5	5512.5

ANOVA

<i>Source of Variation</i>	<i>SS</i>	<i>Df</i>	<i>MS</i>	<i>F</i>	<i>P-value</i>	<i>F crit</i>
Rows	27265.33	1	27265.33	1649.113	0.00071	6.607891
Columns	232.6667	5	46.53333	2.814516	0.140312	5.050329
Error	82.66667	5	16.53333			
Total	27580.67	11				

t-Test: Paired Two Sample for Means of NEIL3 and POT1 in HepG2 cells

	<i>NEIL3</i>	<i>POT1</i>
Mean	183	87.66666667
Variance	9.2	53.86666667
Observations	6	6
Pearson Correlation	0.67381	
Hypothesized Mean Difference	0	
Df	5	
t Stat	40.60927	
P(T<=t) one-tail	8.54E-08	
t Critical one-tail	2.015048	
P(T<=t) two-tail	0.00071	
t Critical two-tail	2.570582	

**Table 5.11:** Anova: Two-Factor Without Replication for NEIL3 and hTERT in HepG2 cells

<i>SUMMARY</i>	<i>Count</i>	<i>Sum</i>	<i>Average</i>	<i>Variance</i>
NEIL3	6	1098	183	9.2
hTERT	6	594	99	50.8
Column 1	2	290	145	3200
Column 2	2	295	147.5	3280.5
Column 3	2	273	136.5	3960.5
Column 4	2	269	134.5	4140.5
Column 5	2	281	140.5	3280.5
Column 6	2	284	142	3362

ANOVA

<i>Source of Variation</i>	<i>SS</i>	<i>df</i>	<i>MS</i>	<i>F</i>	<i>P-value</i>	<i>F crit</i>
Rows	21168	1	21168	1890	0.00012	6.607891
Columns	244	5	48.8	4.357143	0.066037	5.050329
Error	56	5	11.2			
Total	21468	11				

t-Test: Paired Two Sample for Means of NEIL3 and hTERT in HepG2 cells

	<i>NEIL3</i>	<i>hTERT</i>
Mean	183	99
Variance	9.2	50.8
Observations	6	6
Pearson Correlation	0.869625	
Hypothesized Mean Difference	0	
Df	5	
t Stat	43.47413	
P(T<=t) one-tail	6.08E-08	
t Critical one-tail	2.015048	
P(T<=t) two-tail	0.00012	
t Critical two-tail	2.570582	

**Table 5.12:** Anova: Two-Factor Without Replication for NEIL3 in non treated cells and NEIL3 in treated cells with 5  $\mu$ M t-BHP in HepG2 cells

<i>SUMMARY</i>	<i>Count</i>	<i>Sum</i>	<i>Average</i>	<i>Variance</i>
NEIL3 (non treated cells)	6	672	112	2
NEIL3 (treated cells)	6	544	90.66667	30.26667
Column 1	2	194	97	338
Column 2	2	212	106	128
Column 3	2	202	101	242
Column 4	2	196	98	338
Column 5	2	208	104	162
Column 6	2	204	102	200

ANOVA

<i>Source of Variation</i>	<i>SS</i>	<i>df</i>	<i>MS</i>	<i>F</i>	<i>P-value</i>	<i>F crit</i>
Rows	1365.333	1	1365.333	160	0.00005	6.607891
Columns	118.6667	5	23.73333	2.78125	0.142988	5.050329
Error	42.66667	5	8.533333			
Total	1526.667	11				

t-Test: Paired Two Sample for Means of NEIL3 in non treated and in treated cells with 5  $\mu$ M t-BHP in HepG2 cells

	<i>NEIL3 (non treated cells)</i>	<i>NEIL3 (treated cells)</i>
Mean	112	90.66667
Variance	2	30.26667
Observations	6	6
Pearson Correlation	0.976823946	
Hypothesized Mean Difference	0	
Df	5	
t Stat	12.64911064	
P(T<=t) one-tail	2.74361E-05	
t Critical one-tail	2.015048373	
P(T<=t) two-tail	0.00005	
t Critical two-tail	2.570581836	

**Table 5.13:** Anova: Two-Factor Without Replication for hTERT in non treated and in treated cells with 2.5 uM t-BHP in HepG2 cells

<i>SUMMARY</i>	<i>Count</i>	<i>Sum</i>	<i>Average</i>	<i>Variance</i>
hTERT in non treated cells	6	549.5	91.58333	14.24167
hTERT in treated cells	6	635	105.8333	2.166667
Column 1	2	200	100	50
Column 2	2	194	97	200
Column 3	2	197.5	98.75	105.125
Column 4	2	201	100.5	24.5
Column 5	2	197	98.5	180.5
Column 6	2	195	97.5	112.5

ANOVA

<i>Source of Variation</i>	<i>SS</i>	<i>df</i>	<i>MS</i>	<i>F</i>	<i>P-value</i>	<i>F crit</i>
Rows	609.1875	1	609.1875	48.01478	0.000961	6.607891
Columns	18.60417	5	3.720833	0.293268	0.897821	5.050329
Error	63.4375	5	12.6875			
Total	691.2292	11				

t-Test: Paired Two Sample for Means of hTERT in non treated and in treated cells with 2.5 uM t-BHP in HepG2 cells

	hTERT in non treated cells	hTERT in treated cells
Mean	91.5833333	105.8333333
Variance	14.2416667	2.166666667
Observations	6	6
Pearson Correlation	-0.8070948	
Hypothesized Mean Difference	0	
Df	5	
t Stat	-6.9292697	
P(T<=t) one-tail	0.00048029	
t Critical one-tail	2.01504837	
P(T<=t) two-tail	0.000961	
t Critical two-tail	2.57058184	

**Table 5.14:** Anova: Two-Factor Without Replication for hTERT in non treated and treated HepG2 cells with 5 uM t-BHP

<i>SUMMARY</i>	<i>Count</i>	<i>Sum</i>	<i>Average</i>	<i>Variance</i>
hTERT in non treated cells	6	549.5	91.58333	14.24167
hTERT in treated cells	6	749	124.8333	4.566667
Column 1	2	223	111.5	544.5
Column 2	2	210	105	648
Column 3	2	216.5	108.25	561.125
Column 4	2	223	111.5	420.5
Column 5	2	214	107	648
Column 6	2	212	106	512

ANOVA

<i>Source of Variation</i>	<i>SS</i>	<i>df</i>	<i>MS</i>	<i>F</i>	<i>P-value</i>	<i>F crit</i>
Rows	3316.688	1	3316.688	951.0215	0.00672	6.607891
Columns	76.60417	5	15.32083	4.39307	0.065041	5.050329
Error	17.4375	5	3.4875			
Total	3410.729	11				

t-Test: Paired Two Sample for Means of hTERT in non treated and treated HepG2 cells with 5 uM t-BHP

	<i>hTERT in non treated cells</i>	hTERT in treated cells
Mean	91.58333333	124.8333333
Variance	14.24166667	4.566666667
Observations	6	6
Pearson Correlation	0.733663711	
Hypothesized Mean Difference	0	
Df	5	
t Stat	-30.8386366	
P(T<=t) one-tail	3.36448E-07	
t Critical one-tail	2.015048373	
P(T<=t) two-tail	0.00672	
t Critical two-tail	2.570581836	

**Table 5.15:** Anova: Two-Factor Without Replication for POT1 in non treated and treated HepG2 cells with 2.5 uM t-BHP

<i>SUMMARY</i>	<i>Count</i>	<i>Sum</i>	<i>Average</i>	<i>Variance</i>
POT1 (non treated cells)	6	346	57.66667	3.066667
POT1 (treated cells)	6	538	89.66667	7.466667
Column 1	2	146	73	392
Column 2	2	149	74.5	612.5
Column 3	2	148	74	512
Column 4	2	141	70.5	480.5
Column 5	2	150	75	648
Column 6	2	150	75	450

ANOVA

<i>Source of Variation</i>	<i>SS</i>	<i>df</i>	<i>MS</i>	<i>F</i>	<i>P-value</i>	<i>F crit</i>
Rows	3072	1	3072	667.8261	0.001	6.607891
Columns	29.66667	5	5.933333	1.289855	0.393412	5.050329
Error	23	5	4.6			
Total	3124.667	11				

t-Test: Paired Two Sample for Means of POT1 in non treated and treated HepG2 cells with 2.5 uM t-BHP

	<i>POT1 (non treated cells)</i>	<i>POT1 (treated cells)</i>
Mean	57.66667	89.66667
Variance	3.066667	7.466667
Observations	6	6
Pearson Correlation	0.13932	
Hypothesized Mean Difference	0	
Df	5	
t Stat	-25.8423	
P(T<=t) one-tail	8.1E-07	
t Critical one-tail	2.015048	
P(T<=t) two-tail	0.001	
t Critical two-tail	2.570582	

**Table 5.16:** Anova: Two-Factor Without Replication for POT1 in HepG2 cells treated with 5 uM t-BHP

<i>SUMMARY</i>	<i>Count</i>	<i>Sum</i>	<i>Average</i>	<i>Variance</i>
POT1 (non treated cells)	6	346	57.66667	3.066667
POT1 ( treated cells)	6	244	40.66667	1.466667
Column 1	2	100	50	162
Column 2	2	99	49.5	112.5
Column 3	2	98	49	162
Column 4	2	97	48.5	84.5
Column 5	2	96	48	162
Column 6	2	100	50	200

ANOVA

<i>Source of Variation</i>	<i>SS</i>	<i>df</i>	<i>MS</i>	<i>F</i>	<i>P-value</i>	<i>F crit</i>
Rows	867	1	867	270.9375	0.001	6.607891
Columns	6.666667	5	1.333333	0.416667	0.820656	5.050329
Error	16	5	3.2			
Total	889.6667	11				

t-Test: Paired Two Sample for Means of POT1 in HepG2 cells treated with 5 uM t-BHP

	<i>POT1 (non treated cells)</i>	<i>POT1 ( treated cells)</i>
Mean	57.66666667	40.66667
Variance	3.066666667	1.466667
Observations	6	6
Pearson Correlation	-0.440086229	
Hypothesized Mean Difference	0	
Df	5	
t Stat	16.46017922	
P(T<=t) one-tail	7.55229E-06	
t Critical one-tail	2.015048373	
P(T<=t) two-tail	0.001	
t Critical two-tail	2.570581836	

**Table 5.17:** Anova: Two-Factor Without Replication for ALL cells treated with t-BHP

<i>SUMMARY</i>	<i>Count</i>	<i>Sum</i>	<i>Average</i>	<i>Variance</i>
Row 1	2	200	100	0
Row 2	2	128.3636	64.18182	1927.117
Row 3	2	88.07136	44.03568	2160.766
Row 4	2	61.37079	30.68539	864.8694
Row 5	2	52.58373	26.29186	557.8225
Row 6	2	46.28544	23.14272	374.891
Row 7	2	33.33516	16.66758	107.6214
Row 8	2	28.75682	14.37841	48.54599
CEM-1-15	8	446.743	55.84287	976.9338
CEM-7-14	8	192.0239	24.00299	1009.915

ANOVA

<i>Source of Variation</i>	<i>SS</i>	<i>Df</i>	<i>MS</i>	<i>F</i>	<i>P-value</i>	<i>F crit</i>
Rows	11921.42	7	1703.06	6.001157	0.015305	3.787044
Columns	4055.113	1	4055.113	14.2892	0.006891	5.591448
Error	1986.52	7	283.7886			
Total	17963.05	15				

t-Test: Paired Two Sample for Means of ALL cells treated with t-BHP

	<i>CEM-1-15</i>	<i>CEM-7-14</i>
Mean	55.84287	24.00299
Variance	976.9338	1009.915
Observations	8	8
Pearson Correlation	0.714431	
Hypothesized Mean Difference	0	
Df	7	
t Stat	3.780106	
P(T<=t) one-tail	0.003446	
t Critical one-tail	1.894579	
P(T<=t) two-tail	0.006891	
t Critical two-tail	2.364624	



**Table 5.18:** Anova: Two-Factor Without Replication for ALL cells treated with cisplatin

<i>SUMMARY</i>	<i>Count</i>	<i>Sum</i>	<i>Average</i>	<i>Variance</i>
Row 1	2	200	100	0
Row 2	2	192.6122	96.3061	8.146835
Row 3	2	165.5068	82.7534	8.314118
Row 4	2	124.7543	62.37713	5.40314
Row 5	2	99.23012	49.61506	32.91925
Row 6	2	66.76327	33.38163	176.1725
Row 7	2	50.2919	25.14595	58.70611
Row 8	2	40.73386	20.36693	6.315354
CEM-1-15	8	492.2478	61.53097	860.6168
CEM-7-14	8	447.6446	55.95558	1172.713

ANOVA

<i>Source of Variation</i>	<i>SS</i>	<i>Df</i>	<i>MS</i>	<i>F</i>	<i>P-value</i>	<i>F crit</i>
Rows	14061.67	7	2008.81	81.92663	3.5E-06	3.78704
Columns	124.34	1	124.34	5.071039	0.05903	4
Error	171.6374	7	24.51962		3	8
Total	14357.65	15				

**Table 5.19:** Anova: Two-Factor Without Replication for ALL cells treated with doxorubicin

<i>SUMMARY</i>	<i>Count</i>	<i>Sum</i>	<i>Average</i>	<i>Variance</i>
Row 1	2	200	100	0
Row 2	2	144.1856	72.0928	378.3
Row 3	2	92.31662	46.15831	6.3435
Row 4	2	83.83277	41.91638	8
Row 5	2	68.98179	34.49089	2.1095
Row 6	2	67.6233	33.81165	1
Row 7	2	61.65203	30.82601	24.100
Row 8	2	56.41923	28.20961	83
CEM-1-15	8	381.7358	47.71698	15.591

					98
					790.49
CEM-7-14	8	393.2755	49.15944		5

ANOVA

<i>Source of Variation</i>	<i>SS</i>	<i>df</i>	<i>MS</i>	<i>F</i>	<i>P-value</i>	<i>F crit</i>
	8787.479			20.711	0.00035	3.78704
Rows	39	7	1255.354	81	7	4
	8.322704			0.1373	0.72192	5.59144
Columns	28	1	8.322704	14	5	8
	424.2738					
Error	93	7	60.61056			
	9220.075					
Total	99	15				